

DISSERTATION

REMEDICATION OF SOIL IMPACTED WITH CHLORINATED ORGANIC COMPOUNDS:

SOIL MIXING WITH ZERO VALENT IRON AND CLAY

Submitted by

Mitchell R. Olson

Department of Civil and Environmental Engineering

In partial fulfillment of the requirements

For the Degree of Doctor of Philosophy

Colorado State University

Fort Collins, Colorado

Spring 2014

Doctoral Committee:

Advisor: Tom Sale

David Dandy

Susan De Long

Charles Shackelford

Copyright by Mitchell Olson 2014

All Rights Reserved

## ABSTRACT

### REMEDIATION OF SOIL IMPACTED WITH CHLORINATED ORGANIC COMPOUNDS: SOIL MIXING WITH ZERO VALENT IRON AND CLAY

Chlorinated solvents in the environment continue to present an enormous remediation challenge. A primary reason for the difficulty in cleaning up chlorinated solvent source zones involves heterogeneous distributions of permeability and contaminants in natural porous media. A method that can be used to overcome heterogeneity involves use of soil mixing techniques to deliver reagents and homogenize soils. A typical soil mixing application involves admixing contaminated soil with zero valent iron (ZVI) and bentonite (clay). This technology, herein referred to as ZVI-Clay, combines ZVI-mediated degradation of chlorinated solvents with bentonite-induced stabilization.

As of December 2013, ZVI-Clay has been applied in 13 field applications, all of which have been viewed as being successful in achieving site remediation objectives. However, our understanding of the processes governing treatment in the ZVI-Clay mixed soil system is rather limited. The overarching goal of the research presented herein is to broaden our understanding of the processes controlling degradation and transport in soils treated via soil mixing with ZVI (or similar reactive media) and bentonite. In support of this objective, research included (a) analysis of field data, (b) initial rate studies, (c) hydraulic conductivity testing, (d) reactive-transport modeling coupled with column experiments, and (e) treatment of hydrophobic compounds.

Field data analysis was based on performance data from a ZVI-Clay field application at Camp Lejeune, NC, in which 23,000 m<sup>3</sup> of soil initially contaminated with trichloroethene (TCE) and 1,1,2,2-tetrachloroethane (TeCA) were treated with 2% ZVI and 3% bentonite. Within one year of treatment, total chlorinated organic compound (COC) concentrations in soils were decreased by average and median values of 97% and >99%, respectively. Total COC concentrations in groundwater were reduced by

average and median values of 81% and >99%, respectively. Total COC reductions by 99.9% or greater were observed in most soil and water sampling locations. Hydraulic conductivity in the treated soil zone was reduced by an average of about 2.5 orders of magnitude.

To explain the variations in kinetic data observed following ZVI-Clay field applications, initial-rate batch-reactor studies were conducted under a range of initial TCE concentrations and ZVI concentrations. When TCE concentrations were less than solubility, the Michaelis-Menton kinetic model provided an excellent fit of experimental data. When TCE concentrations were above solubility (i.e., NAPL was present), the degradation rate was independent of the amount of NAPL in the system. The presence of NAPL appears to have had a minor impact (~20% reduction) on the TCE degradation rate. A linear relationship between TCE degradation rate and ZVI amount was observed.

Hydraulic characteristics of soils mixed with bentonite were evaluated by conducting column studies and MODFLOW modeling of field-scale systems. Experiments were conducted to evaluate the hydraulic conductivity,  $K$ , in two soils types mixed with 0.5 to 4% bentonite (i.e., the range of values typical for ZVI-Clay field applications). In a well-sorted fine sand, with a moderately high initial  $K$  ( $10^{-4}$  m·s<sup>-1</sup>), the value of  $K$  was reduced by about a factor of 10 for each 1% bentonite added to the soils. In a moderately-sorted fine sand with silt, with a low initial  $K$  ( $10^{-8}$  m·s<sup>-1</sup>), addition of up to 4% bentonite had only minor impacts on  $K$ . MODFLOW modeling indicated that surrounding groundwater flow patterns tend to bypass the treated soil body, under steady state conditions, given a reduction in  $K$  by at least an order of magnitude. Within the treated soil body, contaminant residence time is extended in approximate proportion to the reduction in  $K$ .

The concepts of NAPL dissolution, ZVI-mediated degradation, and flow reduction were combined in a mathematical model. The model was then tested using column reactor studies containing NAPL-phase TCE and soils treated with 2% ZVI. The model adequately described TCE elution and formation of degradation products. The model was then used to predict treatment performance following

field-scale implementation of ZVI-Clay. Model output predicts that the benefits of reaction are most effectively utilized with a reduction in flow rate by at least 2 orders of magnitude.

Finally, enhancements to the ZVI-Clay treatment process were evaluated for treatment of polychlorinated biphenyls (PCBs). Due to their strong hydrophobicity and stable molecular structure, PCBs in the environment have been shown to be much more difficult to degrade than many of the common chlorinated solvents. Thus, alternative types of reactive media were evaluated. Batch experiments were conducted to evaluate zero valent metals (ZVM), ZVM + Pd-catalysis, and emulsified zero valent iron (EZVI) for dechlorination of PCBs in systems with and without soil. In water-based systems, ZVM with a Pd-catalyst facilitated rapid destruction of 2-chlorobiphenyl (half-life < 2 hr), while ZVM alone did not achieve any measurable degradation. In the presence of soils, EZVI was the only approach that resulted in a clear enhancement in PCB dechlorination rates. The results suggest treatment of PCBs in the presence of soil presents a much greater challenge than treatment of aqueous phase PCBs; however, treatment of PCBs in soil can benefit from enhanced desorption and a persistent reactive media.

## ACKNOWLEDGEMENTS

I would like to thank my advisor, Dr. Tom Sale, for giving me this opportunity. I would not be here if not for his encouragement and support. I also thank my committee members, Dr. David Dandy, Dr. Susan De Long, and Dr. Charles Shackelford, for their advisement throughout the process. In conducting the research described herein, help was provided by Center for Contaminant Hydrology staff including Aaron Bailey, Gabi Davis, Gary Dick, Sonja Koldewyn, Kim LeMonde, and Natalie Zeman. Dr. Dave Gilbert played a large role in our early ZVI-Clay development work, but left us far too soon. Additional advice was provided by co-authors of manuscripts included herein, who include Dr. Thomas Borch and Dr. Jens Blotevogel (Colorado State University), Chris Bozzini and Jessica Skeeane (CH2M HILL), Dr. Matt Petersen and Dr. Rich Royer (GE). In our early days working with ZVI-Clay, expert advice was provided by Dr. Bob Gillham (University of Waterloo) as well as John Vogan and Mike Duchesne (Environmental Technologies, Inc.).

Much of the funding for this work came from royalty revenues generated by the ZVI-Clay patents, which were generously donated to Colorado State University by DuPont. The research questions addressed herein were largely derived from treatability studies sponsored by AECOM, ARCADIS, CH2M HILL, DuPont, Golder Associates, General Electric, Groundwater Services Inc., NIRAS, St. John Mittelhauser, TetraTech, URS, US DoD, and US EPA. Financial contributions were also provided by the University Consortium for Field-Focused Groundwater Remediation.

Last but not least, I would like to thank my family – Sara, Paul, and Charley – for their patience and support.

## TABLE OF CONTENTS

CHAPTER 1: INTRODUCTION .....	1
CHAPTER 2: CHLORINATED SOLVENT SOURCE-ZONE REMEDIATION VIA ZVI- CLAY SOIL MIXING: ONE-YEAR RESULTS .....	23
CHAPTER 3: INITIAL RATE STUDIES EVALUATING REACTION KINETICS IN SYSTEMS CONTAINING ZERO VALENT IRON AND NAPL-PHASE TCE.....	52
CHAPTER 4: HYDRAULIC IMPLICATIONS OF BENTONITE ADDITION DURING ZVI- CLAY SOIL MIXING.....	73
CHAPTER 5: DISSOLUTION, TRANSPORT, AND DEGRADATION OF TCE NAPL IN SOILS MIXED WITH ZVI AND BENTONITE: COLUMN STUDIES AND MODELING .....	90
CHAPTER 6: LONG-TERM POTENTIAL OF IN SITU CHEMICAL REDUCTION FOR TREATMENT OF POLYCHLORINATED BIPHENYLS IN SOILS .....	136
CHAPTER 7: CONCLUSIONS AND RECOMMENDATIONS .....	154
APPENDIX A: SUPPORTING INFORMATION FOR DISSOLUTION, TRANSPORT, AND DEGRADATION OF TCE NAPL IN SOILS MIXED WITH ZVI AND BENTONITE: COLUMN STUDIES AND MODELING .....	161
APPENDIX B: SUPPORTING INFORMATION FOR LONG-TERM POTENTIAL OF IN SITU CHEMICAL REDUCTION FOR TREATMENT OF POLYCHLORINATED BIPHENYLS IN SOILS .....	168

# CHAPTER 1

## INTRODUCTION

The industrial revolution spawned unprecedented economic and population growth but forever changed the way humans interact with their planet. The industrialization of society has benefited enormously from the production of an ever-increasing catalog of chemicals. A significant number of these chemicals are anthropogenic, hence, are not found in nature in significant quantities. However, historical handling and disposal practices have resulted in the release of large amounts of anthropogenic chemicals into the environment. Chlorinated organic compounds (COCs) are among the most prominent of the anthropogenic environmental contaminants due to the vast scale at which they were produced and subsequently released into the subsurface environment. Releases commonly originated from leaky plumbing, storage tanks, or transportation vessels. Often, releases resulted from well-intentioned end-users who followed the instructions for disposal as published by the Manufacturing Chemist's Association – “may be poured onto dry sand... and allowed to evaporate” (Pankow and Cherry 1996).

### **1.1 Chlorinated Compounds in the Environment**

When Albert Einstein said that today's problems cannot be solved by the same level of thinking that was used to create them (or something to that effect, as sources tend to differ), he probably was not referring to remediation of COCs in soils, but the quote certainly applies. Although COCs were widely produced throughout the 20<sup>th</sup> century, only in the 1970s did humans first become aware of their presence in the subsurface and subsequent impacts on human health and the environment. Early remediation attempts primarily involved pumping of groundwater for above-ground treatment (pump-and-treat). Unfortunately, pump-and-treat systems have proven to be mostly ineffective in reducing source-zone COC concentrations to drinking water standards (Mackay and Cherry 1989; Mackay et al. 2000; Rivett et

al. 2006). A primary factor limiting the effectiveness of groundwater extraction is subsurface heterogeneity – specifically, the presence of low-permeability (low-k) soil zones. Diffusion can drive a significant fraction of contaminant mass into low-k soils, where groundwater extraction has limited impact. Pump-and-treat can provide effective hydraulic containment by preventing advective discharge from the recovery zone but such systems are often expensive and must be operated indefinitely (EPA 2003).

More recent developments for remediation of COC source zones involve *in situ* chemical oxidation (ISCO), *in situ* chemical reduction (ISCR), enhanced bioremediation, surfactant or cosolvent flushing, and thermal-based technologies. ISCO and ISCR applications typically involve delivery of chemical oxidants, such as persulfate (Petri et al. 2011), or reductants, such as nm-sized ZVI (Elliott and Zhang 2001; Quinn et al. 2005), via injection wells. Enhanced bioremediation technologies involve delivery of substrate (biostimulation) or specific microbes (bioaugmentation) that facilitate *in situ* biodegradation of COCs (Major et al. 2002). Surfactant and cosolvent technologies involve flushing of materials designed to enhance the quantities of COCs in the aqueous-phase, thus improving recoverability as compared to traditional pump-and-treat systems (Jawitz et al. 2003). Thermal technologies involve *in situ* heating of contaminated soil to facilitate volatilization of contaminants such that vapors can be collected and treated or, in some cases, driving *in situ* thermal destruction of contaminant molecules (Kingston et al. 2010).

Under certain circumstances, each of these approaches is capable of achieving considerable contaminant mass reduction (McGuire et al. 2006). However, ISCO, ISCR, enhanced bioremediation, and flushing are primarily effective in treating contaminants in highly transmissive zones. After treatment is stopped, back-diffusion of COCs from low-k zones can restore elevated transmissive-zone concentrations. Thermal remediation techniques are capable of treating contaminants in both high-k and low-k zones (Stroo et al. 2012). Limitations of thermal remediation techniques include a potential re-

mobilization of contaminants, extreme conditions required within the subsurface (i.e., high energy input), and the need to collect and treat vapors generated during treatment (Kingston et al. 2010).

An emerging method for treatment of COC source zones involves use of soil mixing techniques to deliver reactive media and stabilizing agents into COC-contaminated soils. Soil mixing is a technique that was originally developed to improve geotechnical properties such as strength or permeability (Day and Ryan 1995). Through use of soil mixing to deliver amendments, natural subsurface soil strata of various particle sizes are homogenized and reagents are distributed throughout the mixed zone. Thus, reagent-contaminant contact issues associated with many *in situ* technologies can be overcome and treatment of contaminants in low-k soils is possible. To achieve contaminant mass removal, soil mixing has been combined with vapor stripping (Siegrist et al. 1995), chemical oxidation (Gates and Siegrist 1995; Siegrist et al. 2011), and chemical reduction technologies (Wadley et al. 2005; Fjordboge et al. 2012a; Olson et al. 2012).

## **1.2 ZVI-Clay Remediation of Chlorinated Compounds**

For remediation of COCs, a typical application of the soil mixing technique, herein referred to as ZVI-Clay, involves the use of soil mixing for delivery of zero valent iron (ZVI) and clay (e.g., bentonite) into soils contaminated with chlorinated solvents (Shackelford et al. 2005; Wadley et al. 2005; Bozzini et al. 2006; Shackelford and Sale 2011; Fjordboge et al. 2012a; Olson et al. 2012). An illustration of the ZVI-Clay implementation process is shown in Figure 1-1. Soil mixing with ZVI and bentonite utilizes two well-established concepts: (1) ZVI-mediated degradation of chlorinated solvents and (2) bentonite-induced contaminant stabilization. Each of these concepts is discussed in the following sections.

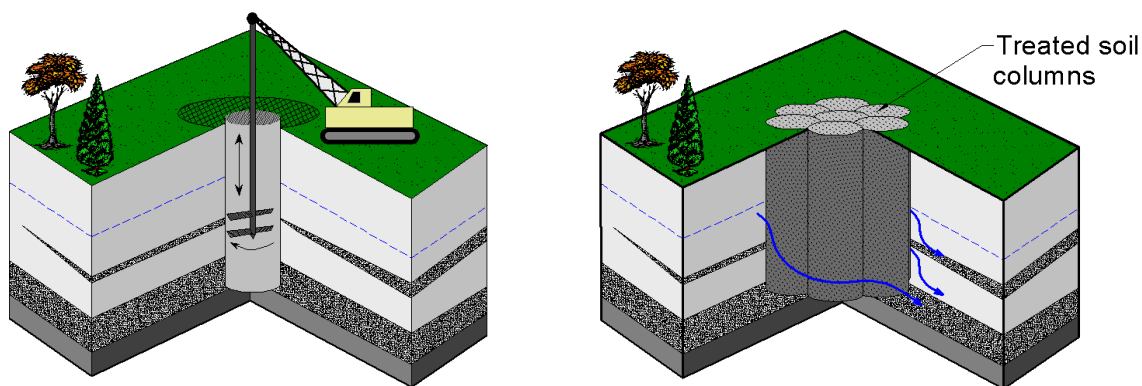


Figure 1-1. For implementation of ZVI-Clay, a soil mixing tool is simultaneously turned and driven vertically in down-up mixing passes, creating a series of overlapping mixed soil columns (left). ZVI and clay are distributed throughout each of the mixed soil columns. After mixing (right), the heterogeneous source zone is transformed into a low-permeability body of treated soils.

### 1.2.1 ZVI-Mediated Degradation of Chlorinated Solvents

Over the past 20 years, ZVI-mediated degradation of chlorinated compounds has generated a substantial amount of research (Gillham and O'Hannesin 1994; Johnson et al. 1996; Scherer et al. 1998; Arnold and Roberts 2000b; Tratnyek et al. 2001; Ritter et al. 2002; Grant and Kueper 2004; Bi et al. 2010; Phillips et al. 2010; Jeon et al. 2011), most of which has been conducted in the context of ZVI-based permeable reactive barriers (PRBs). Common research topics include surface chemistry (Ritter et al. 2002), kinetic modeling (Johnson et al. 1996; Arnold and Roberts 2000a, 2000b), water chemistry effects (Farrell et al. 2000; Devlin and Allin 2005), and long-term performance of PRBs (Puls et al. 1999; Guilbeault et al. 2005; Henderson and Demond 2007; Kouznetsova et al. 2007; Phillips et al. 2010; ITRC 2011; Jeon et al. 2011). From this body of literature, a basic process description of ZVI-mediated degradation of chlorinated solvents is as follows:

- The basic form of the reactions describing ZVI-mediated degradation of a chlorinated hydrocarbon,  $RCl$ , is shown in Equations 1 and 2 (Gillham and O'Hannesin 1994). Alternative reaction pathways can change the form of Equation 2 (for example,  $\beta$ -elimination pathways can result in formation of  $\pi$ -bonds), but the general sequence is similar: anaerobic corrosion of ZVI

produces electrons (Equation 1), which in turn are consumed in a reductive dechlorination reaction (Equation 2).



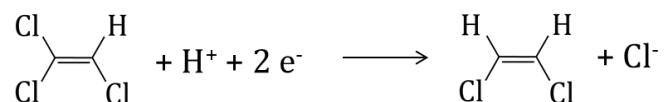
- Degradation is a ZVI surface-mediated process (Matheson and Tratnyek 1994). The iron particle consists of an iron-oxide coating around a ZVI core. Electrons are conducted through the oxide shell to the surface, where degradation occurs (Ritter et al. 2002).
- Chlorinated ethenes (TCE and PCE) tend to degrade via the  $\beta$ -elimination pathway, which bypasses formation of hazardous intermediates *c*DCE and VC (Arnold and Roberts 2000b).
- Degradation kinetics can be modeled as pseudo-first order under a limited range of conditions. More elaborate kinetic models may be applied to describe the system with greater flexibility (e.g., Johnson et al. 1996; Arnold and Roberts 2000a; Bi et al. 2010; Jeon et al. 2011).
- Aqueous chemistry can affect ZVI reactivity and longevity. Certain ions, such as  $Cl^-$  and  $SO_4^{2-}$ , can facilitate ZVI corrosion, thus enhancing reactivity (Devlin and Allin 2005). Other dissolved species, such as  $NO_3^-$ ,  $PO_4^{2-}$ ,  $CO_3^{2-}$ , silica, and dissolved organic matter, can inhibit reactivity of ZVI toward chlorinated solvents (Farrell et al. 2000; Tratnyek et al. 2001; Klausen et al. 2003; Devlin and Allin 2005).
- After 5 to 15 years of operation, many PRBs continue to function well. Failures have generally been attributed to poor design, flow mischaracterization, or mineral precipitation (Henderson and Demond 2007).

Additional discussion on pathways and kinetics are discussed subsequently.

*Reaction Pathways.* ZVI-mediated dechlorination of chlorinated solvents under reducing conditions has several reaction pathways (Figure 1-2). This discussion focuses on chlorinated ethenes, such as trichloroethene (TCE) and tetrachloroethene (PCE), which have been selected as the model compounds for most of the research described in this dissertation. For chlorinated ethenes, primary

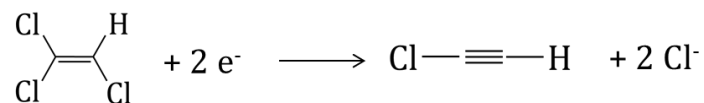
reductive dechlorination pathways include hydrogenolysis and  $\beta$ -elimination (Arnold and Roberts 2000b).

Hydrogenolysis involves replacement of a chlorine atom by hydrogen, such as conversion of TCE to *cis*-1,2-dichloroethylene (*c*DCE):



For degradation of highly chlorinated ethenes such as TCE and PCE, a disadvantage of the hydrogenolysis pathway is the potential for formation of toxic intermediate products including *c*DCE and vinyl chloride (VC). The  $\beta$ -elimination pathway involves removal of chlorine atoms associated with adjacent carbon atoms and subsequent formation of an additional C-C bond (Schwarzenbach et al. 2003).

For example,  $\beta$ -elimination of TCE forms chloroacetylene:



For ZVI, less than 10% of PCE and TCE are typically reported to be degraded through the sequential hydrogenolysis pathway (Gillham and O'Hannesin 1994; Arnold and Roberts 2000b), thus substantially bypassing formation of *c*DCE and VC. Indeed, formation of *c*DCE and VC is often cited as being evidence of degradation being biologically-mediated, rather than ZVI-mediated (Lampron et al. 2001, see Chapter 2). The  $\beta$ -elimination pathway leads to formation of chloroacetylenes, which are rapidly degraded via hydrogenolysis and hydrogenation (replacement of a C-C bond with two hydrogen atoms) pathways to form primarily ethene and ethane (Arnold and Roberts 2000b).

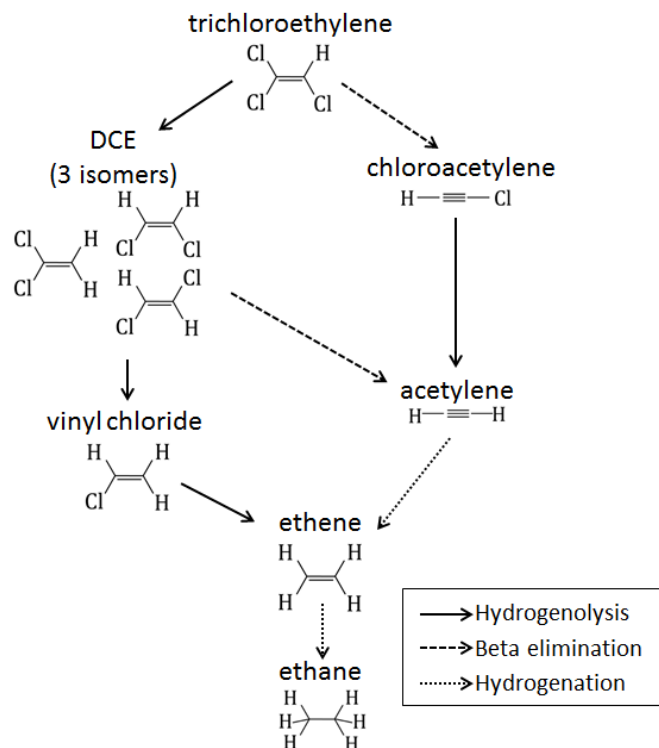


Figure 1-2. Degradation pathways for chlorinated ethenes (after Arnold and Roberts 2000b).

*Reaction Kinetics.* Several kinetic models have been proposed to describe the ZVI-mediated degradation of chlorinated solvents. As a first approximation, a pseudo-first order kinetic model has been used (Gillham and O'Hannesin 1994; Matheson and Tratnyek 1994; Orth and Gillham 1996; Dries et al. 2004; Song and Carraway 2006):

$$\frac{dC}{dt} = -kC \quad (3)$$

where  $k$  ( $d^{-1}$ ) is the first-order rate coefficient,  $C$  ( $mol \cdot L^{-1}$ ) is the aqueous phase contaminant concentration, and  $t$  (d) is the time. Building on the basic pseudo-first order kinetic model, enhanced models have been used to provide additional mechanistic insights. For example, a ZVI-normalized reaction model may be used to compare systems containing variable amounts of ZVI (Johnson et al. 1996):

$$\frac{dC}{dt} = -k_{Fe}\rho_{Fe}C \quad (4)$$

where  $k_{Fe}$  ( $L \cdot g^{-1}d^{-1}$ ) is the ZVI-concentration-normalized rate coefficient and  $\rho_{Fe}$  ( $g \cdot L^{-1}$ ) is the ZVI concentration. Alternatively, the ZVI surface area concentration,  $\rho_a$  ( $m^2 \cdot L^{-1}$ ), can be used in Eqn 5 instead of  $\rho_{Fe}$ , with units of  $k_{Fe}$  changing accordingly. In addition, several models have been published describing competition for a limited number of reactive sites on the ZVI surface. The basic form of this model is analogous to Michaelis-Menton kinetics (Wust et al. 1999; Johnson and Goody 2011):

$$\frac{dC}{dt} = -\frac{k_0C}{K + C} \quad (5)$$

where  $k_0$  ( $mol \cdot L^{-1}d^{-1}$ ) is the maximum degradation rate and  $K$  ( $mol \cdot L^{-1}$ ) is a parameter that represents sorption affinity to the ZVI surface. Additional kinetic models have incorporated competition for reactive sites (Arnold and Roberts 2000a; Grant and Kueper 2004), sorption to reactive and non-reactive sites (Burriss et al. 1995; Bi et al. 2010) and changing reactivity of ZVI over time (Kouznetsova et al. 2007; Jeen et al. 2011).

*ZVI Treatment of Non-Aqueous Phase Liquids.* As compared to ZVI-based PRBs, which target aqueous-phase contaminants, a relatively small volume of literature addresses ZVI-mediated degradation of chlorinated solvent DNAPL. In recent literature, the primary context of ZVI-DNAPL interaction involves injection-based delivery of nm-sized ZVI (nZVI) particles into chlorinated solvent source zones (Quinn et al. 2005; Berge and Ramsburg 2010; Taghavy et al. 2010; Fagerlund et al. 2012). Results have shown that source-zone treatment via injection of nZVI can achieve substantial contaminant mass reduction. However, given current methodologies, injection of nZVI is unlikely to achieve closure status at most sites contaminated with chlorinated solvent DNAPL. The primary limitations include limited nZVI longevity, difficulty in achieving a uniform reagent distribution, and inability to treat contaminants residing in low-k zones. Furthermore, fate and transport of nZVI in the environment is a current source of discussion (e.g., Grieger et al. 2010).

Soil mixing provides an alternative method for delivery of ZVI into chlorinated solvent source zones. The nature of the technique allows for delivery of sub-mm-sized ZVI particles (e.g., -50 mesh), which are much less expensive than nZVI (Lowry and Johnson 2004). Soil mixing for delivery of ZVI has been evaluated in a field demonstration (Wadley et al. 2005) and in full-scale field applications at Martinsville, VA in 2002 (Shackelford et al. 2005), and at Camp Lejeune, NC in 2006 (Bozzini et al. 2006). Wadley et al. (1995) conducted a field demonstration of mixing ZVI and bentonite in PCE NAPL at Canadian Forces Base Borden (Borden, ON). A PCE degradation half-life of about 16 days was reported; soil concentrations were reduced to levels at or near detection limits ( $2 \text{ mg}\cdot\text{kg}^{-1}$ ) within 400 days of mixing. In full-scale field remediation of a carbon tetrachloride source zone, total COCs were reduced by >99% within the first year after completion of mixing (Shackelford et al. 2005). Bozzini et al. (2006) reported average and median reductions in soil concentrations of 82 and 99%, respectively, within one year after field remediation of a PCE source zone. In addition, hydraulic conductivity was reduced by two or more orders of magnitude (Bozzini et al. 2006). These field results indicate that ZVI-Clay is capable of achieving multiple order-of-magnitude reductions in both contaminant concentrations and groundwater advective flow. Furthermore, Colorado State University has conducted approximately 20 treatability studies evaluating ZVI-Clay for remediation under site-specific conditions. Treatability study data (not published) provide further evidence that ZVI is capable of treating soils with DNAPL present under a variety of site-specific conditions.

### 1.2.2 Bentonite-Induced Flow Reduction

As with ZVI-mediated degradation of chlorinated solvents, mixing of bentonite with porous media to reduce hydraulic conductivity,  $K$ , is a well-established remediation approach. Primarily, related research has addressed hydraulic containment structures such as vertical cutoff walls or horizontal liners to waste contaminant systems (Kenney et al. 1992; Yeo et al. 2005). In such applications, bentonite is typically mixed with soils at levels greater than 5% to obtain target  $K$  values of less than  $10^{-9} \text{ m}\cdot\text{s}^{-1}$ . In

vertical cut-off walls, such  $K$ -values (combined with a low hydraulic gradient) can provide long-term isolation of a contamination source by reducing advective discharge to a level where diffusion becomes the predominant transport mechanism (Shackelford 1990) and solute transport rates are restricted (Yeo et al. 2005).

In ZVI-Clay systems, the reduction in  $K$  is coupled with ZVI-mediated degradation. Thus, the objective of including bentonite in ZVI-Clay applications is not permanent isolation of a source, but rather to enhance the benefits of ZVI-mediated degradation by extending the residence time of contaminants (and reactants) within the system. Typical ZVI-Clay applications have involved admixing soils with 1 to 3% bentonite. In laboratory column experiments in fine-grained sand media mixed with 0.6 to 8% bentonite, Castelbaum and Shackelford (2009) reported that measured  $K$ -values declined from about  $10^{-4} \text{ m}\cdot\text{s}^{-1}$  in unmixed sands to about  $10^{-8} \text{ m}\cdot\text{s}^{-1}$  at bentonite contents of greater than 3%. Following a field application that involved mixing contaminated soils with 2% ZVI and 1% bentonite, Bozzini et al. (2006) reported that post-mixing  $K$  values were reduced by about an order of magnitude. Olson et al. (2012) presented a field-application case study wherein mixing of soils with 2% ZVI and 3% bentonite resulted in reduction in  $K$  from  $1.7 \times 10^{-5} \text{ m}\cdot\text{s}^{-1}$  (pre-mixing) to  $5.2 \times 10^{-8} \text{ m}\cdot\text{s}^{-1}$  (post-mixing), a reduction of about 2.5 orders of magnitude. These results suggest that the  $K$  of treated soils can be engineered, to an extent, by the amount of bentonite added. However, only limited information has appeared in the literature on (a) the ability to control  $K$  values in soils mixed with low amounts (i.e., < 5%) of bentonite and (b) subsequent impacts on regional water flow patterns.

### 1.2.3 ZVI-Clay Technology Development Status

The concept of using soil mixing to deliver reactive media and stabilizing agents (e.g., ZVI-Clay) was independently developed by DuPont and the University of Waterloo. Early field applications were conducted by DuPont in Kinston, SC (1998) and Martinsville, VA (2002) and by the University of Waterloo at Canadian Forces Base Borden (Wadley et al. 2005). The technology is the subject of two

patents (Batchelor et al. 1998, 2002) that were donated by DuPont to Colorado State University in 2003. As of December 2013, thirteen field-scale ZVI-Clay projects have been completed (Table 1-1). According to data shown in Table 1-1, approximately 60,000 m<sup>3</sup> (80,000 yd<sup>3</sup>) of contaminated soil have been treated and an estimated 73,000 kg (80 tons) of chlorinated solvents have been removed from the environment as a result of ZVI-Clay field applications. While the ZVI-Clay technology has been shown to work effectively in field applications, much remains to be learned about the processes that govern contaminant degradation and transport in ZVI-Clay treated soils.

**Table 1-1. Summary of ZVI-Clay field projects**

<i>Site</i>	<i>Year</i>	<i>Primary Contaminant/ Initial Conc./ Amount</i>	<i>Treated Soil Volume (yd<sup>3</sup>)</i>	<i>Treatment</i>	<i>Mixing Method</i>	<i>Treatment notes</i>	<i>Reference(s)</i>
Kinston, NC	1999	TCE 100 mg/kg 150 mg/L	200	Peerless ZVI (-50 mesh) Kaolin clay	Jetting	TCE and degradation products non-detect in 14 of 16 cores collected one year after mixing. Jetting method resulted in mixing on the scale of inches.	(EPA 2003)
Martinsville, VA	2002	CT Up to 30,000 mg/kg 22,000 kg total	3,800	2-6% ZVI 6% Kaolin	Auger, crane-mounted	After 2 years, soil sampling indicates 99.99% removal of CT and 99% reduction in total CVOCs. Dichloromethane after 2 years accounted for approximately 1% of initial CT.	(Shackelford et al. 2005)
CFB Borden, Ontario	2003	PCE Up to 4,000 mg/kg	NA (field demo)	0, 5, and 10% ZVI 1-5% bentonite	Hollow-stem auger rig; 60-80cm dia. mixing tool	Concentrations reduced from NAPL levels to <2 mg/kg over most of the mixed region.	(Wadley et al. 2005)
Camp Lejeune, NC (Site 88)	2005	PCE average post-mixing conc.: 1100 mg/kg  10,000 kg total	7,000	2% ZVI 1% bent.	Auger, crane-mounted. 10-ft dia.	82% average removal in soils over 12 months; >99% removal observed over most of the treated soil zone. Greater than 96% removal of PCE in ground water.  Hydraulic conductivity reduced by a factor of 10.  Parking lot constructed over treated soils; surface soils cement-stabilized 6 weeks after treatment.	(Bozzini et al. 2006)
Arnold AFB, TN	2005	TCE Up to 27 mg/L DNAPL suspected	1,600	1.5% ZVI 2% bent.	Mixed using Lang tool in 6-ft. lifts	70% reduction in downgradient water concentrations in year after mixing.	(Palaia 2007)
Warrenton, VA	2006	PCE, TCE, DCM TCA, DCA 10 mg/L	1,150	2% ZVI 1.2% bent. 0.12% EOS veg. oil	Auger, backhoe-mounted. 8.5-ft. dia.	Total VOCs: >98% removal; reached MCLs in water within two years of mixing; met site cleanup criteria.	(Ruffing et al. 2008)
Lake City, MO	2007	TCE 10,000 kg total	7,000	2% ZVI 1% bent.	Auger, crane-mounted. 9-ft dia.	Mixed in silty-clay colluvium to 45 ft in depth.  American Academy of Environmental Engineers and Scientists award for ARCADIS (2011).	(Killenbeck et al. 2008)
Manufacturing facility, SC	2007	CF, TeCA, CT, + aromatics Up to 13,000 mg/L 1000 kg total	1,200	1.5-2.5% ZVI 4% bent.	Lang tool	CF, CT, and TeCA were initially present at 6100, 390, and 1500 mg/kg. All were below detection limits (0.03 mg/kg) in cores collected four years after treatment.	(Ovbey et al. 2010)

**Table 1-1. Summary of ZVI-Clay field projects (continued)**

<i>Site</i>	<i>Year</i>	<i>Primary Contaminant</i>	<i>Treated Soil Volume (yd<sup>3</sup>)</i>	<i>Treatment</i>	<i>Method</i>	<i>Treatment notes</i>	<i>Reference(s)</i>
Camp Lejeune, NC (Site 89)	2008	TCE and TeCA 20,000 kg total	30,000	2% ZVI 3% bentonite	Auger, crane-mounted. 10-ft dia.	PCA and TCE reduced to detection limits in former DNAPL source zone within 12 months. Overall contaminant concentrations in soil and water reduced by 97 and 81% in one year, with additional degradation observed over time.  Hydraulic conductivity reduced by 2.5 orders of magnitude.  Engineering Excellence Award for CH2M HILL from the American Council of Engineering Companies of North Carolina (ACEC/NC).	(Olson et al. 2012)
Skuldelev, Denmark	2008	PCE up to 12000 mg/kg 100 kg total	260	3% ZVI 1% bent.	Auger, crane-mounted.	Within one year after mixing, PCE concentrations reduced by 99% and total chlorinated compounds reduced by 91%, with additional degradation expected.  Discharge in well transect 3-m downgradient reduced by 76% after one year.	(Fjordboge et al. 2012a; Fjordboge et al. 2012b)
Eunice, LA	2011	12-DCP	11,000	6% ZVI 1% bent.	Auger, crane-mounted (in situ). Pug mill (ex situ)	In situ and ex situ treatment performed. All soil sample concentrations reduced below target levels - remediation objectives completed at the site.	(ARCADIS 2012)
Treatment Lagoon, Alberta	2012	PCE	9,800	NA	NA	NA	NA
Waukegan, IL	2012	TCE Up to 700 mg/kg 10,000 kg total	9,000	2.4% ZVI 1.3% bent.	Auger, backhoe-mounted. 9-ft. dia.	Reduction in soil concentrations by >99% within two months of treatment.	(CH2M HILL 2012)

\*NA: no information is publicly available for this site.

\*\*TCE = trichloroethene; PCE = perchloroethene; CT = carbon tetrachloride; CF = chloroform; DCM = dichloromethane; TeCA = 1,1,2,2-tetrachloroethane; 12-DCP = 1,2-dichloropropane; DCA = 1,2-dichloroethane; TCA = 1,1,2-trichloroethane

### 1.3 Research Objectives

Although ZVI-Clay field applications have generally been successful in meeting site remediation goals, there exists a knowledge gap in terms of our understanding of the processes governing treatment. For example, variations in contaminant degradation rates have been noted across field sites after mixing, even though quality control (QC) testing has indicated post-mixing ZVI concentrations are fairly uniform. Thus, the research objectives described herein were developed to address the shortcomings of our current knowledge and broaden our understanding of the processes controlling degradation and transport in soils treated using ZVI-Clay. Specific objectives included the following:

- (1) Characterizing field-scale treatment processes, including reaction kinetics and groundwater flow properties, through analysis of data collected following field-scale implementation of the ZVI-Clay soil mixing technology. Although nearly all field applications have involved collection of some level of performance monitoring data, a rigorous analysis of field-scale kinetics and hydraulic conductivity reduction has not been conducted.
- (2) Evaluating the effects of (a) variable initial COC concentrations and (b) variable ZVI concentrations on degradation kinetics in a ZVI/Non-Aqueous Phase Liquid (NAPL) system.
- (3) Evaluating flow characteristics, including  $K$  reduction and effects on regional groundwater flow patterns, in soils mixed with relatively small quantities of bentonite (< 5%).
- (4) Evaluating the interaction between ZVI-mediated degradation of NAPL-phase COCs (see Objective 2) and enhanced residence time resulting from bentonite-induced flow reduction (see Objective 3).
- (5) Evaluating the potential for using the soil-mixing treatment approach to degrade persistent and hydrophobic compounds, such as polychlorinated biphenyls (PCBs), using reactive materials including zero-valent metals, Pd-catalyst, and emulsified zero valent iron, in soil-water systems.

In support of these objectives, Chapter 2 presents analysis of soil and water data collected over the 12-month period after soil mixing was completed at Site 89, Marine Corps Base Camp Lejeune, North Carolina. Reaction kinetic experiments in a ZVI/TCE-NAPL system are addressed in Chapter 3, wherein initial rate studies were conducted under a range of initial TCE concentrations and ZVI concentrations. Chapter 4 presents results of hydraulic conductivity testing under a range of bentonite loadings (0.5 to 4%) and MODFLOW modeling of groundwater flow in a hypothetical source zone following ZVI-Clay treatment. Chapter 5 presents (a) reactive-transport modeling, including NAPL-dissolution, transport, and reaction processes, and (b) column reactor studies conducted to evaluate the interaction between concepts initially explored in Chapter 3 (reaction kinetics) and Chapter 4 (flow rate). Building on this, Chapter 5 also presents modeled prediction of contaminant discharge and NAPL longevity following field-scale implementation under ranges of groundwater-flow and reaction conditions. Chapter 6 presents long-term (>1 year) batch experiments that were conducted to evaluate strong reductants, including zero-valent metals, palladium catalysis, and emulsified zero valent iron, to degrade polychlorinated biphenyls (PCBs) in water-only and soil-water systems. Conclusions are presented in Chapter 7.

#### **1.4 Publication Status**

Chapter 1 presents introductory material that is not intended for publication outside of this dissertation. Chapter 2 has been published in the National Groundwater Association journal *Groundwater Monitoring & Remediation* (Olson et al. 2012). Chapter 3 is intended to be submitted to the American Chemical Society journal *Environmental Science & Technology*, after completion of supplemental experimental work and modeling (in progress). Chapter 4 presents work that was conducted in support of research presented in Chapter 5, and is not intended for publication outside of this dissertation. Chapter 5 is intended for publication in the Elsevier *Journal of Contaminant Hydrology*. Chapter 6 was submitted to the Elsevier journal *Chemosphere* (June 2013) and is currently in review

(Olson et al. 2013). Chapter 7 presents conclusions and is not intended for publication outside of this dissertation.

## REFERENCES

ARCADIS. 2012. Remedial Action Report, Eunice Train Derailment, May 27, 2000; Agency Interest No. 85276. Baton Rouge, Louisiana.

Arnold, W. A., and A. L. Roberts. 2000a. Inter- and intraspecies competitive effects in reactions of chlorinated ethylenes with zero-valent iron in column reactors. *Environmental Engineering Science* 17 (5):291-302.

Arnold, W. A., and A. L. Roberts. 2000b. Pathways and kinetics of chlorinated ethylene and chlorinated acetylene reaction with Fe(0) particles. *Environmental Science & Technology* 34 (9):1794-1805.

Batchelor, B. , A. M. Hapka, G. J. Igwe, R. H. Jensen, M.F. McDevitt, D.S. Schultz, and J.M. Whang. 1998. Method for Remediating Contaminated Soils edited by U. S. P. a. T. Office. United States: E. I. du Pont de Nemours and Company.

Batchelor, B. , A. M. Hapka, G. J. Igwe, R. H. Jensen, M.F. McDevitt, D.S. Schultz, and J.M. Whang. 2002. Method for Remediating Contaminated Soils edited by U. S. P. a. T. Office. United States: E. I. du Pont de Nemours and Company.

Berge, N. D., and C. A. Ramsburg. 2010. Iron-mediated trichloroethene reduction within nonaqueous phase liquid. *Journal of Contaminant Hydrology* 118 (3-4):105-116.

Bi, E. P., J. F. Devlin, B. Huang, and R. Firdous. 2010. Transport and Kinetic Studies To Characterize Reactive and Nonreactive Sites on Granular Iron. *Environmental Science & Technology* 44 (14):5564-5569.

Bozzini, C., T. Simpkin, T. Sale, D. Hood, and B. Lowder. 2006. DNAPL Remediation at Camp Lejeune using ZVI-Clay Soil Mixing. In *Fifth Battelle Conference on Remediation of Chlorinated and Recalcitrant Compounds*. Monterrey, CA.

Burris, D. R., T. J. Campbell, and V. S. Manoranjan. 1995. Sorption of trichloroethylene and tetrachloroethylene in a batch reactive metallic iron-water system. *Environmental Science & Technology* 29 (11):2850-2855.

Castelbaum, D., and C. D. Shackelford. 2009. Hydraulic conductivity of bentonite slurry mixed sands. *Journal of Geotechnical and Geoenvironmental Engineering* 135 (12):1941-1956.

CH2M HILL. 2012. Final Remedial Action Report, OMC Plant 2 Site (OU4), In Situ Soil Mixing Remedy, Waukegan, Illinois, WA No. 151-RARA-0528/Contract No. EP-S5-06-01. September 2012. Chicago, Illinois.

Day, S. R., and C. Ryan. 1995. Containment, stabilization and treatment of contaminated soils using in-situ soil mixing. In *Geoenvironment 2000: Characterization, Containment, Remediation, and Performance in Environmental Geotechnics, Vols 1 and 2*, edited by Y. B. Acar and D. E. Daniel. New York: ASCE.

Devlin, J. F., and K. O. Allin. 2005. Major anion effects on the kinetics and reactivity of granular iron in glass-encased magnet batch reactor experiments. *Environmental Science & Technology* 39 (6):1868-1874.

- Dries, J., L. Bastiaens, D. Springael, S. N. Agathos, and L. Diels. 2004. Competition for sorption and degradation of chlorinated ethenes in batch zero-valent iron systems. *Environmental Science & Technology* 38 (10):2879-2884.
- Elliott, D. W., and W. X. Zhang. 2001. Field assessment of nanoscale biometallic particles for groundwater treatment. *Environmental Science & Technology* 35 (24):4922-4926.
- EPA. 2003. *The DNAPL remediation challenge: Is there a case for source depletion?* Edited by M. C. Kavanaugh and P. S. C. Rao. Cincinnati, OH: U.S. Environmental Protection Agency, National Risk Management Research Laboratory.
- Fagerlund, F., T. H. Illangasekare, T. Phenrat, H. J. Kim, and G. V. Lowry. 2012. PCE dissolution and simultaneous dechlorination by nanoscale zero-valent iron particles in a DNAPL source zone. *Journal of Contaminant Hydrology* 131 (1-4):9-28.
- Farrell, J., N. Melitas, M. Kason, and T. Li. 2000. Electrochemical and column investigation of iron-mediated reductive dechlorination of trichloroethylene and perchloroethylene. *Environmental Science & Technology* 34 (12):2549-2556.
- Fjordboge, A. S., I. V. Lange, P. L. Bjerg, P. J. Binning, C. Riis, and P. Kjeldsen. 2012a. ZVI-Clay remediation of a chlorinated solvent source zone, Skuldelev, Denmark: 2. Groundwater contaminant mass discharge reduction. *Journal of Contaminant Hydrology* 140:67-79.
- Fjordboge, A. S., C. Riis, A. G. Christensen, and P. Kjeldsen. 2012b. ZVI-Clay remediation of a chlorinated solvent source zone, Skuldelev, Denmark: 1. Site description and contaminant source mass reduction. *Journal of Contaminant Hydrology* 140:56-66.
- Gates, D. D., and R. L. Siegrist. 1995. In situ chemical oxidation of trichloroethylene using hydrogen-peroxide. *Journal of Environmental Engineering-ASCE* 121 (9):639-644.
- Gillham, R. W., and S. F. O'Hannesin. 1994. Enhanced degradation of halogenated aliphatics by zero-valent iron. *Ground Water* 32 (6):958-967.
- Grant, G. P., and B. H. Kueper. 2004. The influence of high initial concentration aqueous-phase TCE on the performance of iron wall systems. *Journal of Contaminant Hydrology* 74 (1-4):299-312.
- Grieger, K. D., A. Fjordboge, N. B. Hartmann, E. Eriksson, P. L. Bjerg, and A. Baun. 2010. Environmental benefits and risks of zero-valent iron nanoparticles (nZVI) for in situ remediation: Risk mitigation or trade-off? *Journal of Contaminant Hydrology* 118 (3-4):165-183.
- Guilbeault, M. A., B. L. Parker, and J. A. Cherry. 2005. Mass and flux distributions from DNAPL zones in sandy aquifers. *Ground Water* 43 (1):70-86.
- Henderson, A. D., and A. H. Demond. 2007. Long-term performance of zero-valent iron permeable reactive barriers: A critical review. *Environmental Engineering Science* 24 (4):401-423.
- ITRC. 2011. Permeable Reactive Barrier: Technology Update. In *Technical/Regulatory Guidance*. Washington, D.C.: Interstate Technology & Regulatory Council.
- Jawitz, James W., Dongping Dai, P. Suresh C. Rao, Michael D. Annable, and R. Dean Rhue. 2003. Rate-Limited Solubilization of Multicomponent Nonaqueous-Phase Liquids by Flushing with Cosolvents and

Surfactants: Modeling Data from Laboratory and Field Experiments. *Environmental Science & Technology* 37 (9):1983-1991.

Jeen, S. W., R. W. Gillham, and A. Przepiora. 2011. Predictions of long-term performance of granular iron permeable reactive barriers: Field-scale evaluation. *Journal of Contaminant Hydrology* 123 (1-2):50-64.

Johnson, K. A., and R. S. Goody. 2011. The Original Michaelis Constant: Translation of the 1913 Michaelis-Menten Paper. *Biochemistry* 50 (39):8264-8269.

Johnson, T. L., M. M. Scherer, and P. G. Tratnyek. 1996. Kinetics of halogenated organic compound degradation by iron metal. *Environmental Science & Technology* 30 (8):2634-2640.

Kenney, T. C., W. A. Vanveen, M. A. Swallow, and M. A. Sungaila. 1992. Hydraulic Conductivity of Compacted Bentonite Sand Mixtures. *Canadian Geotechnical Journal* 29 (3):364-374.

Killenbeck, E., E. Panhorst, F. Lenzo, A. Faulkner, and F. Payne. 2008. Field Implementation of ZVI and Clay Soil Mixing for a Multicomponent NAPL. In *Proceedings of the Seventh International Conference on Remediation of Chlorinated and Recalcitrant Compounds*. Monterrey, California.

Kingston, J. L. T., P. R. Dahlen, and P. C. Johnson. 2010. State-of-the-practice review of in situ thermal technologies. *Ground Water Monitoring and Remediation* 30 (4):64-72.

Klausen, J., P. J. Vikesland, T. Kohn, D. R. Burris, W. P. Ball, and A. L. Roberts. 2003. Longevity of granular iron in groundwater treatment processes: Solution composition effects on reduction of organohalides and nitroaromatic compounds. *Environmental Science & Technology* 37 (6):1208-1218.

Kouznetsova, I., P. Bayer, M. Ebert, and M. Finkel. 2007. Modelling the long-term performance of zero-valent iron using a spatio-temporal approach for iron aging. *Journal of Contaminant Hydrology* 90 (1-2):58-80.

Lampron, K. J., P. C. Chiu, and D. K. Cha. 2001. Reductive dehalogenation of chlorinated ethenes with elemental iron: The role of microorganisms. *Water Research* 35 (13):3077-3084.

Lowry, G. V., and K. M. Johnson. 2004. Congener-specific dechlorination of dissolved PCBs by microscale and nanoscale zerovalent iron in a water/methanol solution. *Environmental Science & Technology* 38 (19):5208-5216.

Mackay, D. M., and J. A. Cherry. 1989. Groundwater contamination: Pump-and-treat remediation. *Environmental Science & Technology* 23 (6):630-636.

Mackay, D. M., R. D. Wilson, M. J. Brown, W. P. Ball, G. Xia, and D. P. Durfee. 2000. A controlled field evaluation of continuous vs. pulsed pump-and-treat remediation of a VOC-contaminated aquifer: site characterization, experimental setup, and overview of results. *Journal of Contaminant Hydrology* 41 (1-2):81-131.

Major, D. W., M. L. McMaster, E. E. Cox, E. A. Edwards, S. M. Dworatzek, E. R. Hendrickson, M. G. Starr, J. A. Payne, and L. W. Buonamici. 2002. Field demonstration of successful bioaugmentation to achieve dechlorination of tetrachloroethene to ethene. *Environmental Science & Technology* 36 (23):5106-5116.

Matheson, L. J., and P. G. Tratnyek. 1994. Reductive Dehalogenation of Chlorinated Methanes by Iron Metal. *Environmental Science & Technology* 28 (12):2045-2053.

McGuire, T. M., J. M. McDade, and C. J. Newell. 2006. Performance of DNAPL source depletion technologies at 59 chlorinated solvent-impacted sites. *Ground Water Monitoring and Remediation* 26 (1):73-84.

Olson, M. R., J. Blotevogel, T. Borch, T.C. Sale, M.A. Petersen, and R.A. Royer. 2013. Long-Term Potential of In Situ Chemical Reduction for Treatment of Polychlorinated Biphenyls in Soils *Chemosphere* in review.

Olson, Mitchell R., Thomas C. Sale, Charles D. Shackelford, Christopher Bozzini, and Jessica Skeean. 2012. Chlorinated Solvent Source-Zone Remediation via ZVI-Clay Soil Mixing: 1-Year Results. *Ground Water Monitoring & Remediation* 32 (3):63-74.

Orth, W. S., and R. W. Gillham. 1996. Dechlorination of trichloroethene in aqueous solution using Fe-O. *Environmental Science & Technology* 30 (1):66-71.

Ovbey, T.W., M.M. Thomson, and C. Bozzini. 2010. In Situ Remediation of Chlorinated Solvent Source Zone using ZVI-Clay Treatment Technology. In *Proceedings of the Seventh International Conference on Remediation of Chlorinated and Recalcitrant Compounds*. Monterey, California.

Palaia, T. 2007. Resurgence of In Situ Soil Mixing for Treating NAPL Source Areas. In *2007 Air Force ESOH Training Symposium*.

Petri, Benjamin G., Richard J. Watts, Aikaterini Tsitonaki, Michelle Crimi, Neil R. Thomson, and Amy L. Teel. 2011. Fundamentals of ISCO Using Persulfate

In Situ Chemical Oxidation for Groundwater Remediation, edited by R. L. Siegrist, M. Crimi and T. J. Simpkin: Springer New York.

Phillips, D. H., T. Van Nooten, L. Bastiaens, M. I. Russell, K. Dickson, S. Plant, J. M. E. Ahad, T. Newton, T. Elliot, and R. M. Kalin. 2010. Ten year performance evaluation of a field-scale zero-valent iron permeable reactive barrier installed to remediate trichloroethene contaminated groundwater. *Environmental Science & Technology* 44 (10):3861-3869.

Puls, R. W., D. W. Blowes, and R. W. Gillham. 1999. Long-term performance monitoring for a permeable reactive barrier at the US Coast Guard Support Center, Elizabeth City, North Carolina. *Journal of Hazardous Materials* 68 (1-2):109-124.

Quinn, J., C. Geiger, C. Clausen, K. Brooks, C. Coon, S. O'Hara, T. Krug, D. Major, W. S. Yoon, A. Gavaskar, and T. Holdsworth. 2005. Field demonstration of DNAPL dehalogenation using emulsified zero-valent iron. *Environmental Science & Technology* 39 (5):1309-1318.

Ritter, K., M. S. Odziemkowski, and R. W. Gillham. 2002. An in situ study of the role of surface films on granular iron in the permeable iron wall technology. *Journal of Contaminant Hydrology* 55 (1-2):87-111.

Rivett, M. O., S. W. Chapman, R. M. Allen-King, S. Feenstra, and J. A. Cherry. 2006. Pump-and-treat remediation of chlorinated solvent contamination at a controlled field-experiment site. *Environmental Science & Technology* 40 (21):6770-6781.

- Ruffing, S., C. Pike, M. Speranza, and N. Flaherty. 2008. Remediation of Chlorinated Hydrocarbons Utilizing Zero-Valent Iron via Soil Mixing. In *Proceedings of the Seventh International Conference on Remediation of Chlorinated and Recalcitrant Compounds*. Monterrey, California.
- Scherer, M. M., B. A. Balko, D. A. Gallagher, and P. G. Tratnyek. 1998. Correlation analysis of rate constants for dechlorination by zero-valent iron. *Environmental Science & Technology* 32 (19):3026-3033.
- Schwarzenbach, R. P., P. M. Gschwend, and D. M. Imboden. 2003. *Environmental Organic Chemistry*. 2nd ed. New York: Wiley.
- Shackelford, C. D. 1990. Transit-Time Design of Earthen Barriers. *Engineering Geology* 29 (1):79-94.
- Shackelford, C. D., and T. C. Sale. 2011. Using the ZVI-clay technology for source zone remediation. *Geo-Strata* 15 (2):36-42.
- Shackelford, C. D., T. C. Sale, and M.R. Liberati. 2005. In-situ remediation of chlorinated solvents using zero valent iron and clay mixtures: A case history. In *Waste Containment and Remediation*, edited by A. Alshawabkeh, C. H. Benson, P. J. Culligan, J. C. Evans, B. A. Gross, D. Narejo, R. Reddy, C. D. Shackelford and J. G. Zornberg. Geotechnical Special Publication 142 (CD ROM), Reston, VA: ASCE.
- Siegrist, R. L., O. R. West, M. I. Morris, D. A. Pickering, D. W. Greene, C. A. Muhr, D. D. Davenport, and J. S. Gierke. 1995. In-situ mixed region vapor stripping in low-permeability media. 2. Full-scale field experiments. *Environmental Science & Technology* 29 (9):2198-2207.
- Siegrist, R.L., M. Crimi, T.J. Simpkin, and R.C. Borden. 2011. *In situ chemical oxidation for groundwater remediation*. Edited by R. L. Siegrist, M. Crimi, T. J. Simpkin and R. C. Borden, *Springer eBook collection*. New York: Springer.
- Song, H., and E. R. Carraway. 2006. Reduction of chlorinated methanes by nano-sized zero-valent iron. Kinetics, pathways, and effect of reaction conditions. *Environmental Engineering Science* 23 (2):272-284.
- Stroo, H. F., A. Leeson, J. A. Marqusee, P. C. Johnson, C. H. Ward, M. C. Kavanaugh, T. C. Sale, C. J. Newell, K. D. Pennell, C. A. Lebron, and M. Unger. 2012. Chlorinated Ethene Source Remediation: Lessons Learned. *Environmental Science & Technology* 46 (12):6438-6447.
- Taghavy, A., J. Costanza, K. D. Pennell, and L. M. Abriola. 2010. Effectiveness of nanoscale zero-valent iron for treatment of a PCE-DNAPL source zone. *Journal of Contaminant Hydrology* 118 (3-4):128-142.
- Tratnyek, P. G., M. M. Scherer, B. L. Deng, and S. D. Hu. 2001. Effects of natural organic matter, anthropogenic surfactants, and model quinones on the reduction of contaminants by zero-valent iron. *Water Research* 35 (18):4435-4443.
- Wadley, S. L. S., R. W. Gillham, and L. Gui. 2005. Remediation of DNAPL source zones with granular iron: Laboratory and field tests. *Ground Water* 43 (1):9-18.
- Wust, W. F., R. Kober, O. Schlicker, and A. Dahmke. 1999. Combined zero- and first-order kinetic model of the degradation of TCE and cis-DCE with commercial iron. *Environmental Science & Technology* 33 (23):4304-4309.

Yeo, S. S., C. D. Shackelford, and J. C. Evans. 2005. Membrane behavior of model soil-bentonite backfills. *Journal of Geotechnical and Geoenvironmental Engineering* 131 (4):418-429.

## CHAPTER 2

### CHLORINATED SOLVENT SOURCE-ZONE REMEDIATION VIA ZVI-CLAY

#### SOIL MIXING: ONE-YEAR RESULTS

##### *Synopsis of Chapter*

ZVI-Clay is an emerging remediation approach that combines zero-valent iron (ZVI)-mediated degradation and *in situ* stabilization of chlorinated solvents. Through use of *in situ* soil mixing to deliver reagents, reagent-contaminant contact issues associated with natural subsurface heterogeneity are overcome. This paper describes implementation, treatment performance, and reaction kinetics during the first year after application of the ZVI-Clay remediation approach at Marine Corps Base Camp Lejeune, NC. Primary contaminants included trichloroethylene, 1,1,2,2-tetrachloroethane, and related natural degradation products. For the field application, 22,900 m<sup>3</sup> of soils were treated to an average depth of 7.6 m with 2% ZVI and 3% sodium bentonite (dry weight basis). Performance monitoring included analysis of soil and water samples. After one year, total concentrations of chlorinated volatile organic compounds (CVOCs) in soil samples were decreased by site-wide average and median values of 97% and >99%, respectively. Total CVOC concentrations in groundwater were reduced by average and median values of 81% and >99%, respectively. In several of the soil and groundwater monitoring locations, reductions in total CVOC concentrations of greater than 99.9% were apparent. Further reduction in concentrations of chlorinated solvents is expected with time. Pre- and post-mixing average hydraulic conductivity values were  $1.7 \times 10^{-5}$  and  $5.2 \times 10^{-8} \text{ m}\cdot\text{s}^{-1}$ , respectively, indicating a reduction of about 2.5 orders of magnitude. By achieving simultaneous contaminant mass depletion and hydraulic conductivity reduction, contaminant flux reductions of several orders of magnitude are predicted.

## 2.1 Introduction

Despite substantial attention, chlorinated solvents in the subsurface continue to present an immense remediation challenge (USEPA 2003; NRC 2005). With experience, the remediation community has come to realize that much of the difficulty lies in the heterogeneous nature of subsurface soils, including irregular distributions of hydraulic conductivity and contaminant mass (Mackay and Cherry 1989; Chapman and Parker 2005; Guilbeault et al. 2005; Sale et al. 2008). This challenge is exacerbated by the fact that chlorinated solvents can occur as non-aqueous, aqueous, sorbed, and vapor phases in transmissive and low-permeability zones (Pankow and Cherry 1996). Due to mass transfer constraints in heterogeneous media, remedies involving flushing (e.g., pump-and-treat, soil vapor extraction, or surfactant-cosolvent flushing) frequently require extended periods of operation (Mackay and Cherry 1989). Similarly, injection-based technologies (e.g., injection of chemical oxidants or reductants) can be limited in their ability to achieve reagent-contaminant contact due to preferential flow paths and irregular contaminant distributions (Siegrist et al. 1999; McGuire et al. 2006).

*In situ* soil mixing provides a means to overcome the challenge of subsurface heterogeneity. Soil stabilization via *in situ* soil mixing has been a common practice in geotechnical engineering since the 1960s (Jasperse and Ryan 1987). The primary purpose of this practice has been either to improve the mechanical properties (e.g., compressibility or strength) of foundation soils at sites where such properties are intrinsically unsuitable or to provide for subsurface hydraulic control. In terms of remediation, *in situ* stabilization has been used to immobilize contaminants via the addition of pozzolanic materials, such as cement, lime, and fly or bottom ashes (Day and Ryan 1995). More recently, *in situ* soil mixing techniques have been further refined to remove contaminant mass via delivery of reactive media (Day et al. 1999) or by stripping using air or steam (Siegrist et al. 1995).

For treatment of chlorinated solvents, the use of zero-valent iron (ZVI) to drive degradation of certain chlorinated solvents is well established (Gillham and O'Hannesin 1994; Johnson et al. 1996;

Roberts et al. 1996). For example, granulated ZVI has been used as a reactive medium in a permeable reactive barrier (PRB) (Day and Ryan 1995; Puls et al. 1999; Phillips et al. 2010). ZVI also has been evaluated for source-zone treatment via injection of nano-scale ZVI (Zhang 2003) or emulsified ZVI (Quinn et al. 2005). However, injection techniques may be limited in their ability to achieve reagent-contaminant contact in heterogeneous subsurface settings (USEPA 2003; McGuire et al. 2006).

An emerging remediation approach, herein referred to as the ZVI-Clay technology, combines stabilization techniques with ZVI-mediated degradation of chlorinated solvents (e.g., Shackelford and Sale 2011). Using this approach, soil mixing overcomes reagent delivery issues associated with natural subsurface heterogeneity. Reagents (e.g., ZVI) are distributed throughout the mixed soil body and brought into close contact with the contaminant mass in the mixed region, including dense non-aqueous phase liquids (DNAPLs). Assuming homogeneous delivery of 0.5 to 3% (on a dry soil weight basis) of a fine-grained ZVI particle (e.g., 50 to 100 mesh), the spacing between ZVI particles in treated soils may be on the order of 1 mm (Olson 2005). ZVI is delivered into the subsurface via a clay (e.g., sodium bentonite) and water-based grout. Sodium bentonite thickens the grout, preventing settlement of ZVI granules. The grout also functions as a drilling fluid, which reduces the energy required to overcome friction during mixing. Furthermore, soil mixing with sodium bentonite can stabilize contaminants by reducing the hydraulic conductivity of the contaminated soil (Castelbaum and Shackelford 2009). The combined benefits of degradation and stabilization can greatly reduce contaminant mass flux, as has been demonstrated in the context of grout walls (Rabideau et al. 1999) and containment liners (Shimotori et al. 2004).

The use of soil mixing to apply ZVI-Clay directly to a DNAPL source zone has been demonstrated in the laboratory (Olson 2005), in a field demonstration at Canadian Forces Base Borden (Wadley et al. 2005), and in full-scale field applications (Shackelford et al. 2005). The purpose of this paper is to describe implementation and treatment performance during the first year after application of ZVI-Clay to a chlorinated solvent DNAPL source zone at Site 89, Marine Corps Base Camp Lejeune, NC

(Camp Lejeune). Performance monitoring criteria within the treated soil zone consisted of soil and water sample collection for one year after mixing. One-year performance data have been supplemented by recent data, as necessary, to complete relevant analyses.

## 2.2 Methods and Materials

### 2.2.1 Site Description

Camp Lejeune covers approximately 61,100 ha (236 sq. miles) and is located approximately 24 km (15 mi) inland from the Atlantic Ocean. Prior to remediation, most of the zone targeted for treatment was covered with asphalt or grass. Surrounding terrain includes buildings to the north and east and forests to the south and west. A creek runs adjacent to Site 89, approximately 20 m south/southwest of the targeted treatment zone. Site geology consists of interbedded sands and silts. The typical depth to groundwater across the site is 2 m.

Historical activities at Site 89, which include use as a Defense Reutilization Marketing Office (DRMO), have resulted in subsurface soils and groundwater impacted by chlorinated solvents including trichloroethylene (TCE) and 1,1,2,2-tetrachloroethane (TeCA). In addition, natural processes have led to formation of degradation products including *cis*-1,2-dichloroethylene (*c*DCE), *trans*-1,2-dichloroethylene (*t*DCE), and vinyl chloride (VC). Measured soil and groundwater concentrations indicated that DNAPL likely was present at the site prior to remediation activities. The total mass of chlorinated solvents within the target treatment zone was estimated to be 28,000 kg (AGVIQ-CH2M HILL 2010). Contamination is present to a depth of 8.5 m below ground surface (bgs).

A pilot-scale demonstration of electrical resistive heating (ERH) was conducted at Site 89 in 2001 to 2002. The demonstration involved heating of soils to a target level of 60 °C and subsequent collection of vapors generated. The zone targeted for ZVI-Clay soil mixing overlapped slightly with the ERH demonstration area (Figure 2-1).

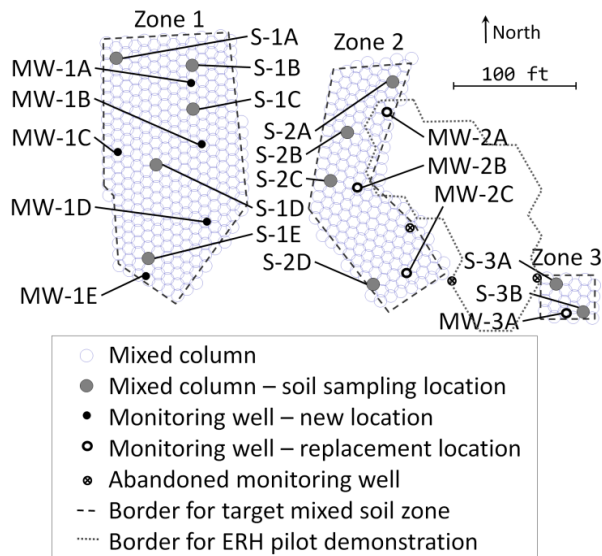


**Figure 2-1. Mixed column layout with sampling locations.**

### 2.2.2 Materials

Target reagent delivery amounts of 2% ZVI and 3% sodium bentonite on a dry soil weight basis were selected based on results of a laboratory study (not published). The field application required 840,000 kg of ZVI and 1,300,000 kg of sodium bentonite to achieve target levels. In addition, 5,200,000 L of water, obtained from the Camp Lejeune water distribution system, were used for grout preparation. ZVI was supplied by Peerless Metal Powders and Abrasive (Peerless), Detroit, MI (ZVI Cast Iron Aggregate Size 50/200 [mesh]) and GMA Industries (GMA), Romulus, MI (product LT-120, which is nominally of 120 mesh-size). Two sources were required to provide the total amount of ZVI needed for the project. Although the mixing contractor noted the sources of iron used each day, the specific iron product used in each mixed column was not recorded. Sodium bentonite (< 20-mesh particle size) was supplied by Texas Sodium Bentonite, Comanche, TX.

### 2.2.3 Site Preparation

To accommodate soil heave, which is typically 15% in mixed soils (Day and Ryan 1995), approximately 1 m of soil was removed from the surface prior to mixing, and berms were constructed around target treatment zones. In addition, monitoring wells within the mixed zone were abandoned prior to treatment.

### 2.2.4 Soil Mixing

Soil mixing was conducted over 80 days and was completed in August 2008. A total of 515 columns were mixed in three separate treatment zones (Figure 2-1). Mixed columns were 3.0 m in diameter and were overlapped so that treatment was applied to the entire treatment zone. The required overlap to achieve mixing of the entire zone was approximately 18%. An average of four downward and upward mixing passes were completed at each column. Dimensions of the treated zone include a surface footprint of 3,010 m<sup>2</sup>, an average depth of 7.6 m, and a total treatment volume of 22,900 m<sup>3</sup>.

Soil mixing equipment (Figure 2-2) included a Manitowoc 4000 W (Manitowoc, WI) crane, rotary table (Calweld, Inc., McKinney, TX), and mixing auger. The rotary table was capable of producing 600,000 N-m torque. The mixing auger, which was provided by the site contractor, Geo-Con (Monroeville, PA), consisted of three blades mounted to a hollow shaft and was 3.0 m in diameter.

A grout comprising ZVI, bentonite, and water was prepared in a 3.8-m<sup>3</sup>, high-speed, high-shear colloid mixer (also provided by Geo-Con). The grout was pumped through the hollow stem of the Kelly bar and delivered into subsurface soils via ports in the soil mixing tool.



**Figure 2-2. Soil mixing equipment (left) used for ZVI-Clay soil mixing at Camp Lejeune, Site 89, included a crane, crane-mounted rotary table, and hollow kelly bar. Mixing was completed using 3.0-m diameters augers (right).**

Due to the potential for volatilization of chlorinated solvents during mixing, a vapor-collection hood was utilized. The hood consisted of a 4-m-diameter cylinder that was maintained at 7 to 21 kPa of negative pressure using a vacuum blower. Discharge from the hood was drawn through a series of two 680-kg granular activated carbon units. The amount of chlorinated solvents captured by the carbon was not quantified.

To ensure adequate mixing, quality-control soil samples were collected. Samples were collected from depths of 3 and 6 m bgs and were tested for ZVI and gravimetric water content. ZVI content was measured using magnetic separation techniques, in accordance with the following procedure: (1) each sample was washed to remove dust and fine particles, (2) a magnet, approximately 10-cm in diameter, was used to separate magnetically-susceptible materials from the wet mixture, (3) the collected materials were dried on a hot plate (temperature not specified) and the magnet was once again used to separate magnetically-susceptible materials from the remaining native material, and (4) the magnetically-separated materials were visually inspected to ensure that they consisted primarily of the emplaced ZVI. The iron

content was calculated as ratio of the dry weight of magnetically-separated materials separated to that of the entire soil sample.

### 2.2.5 Sampling Methods

Performance monitoring consisted of soil and groundwater sampling from within the mixed soil body. Eleven of the mixed soil columns were selected for soil sampling (Figure 2-1). Soil samples were collected over time from depths of 3 and 6 m bgs. Baseline (time 0) soil concentrations were determined via grab samples collected immediately after mixing. Subsequent sampling was conducted 1, 3, 6, 9, and 12 months after all mixing at the site was complete (i.e., after August 2008). A Geoprobe<sup>®</sup> (Geoprobe Systems, Salina, KS) was used to collect soil cores from 3 and 6 m bgs in 5.1-cm I.D. acetate sleeves. Subsamples from the cores were placed in laboratory-prepared 125-mL soil jars, which were stored on ice and shipped overnight to CompuChem (Cary, NC). Soil samples were analyzed for volatile organic compounds (VOCs) following EPA method 8260B.

In April 2008, pre-treatment groundwater samples were collected from seven wells within the target treatment zone. These wells were subsequently abandoned prior to mixing. Groundwater samples were collected using low-flow purge methods (0.23 to 0.45 L·min<sup>-1</sup>). In September 2008, after all mixing at the site was complete, seven new groundwater monitoring wells were installed throughout the treated zone (Figure 2-1). Four of these wells were installed in the vicinity of abandoned wells. The new wells were constructed of 5.1-cm I.D. schedule 40 PVC with 0.25-mm slots in the interval of 5.5 to 7.0 m bgs. Post-treatment groundwater samples were collected from all source-area monitoring wells 1, 3, 6, 9, and 12 months after all mixing at the site was complete. Approximately 39 months after mixing was completed, an additional groundwater sample was collected from monitoring well MW-2A. Despite the use of low-flow purge methods, all of the monitoring wells were purged dry during the 1-month sampling event, and the wells were sampled subsequently upon recovery. For subsequent sample events, a Hydrasleeve<sup>™</sup> sampler (GeoInsight, Las Cruces, NM) was used (Parker and Clark 2004). Hydrasleeve<sup>™</sup>

samplers were deployed for a minimum of two weeks before sample collection. Groundwater samples were transferred to laboratory-prepared 40-mL Volatile Organic Analysis (VOA) vials (HCl preserved), placed on ice, and shipped to an analytical laboratory via overnight delivery. All groundwater samples were analyzed by CompuChem with the exception of the December 2011 sample from MW-2A, which was analyzed by ENCO Laboratories, Inc. (Orlando, FL). Groundwater samples were analyzed for volatile organic compounds (VOCs) and chloride following EPA methods 8260B and 325.1/325.3, respectively. In addition, field parameters including pH and ORP were measured using a Horiba U-22 water quality meter (Horiba Instruments Inc., Ann Arbor, MI).

#### 2.2.6 Hydraulic Conductivity

Hydraulic conductivity,  $K$ , values were measured before and after mixing via slug tests conducted in source-area wells. Pre-mixing slug tests for measurement of  $K$  were conducted in the seven source-area wells in April 2008. Post-mixing slug tests were conducted in the replacement source-area wells in February 2009, six months after mixing was complete. Well locations are shown in Figure 2-1.

#### 2.2.7 Reaction Network Modeling

The parent compounds at the site included TeCA and TCE. Primary degradation products present before remediation activities included *c*DCE, *t*DCE, and VC. These degradation products also may be formed during ZVI-mediated degradation of the parent compounds. Due to the potential for formation and subsequent degradation of contaminants of concern (COCs), the reaction system was modeled as a network of first-order reactions, as follows:

$$[TCE]' = -k_{TCE}[TCE]$$

$$[cDCE]' = k_{TCE/cDCE}[TCE] - k_{cDCE}[cDCE]$$

$$[tDCE]' = k_{TCE/tDCE}[TCE] - k_{tDCE}[tDCE]$$

$$[VC]' = k_{cDCE/VC}[cDCE] + k_{tDCE/VC}[tDCE] - k_{VC}[VC]$$

where  $k_{TCE}$ ,  $k_{cDCE}$ ,  $k_{tDCE}$ , and  $k_{VC}$  ( $d^{-1}$ ) are the non-path-specific first-order degradation rate coefficients, and concentrations ( $\mu M$ ) of TCE,  $cDCE$ ,  $tDCE$ , and VC are indicated by brackets. For pathway-specific rate coefficients, the parent compound and product are indicated in the subscript. The parent compound TeCA was excluded from the reaction network, as TeCA had been reduced to levels below detection limits by the time of the second post-treatment sampling event. The reaction network was modeled using Scientist<sup>®</sup> for Windows 3.0 software (Micromath Scientific Software, St. Louis, MO). Reaction rate coefficients were estimated by regression of the model against Site 89 performance monitoring data.

## 2.3 Results and Discussion

### 2.3.1 Evaluation of Homogeneity

The degree of homogeneity achieved during mixing pertains to both (a) soils and contaminants that were present before mixing and (b) reagents delivered during mixing. Evaluating the extent of contaminant and soil homogenization would require depth-discreet sampling on a fine scale, which was not conducted as part of this study. Reagent delivery was evaluated during mixing, as part of the project quality-control protocol, via measurement of ZVI content from grab samples collected from mixed columns at depths of 3 and 6 m bgs. Measured ZVI contents at 3 and 6 m bgs were statistically similar (T-test p-value = 0.6). The average ZVI content, on the basis of 98 samples collected from 49 columns, was  $2.86 \pm 0.09\%$ , where  $\pm$  indicates 95% confidence intervals. None of the samples contained less than 2.0% ZVI. Potential reasons for the actual emplaced iron being higher than the target amounts include (a)

mixing specifications and (b) under-estimation of post mixing bulk (dry) density. The mixing specifications required that all samples be greater than the target level of 2% ZVI. Second, the act of mixing soils with bentonite can result in an increased void ratio (Castelbaum and Shackelford 2009) and therefore a decreased bulk density. Both of these factors could place an upward bias on post-mixing ZVI content.

### 2.3.2 Hydraulic Conductivity

Average pre- and post-mixing  $K$  values were  $1.7 \pm 2.7 \times 10^{-5}$  and  $5.2 \pm 4.7 \times 10^{-8}$   $\text{m}\cdot\text{s}^{-1}$ , respectively. On average, the  $K$  was reduced by about 2.5 orders of magnitude.

### 2.3.3 Soil Sampling Data

In the following analysis, total chlorinated volatile organic compounds (CVOCs) refers to the sum of molar concentrations of TeCA, TCE, *c*DCE, *t*DCE, and VC. Concentration reductions are calculated as  $(C_0 - C_t)/C_0$ , where  $C_0$  is the initial concentration at each location ( $\text{mg}\cdot\text{L}^{-1}$  or  $\text{mg}\cdot\text{kg}^{-1}$ ) and  $C_t$  is the concentration at time  $t$ . Where final concentrations were below detection limits, a minimum level of reduction is estimated based on detection limit values. In comparing the initial (i.e., time 0) to the one-year post-treatment data, total CVOCs in soil samples (by location) were reduced by 69% to >99%. The site-wide average and median reductions of total CVOCs in soil samples were 97% and >99%, respectively. In five of the eleven mixed columns selected for soil sampling, apparent reductions in total CVOC concentrations were 99.9% or greater.

Soil concentration data for the parent compounds, TeCA and TCE, are shown in Figure 2-3. In soil samples, TeCA and TCE were generally below detection limits within 4 months after soil mixing was complete, although low levels (i.e.,  $\leq 0.014$   $\text{mg}\cdot\text{kg}^{-1}$ ) were detected periodically. The site-wide average reductions of TeCA and TCE were both greater than 99%, with detection limits used as conservative (high) estimates of final concentrations for samples reported as non-detect. Degradation products

including *c*DCE and VC were present prior to remediation activities, presumably due to natural degradation of parent compounds, and may have been formed via ZVI-mediated degradation of TeCA and TCE. Soil concentration data for the degradation products are shown in Figure 2-4. The site-wide average reductions of *c*DCE and VC were both approximately 90%. In soil sampling data, *t*DCE was generally below detection limits or, if detected, constituted a small fraction of total CVOCs (i.e.,  $\leq 5\%$  in all but three samples and less than 23% in all samples). No other degradation products were detected in significant quantities.

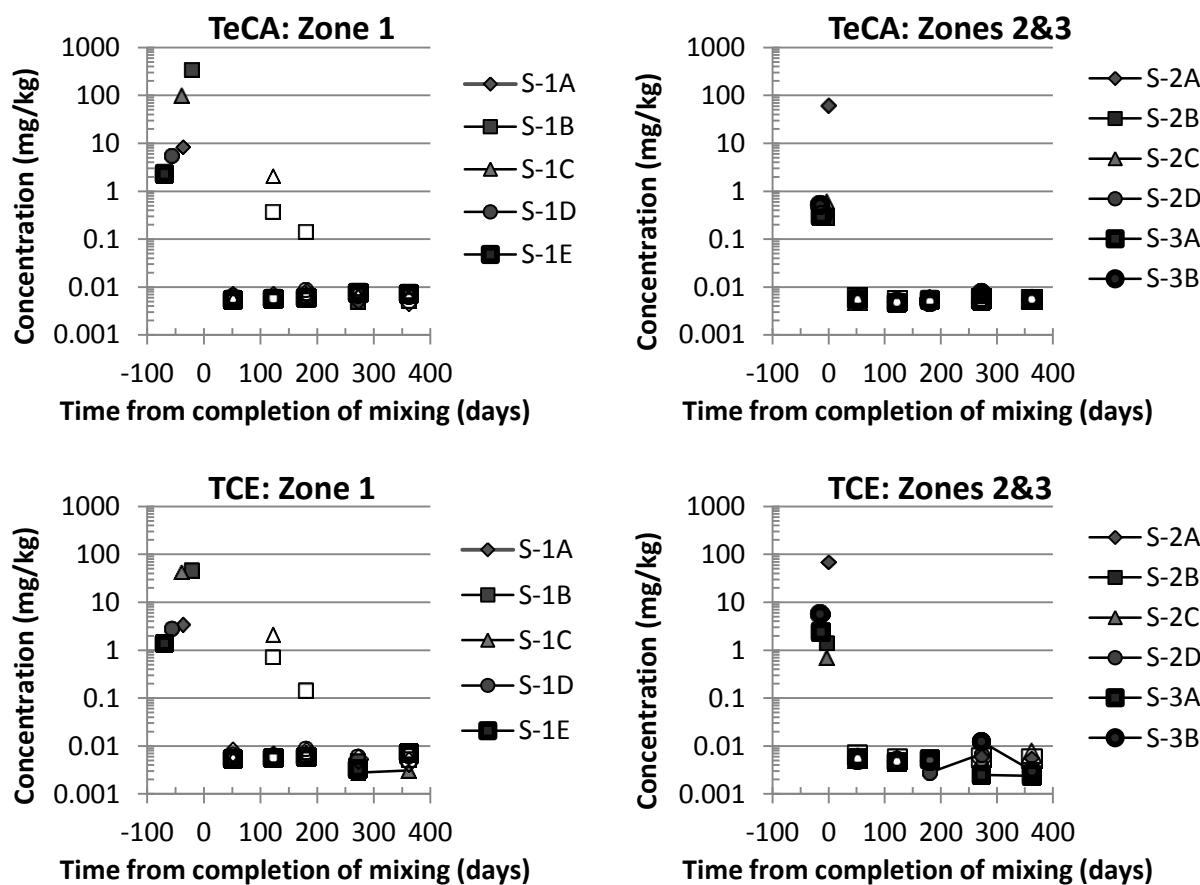


Figure 2-3. Depth-averaged soil concentrations of parent compounds TeCA (upper) and TCE (lower) versus time since completion of mixing in zone 1 (left) and zones 2 and 3 (right). Solid data symbols connected with lines indicate reported concentrations; open data symbols indicate detection limits for samples in which the target compound was not detected. Data corresponding to negative times represent results of samples collected immediately after mixing was complete at that location, with time 0 indicating completion of all mixing at the site.

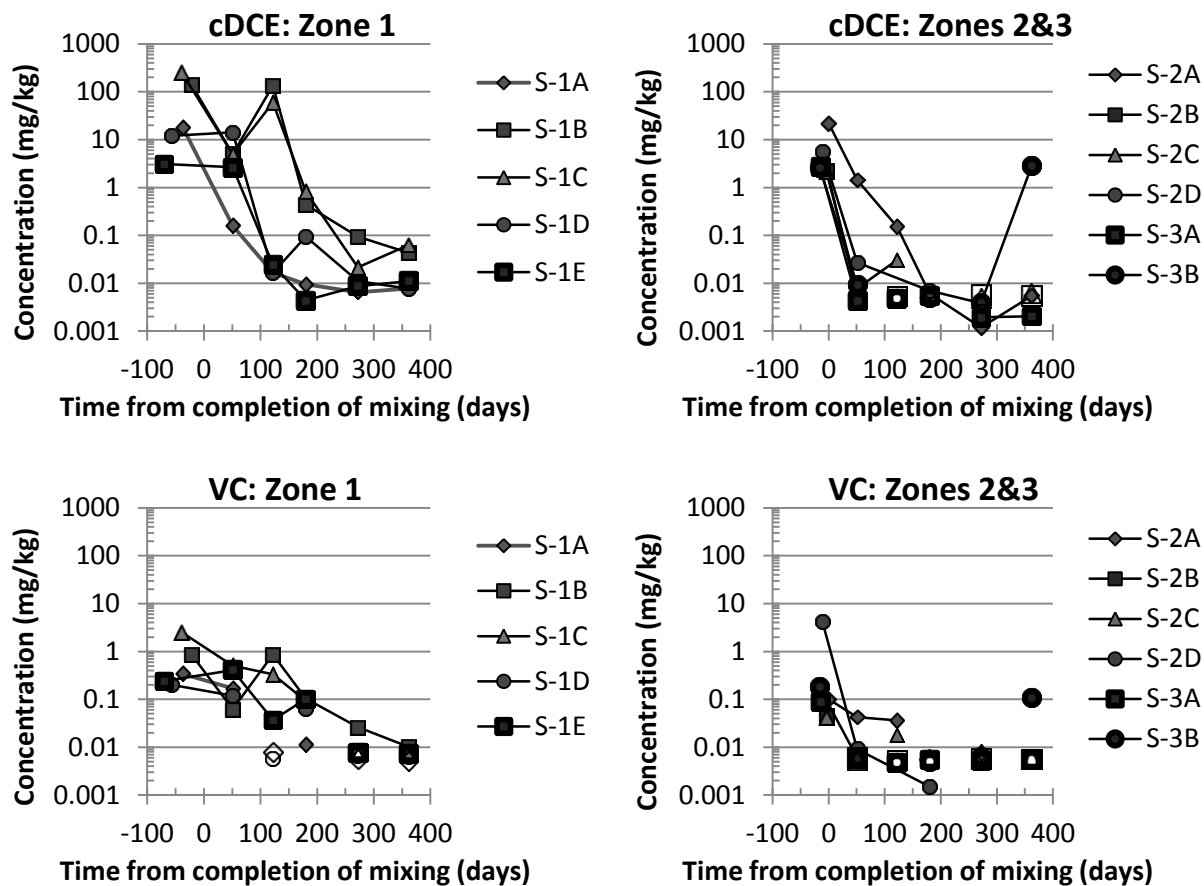


Figure 2-4. Depth-averaged soil concentrations of degradation products *c*DCE (upper) and VC (lower) versus time since completion of mixing in zone 1 (left) and zones 2 and 3 (right). Solid data symbols connected with lines indicate reported concentrations; open data symbols indicate detection limits for samples in which the target compound was not detected. Data corresponding to negative times represent results of samples collected immediately after mixing was complete at that location, with time 0 indicating completion of all mixing at the site.

Although general trends indicate declining soil concentrations in all of the columns selected for soil sampling, some fluctuations are apparent. The apparent deviations from the overall trend of declining concentrations likely result from residual heterogeneity present after mixing. For example, a concentration spike (primarily *c*DCE) is observed at sampling location S-3B in the 363-day sample event (Figure 2-4). Elevated *c*DCE levels in this particular sample indicate that degradation of the parent compounds has occurred and may reflect the sample containing a small clod (possibly on the order of 1-cm) of soil that was not broken up during mixing. However, contaminants that remain in such pockets

after mixing are still susceptible to degradation via diffusion into the surrounding media and subsequent exposure to the widely distributed ZVI particles.

#### 2.3.4 Groundwater Sampling Data

In comparing pre-mixing to one-year post-treatment data (by location), aqueous-phase concentrations of total CVOCs were reduced by 23% to >99%. The site-wide average and median reductions of total CVOCs in groundwater were 81% and >99%, respectively. In three of the four locations where pre- and post-mixing groundwater data were available, apparent reductions of total CVOCs were 99.9% or greater.

Groundwater concentrations for the parent compounds, TeCA and TCE, are shown in Figure 2-5. TeCA and TCE were reduced to concentrations near or below detection limits in all source-area monitoring wells within 4 and 12 months, respectively, after soil mixing was complete. The site-wide average reductions of TeCA and TCE were both greater than 99%, with detection limits used as conservative (high) estimates of final concentrations for samples reported as non-detect. Degradation products including *c*DCE, *t*DCE, and VC were present prior to remediation activities, presumably due to natural degradation of parent compounds, and also may have been formed after treatment via ZVI-mediated degradation of TeCA and TCE. Groundwater data for degradation products are shown in Figure 2-6. Due to nearly complete removal of parent compounds within the first four months after treatment, concentrations of degradation products followed declining trends in all but one monitoring well (MW-2A). In the 12 months after treatment, the site-wide average reductions for *c*DCE and *t*DCE, were 82% and 99%, respectively. The site-wide average VC concentration, considering all monitoring wells, increased by approximately 400% in the year after treatment, with the increase due entirely to MW-2A. Excluding MW-2A, the site-wide average VC concentration decreased by >99%. In a supplemental sampling event conducted approximately three years after treatment, the VC concentration in MW-2A had been reduced by >99%. Compared to the peak concentration (216 days), the apparent VC reduction

was >99.9%. Results of final sampling in MW-2A provide evidence that the degradation reaction continued well after the first year. Additional discussion on MW-2A, including kinetics analysis, is presented in subsequent sections.

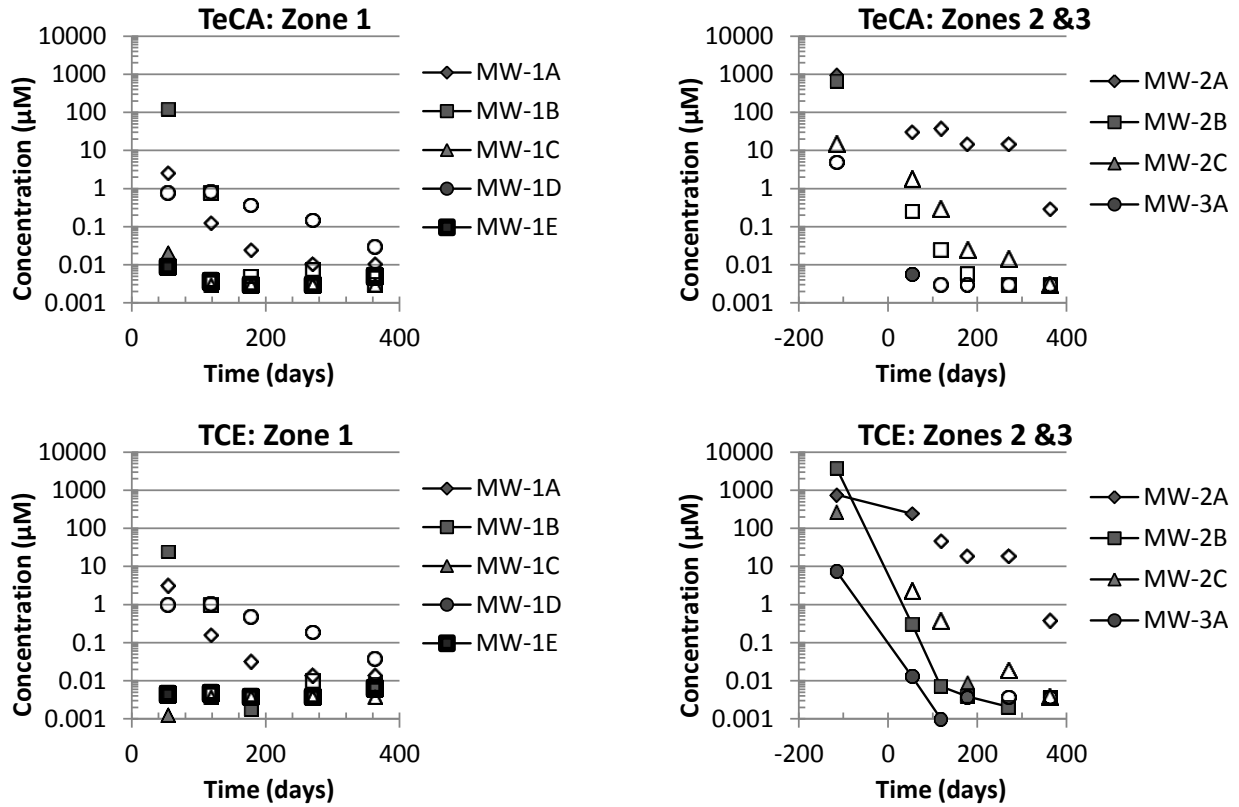


Figure 2-5. Molar groundwater concentrations of parent compounds TeCA (upper) and TCE (lower) in versus time in zone 1 (left) and zones 2 and 3 (right). Solid data symbols with lines indicate reported concentrations; open data symbols indicate detection limits for samples in which the target compound was analyzed for but not detected. Data in zones 2 and 3 corresponding to -115 days represent results of samples collected from monitoring wells in similar locations that were abandoned prior to soil mixing. Time 0 indicates the completion of all mixing at the site.

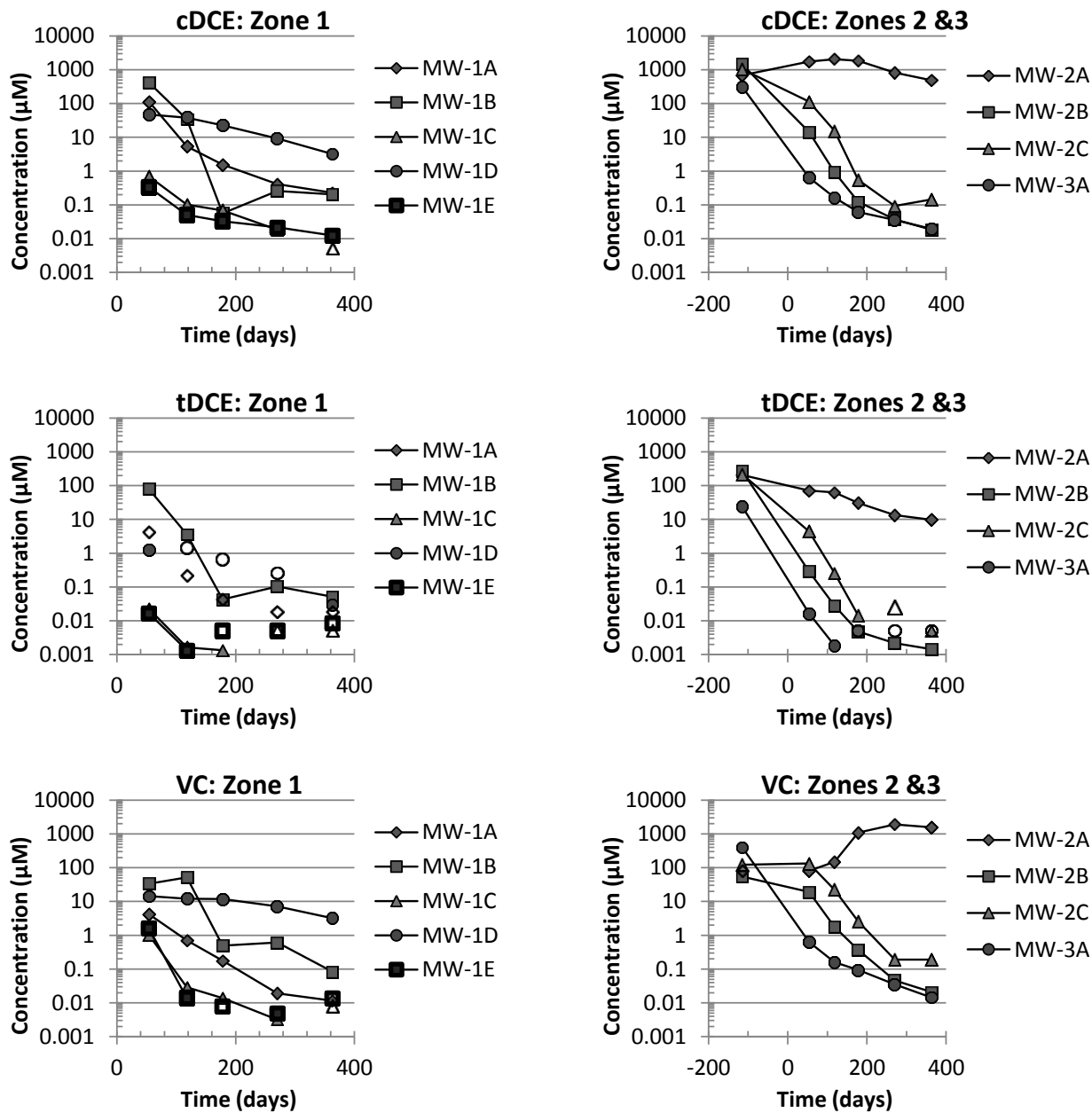


Figure 2-6. Molar groundwater concentrations of degradation products cDCE (upper), tDCE (middle), and VC (lower) versus time in zone 1 (left column) and zones 2 and 3 (right column). Solid data symbols with lines indicate reported concentrations; open data symbols indicate detection limits for samples in which the target compound was analyzed but not detected. Data corresponding to -115 days represent results of samples collected from monitoring wells in similar locations that were abandoned prior to soil mixing. Time 0 indicates the completion of all mixing at the site.

In addition to CVOC data, inorganic parameters measured in groundwater wells included free chloride ( $\text{Cl}^-$ ), pH, and ORP. Chloride data from each monitoring well are presented in Figure 2-7. Background chloride levels in most monitoring wells were 2 to 3 orders of magnitude higher than total CVOC concentrations. As such, changes in chloride concentrations were limited in most locations, with MW-2A as a primary exception. Values of pH in the treated-zone monitoring wells increased from a site-wide average of  $6.3 \pm 0.2$  prior to remediation (calculated from seven locations and one elapsed time) to an average of  $8.4 \pm 0.5$  in the year after treatment (calculated from seven locations and five elapsed times). Values of ORP in the treated-zone monitoring wells decreased from a site-wide average of  $-48 \pm 25$  mV (vs. Ag/AgCl) prior to remediation to an average of  $-282 \pm 50$  mV in the year after treatment.

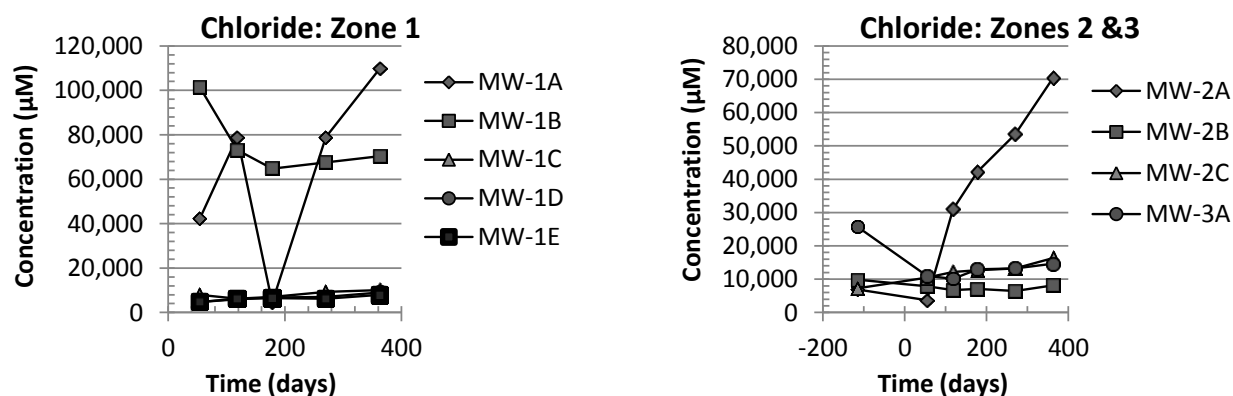


Figure 2-7. Molar groundwater concentration of chloride versus time in zone 1 (left) and zones 2 and 3 (right). Data in zones 2 and 3 corresponding to -115 days represent results of samples collected from monitoring wells in similar locations that were abandoned prior to soil mixing.

### 2.3.5 Degradation Kinetics

Performance data from Site 89 was evaluated to provide insights into reaction kinetics and pathways. Modeling was applied only to post-mixing groundwater data. Although soil data provide an indicator of reduction in total concentrations versus time, the data suffer from the limitation of not being able to collect soil samples from exactly the same location at different times. Of the groundwater data,

only post-mixing data were used for kinetic modeling. The reasons for excluding pre-mixing data from kinetic modeling were as follows: (a) pre-mixing data come from different wells, which were abandoned prior to mixing, and (b) the architecture of surrounding soil and contaminant distribution has been disrupted during mixing, such that groundwater samples collected from pre- and post-mixing wells are representative of different systems. Finally, as noted previously, supplemental sampling was conducted in MW-2A approximately 39 months after completion of soil mixing to resolve long-term treatment trends. The data used for the following analysis include results of this 39-month sampling event from MW-2A.

For statistically valid kinetic modeling, only compounds and locations with at least three data points of known concentration (i.e., above detection limits) were included. TeCA and TCE depletion occurred sufficiently fast, relative to the frequency of sample collection, such that there were not enough reported concentrations to calculate degradation rate coefficients. However, at least three concentration data points existed for *c*DCE, *t*DCE, and VC in most monitoring wells. Degradation rate coefficients for *c*DCE, *t*DCE, and VC are shown by location in Figure 2-8. For *c*DCE, a sufficient number of data points existed to conduct kinetic modeling for all seven monitoring wells. The *c*DCE degradation rate coefficients ranged from 0.0067 to 0.047 d<sup>-1</sup> and averaged 0.028±0.011 d<sup>-1</sup>. *c*DCE rate coefficients for monitoring wells MW-1D and MW-2A were statistically lower than those calculated for the remaining locations. For *t*DCE, kinetic modeling was conducted for five of the seven monitoring wells. The *t*DCE degradation rate coefficients ranged from 0.012 to 0.048 d<sup>-1</sup> and averaged 0.036±0.018 d<sup>-1</sup>. Values were statistically similar at all locations, although 95% confidence intervals for *t*DCE rate coefficients at each location were relatively large. For VC, kinetic modeling was conducted for six of the seven monitoring wells. The VC degradation rate coefficients ranged from 0.0036 to 0.055 d<sup>-1</sup> and averaged 0.029±0.016 d<sup>-1</sup>. VC degradation rate coefficients generally were more variable than those calculated for *c*DCE and *t*DCE.

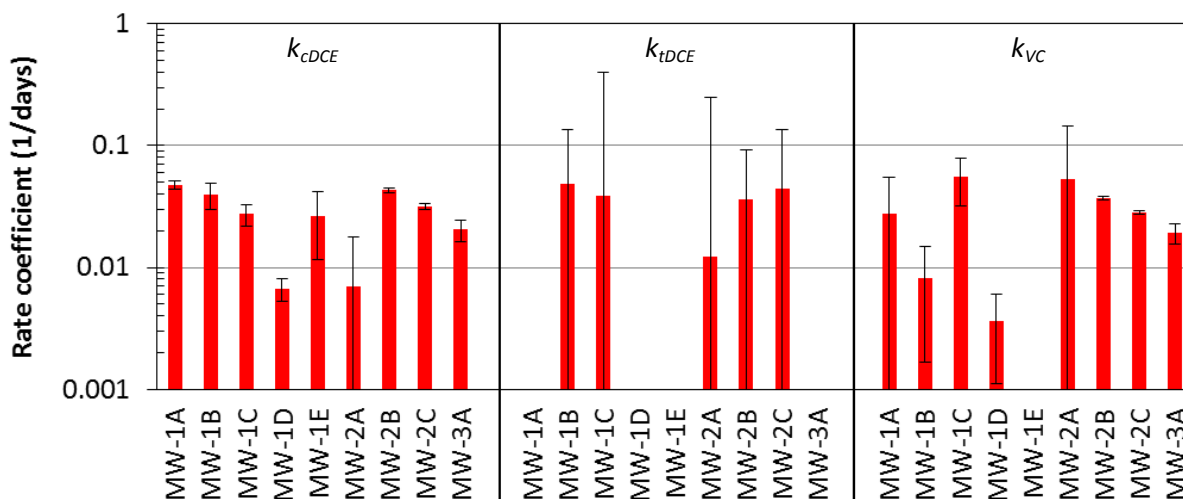


Figure 2-8. Calculated first-order degradation rate coefficients by monitoring well (MW) for *c*DCE, *t*DCE, and VC. Error bars represent 95% confidence intervals (calculated by Scientist® for Windows).

The degradation rate coefficients for *c*DCE, *t*DCE, and VC were of similar magnitude, in general, although some variability was apparent. The hypothesized reasons for variability between monitoring wells include spatial heterogeneity in geochemical conditions and initial total-CVOC concentrations. Geochemical conditions may play a role in affecting iron surface reactivity or availability of CVOCs for reaction. The initial CVOC concentration may impact overall degradation rates, especially at high concentrations, due to saturation of reactive iron-surface sites (Arnold and Roberts 2000a; Grant and Kueper 2004; Bi et al. 2010).

### 2.3.6 Pathways and Products

Reductive degradation of TeCA (Arnold et al. 2002) may lead to formation of TCE (via dehydrochlorination), *c*DCE or *t*DCE (via  $\beta$ -elimination), or 1,1,2-trichloroethane (TCA; via hydrogenolysis). In general, TCA either was not detected or was present in low quantities. If formed, TCA is likely to be subsequently degraded via reaction with ZVI (Scherer et al. 1998). The other potential TeCA degradation products, TCE, *c*DCE, and *t*DCE, were present prior to remediation

activities. Due to the apparently rapid depletion of TeCA relative to the frequency of sampling events, insufficient data exist for a rigorous analysis of TeCA degradation pathways.

Degradation of TCE may lead to formation of *c*DCE or *t*DCE (via hydrogenolysis), or chloroacetylene (via  $\beta$ -elimination). *c*DCE and *t*DCE were both present at Site 89 prior to soil mixing activities and, once formed, are expected to degrade via reaction with ZVI (Arnold and Roberts 2000b). Chloroacetylene was not analyzed. In post-treatment monitoring, an actual increase in *c*DCE concentrations was noted only in monitoring well MW-2A. An increase in *t*DCE concentrations was not observed in any of the treated-zone monitoring wells. However, the lack of an apparent increase in degradation product concentrations does not necessarily mean that temporary increases did not occur, as degradation product concentrations may have increased and subsequently declined between sampling events.

Degradation of *c*DCE and *t*DCE may lead to formation of VC (via hydrogenolysis) or acetylene (via  $\beta$ -elimination). VC was present at Site 89 prior to remediation and, once formed, is expected to be amenable to ZVI-mediated degradation. Temporary increases in VC concentrations were noted in three of the treated-zone monitoring wells: MW-1B, MW-2A, and MW-2C. At each of these locations, VC concentrations reached peak values and subsequently declined. In MW-2A, the reaction sequence required more time to achieve substantial depletion of VC.

### 2.3.7 Analysis of MW-2A

As discussed previously, the apparent degradation trends in MW-2A differed from those observed in other source-area monitoring wells. In MW-2A, substantial increases (and subsequent declines) in *c*DCE and VC concentrations were noted. To evaluate long-term degradation trends, an additional groundwater sample was collected from MW-2A in December 2011, approximately 39 months after mixing was complete.

Groundwater concentration data for MW-2A, shown in Figure 2-9, indicated that the molar concentration of total CVOCs did not change considerably over the first year after treatment, although the composition of CVOCs changed substantially. The *c*DCE degradation rate coefficient (Figure 2-8) was low for MW-2A compared to those associated with all other monitoring wells except for MW-1D. An additional anomaly is that most of the *c*DCE appears to have been degraded via the hydrogenation pathway, leading to formation of VC. For the subsequent reaction step, the VC degradation rate coefficient appears to be similar to those calculated for other locations.

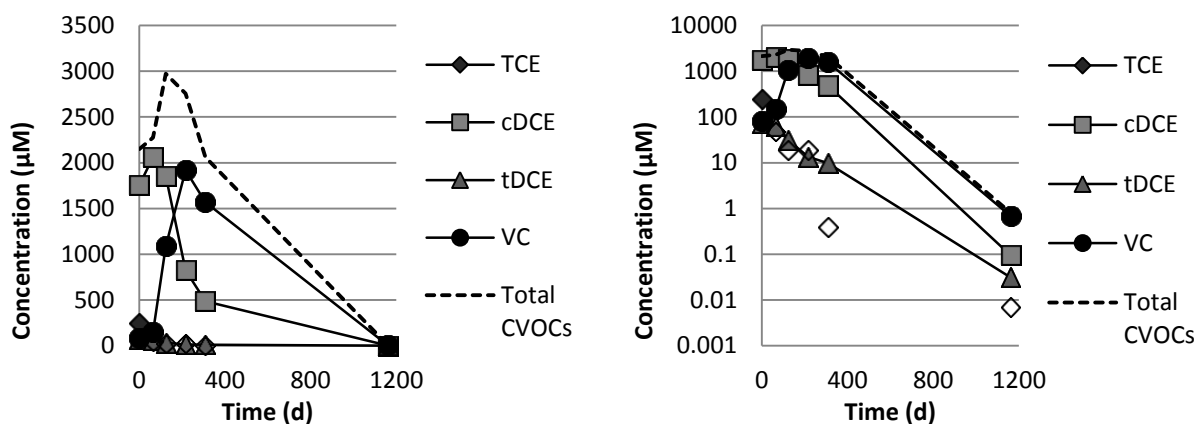


Figure 2-9. Molar concentration of select CVOCs versus time in MW-2A: linear scale (left) and logarithmic scale (right). TeCA was not detected in MW-2A. Open data symbols indicate detection limits where the indicated compound was reported as non-detect.

The reasons for the apparently anomalous treatment pattern in MW-2A are not clear. In evaluating data from ZVI-based PRBs, Jeen et al. (2011) noted that certain chemical species (i.e., sulfides) may have greater impact on iron reactivity toward *c*DCE than more chlorinated compounds such as TCE. Sulfate or sulfide data have not been collected at Site 89, so this potential correlation cannot be evaluated. However, other observations can be made given the available site data, including (a) distinct chemical parameters, (b) high level of chloride production, and (c) occurrence of the well within the

boundary of the electrical resistivity heating (ERH) demonstration. A discussion of these observations follows.

*Chemical parameters:* pH and ORP values in MW-2A were different from those measured in the other Site 89 monitoring wells. Average pH values, based on values at five different elapsed times within the year after mixing, were  $6.7 \pm 0.5$  in MW-2A and  $8.6 \pm 0.5$  in all other locations. Similarly, the average ORP values within the year after mixing were  $-160 \pm 40$  mV (vs. Ag/AgCl) in MW-2A and  $-300 \pm 50$  mV in all other locations. The apparently diminished impact of ZVI on the pH and ORP values in MW-2A may indicate partial passivation of the iron surface.

*Chloride production:* Post-treatment chloride production in MW-2A is greater than that in any other monitoring well. The amount of chloride produced in MW-2A was approximately  $67,000 \mu\text{mol} \cdot \text{L}^{-1}$ . Based on 3 moles of chloride per mole of TCE, this chloride concentration converts to an equivalent TCE concentration of  $22,300 \mu\text{M}$ , which is well above the TCE solubility of  $9,125 \mu\text{M}$  (Pankow and Cherry 1996). This result indicates that non-aqueous phase contaminants, either sorbed or DNAPL, may have existed in the vicinity. If non-aqueous phase contaminants were present, the kinetic coefficients calculated herein may be reduced by an inherent rate-limiting phase transfer step (i.e., for either desorption or dissolution).

*Electrical Resistivity Heating:* Monitoring well MW-2A is the only sampling location that occurred within the boundary of the ERH demonstration (Figure 2-1), which was conducted six years prior to the ZVI-Clay field application. Potential impacts of ERH on water quality include an increase in dissolved organic carbon (Friis et al. 2005), which has been shown to inhibit degradation of TCE by competing for reactive iron-surface sites (Tratnyek et al. 2001). Other possible impacts of ERH on aquifer conditions are also likely (USEPA 2003), although they may be site specific. For example, the possibility of inhibited autoreduction (Ritter et al. 2002) or otherwise diminished reactivity of the iron surface may exist as a result of the ERH activity. Despite the inability of the available data to explain the

exact mechanisms behind the seemingly anomalous treatment pattern in MW-2A, the long-term data indicate that degradation of CVOCs has continued beyond the initial 12-month performance evaluation period.

#### 2.3.8 Contaminant and Groundwater Flux in ZVI-Clay Treated Soils

An emerging metric for source-zone remedies involves quantifying contaminant-mass discharge, which may be calculated as the integrated contaminant mass flux across a plane down-gradient from treated zones (Guilbeault et al. 2005; Brooks et al. 2008). The advective contaminant mass flux is the product of the Darcy liquid flux and the solute concentration (Schwarzenbach et al. 2003). In using contaminant-mass discharge to compare source-zone remediation approaches, a unique feature of ZVI-Clay is the simultaneous reduction of both the Darcy flux, via reduction in hydraulic conductivity, and the concentration. Theoretically, by compounding multiple order-of-magnitude reductions for both Darcy flux and concentration, substantial reductions in contaminant discharge can be achieved. Due to the relatively large uncertainty in the hydraulic gradient in the year immediately following mixing, a contaminant mass flux has not been calculated for Site 89.

In addition to reduced contaminant discharge, the reduction in hydraulic conductivity has other treatment implications, including reduction in recharge of dissolved-phase constituents, accumulation of degradation products, and extension of residence times for all species. Dissolved-phase constituents are effectively limited to those present in the region prior to mixing or generated after treatment. Several studies have noted impacts of dissolved phase species on iron reactivity. For example, a decline in the performance of permeable reactive barriers (PRBs) due to iron-surface passivation has been associated with various species including dissolved nitrate (Farrell et al. 2000; Devlin and Allin 2005), silica (Klausen et al. 2003), and natural organic matter (Tratnyek et al. 2001). Positive impacts on iron reactivity, due to promotion of iron surface activation, may result from dissolved species including sulfate or chloride (Devlin and Allin 2005).

Another contrast to PRBs is that degradation products are not rapidly removed from the system. This delayed removal may lead to local accumulation of reaction products such as hydrogen (Reardon 2005), ferrous iron, chloride, and lesser-chlorinated CVOCs (Wadley et al. 2005). Degradation products may compete with parent compounds for reactive iron-surface sites (Arnold and Roberts 2000a), which could potentially limit degradation rates. However, the residence time for reactions to proceed also is extended. The potential benefit of the extended residence time is apparent in analysis of data from MW-2A, whereby three years were required to reduce the total CVOCs by approximately 99%. Effects of these conditions on iron reactivity have been well evaluated with respect to PRBs. However, reactive transport processes are quite different in ZVI-Clay treated soils. Additional research into the effects of such conditions on the efficacy of ZVI-Clay is needed for continued development of the technology.

## 2.4 Conclusions

The ZVI-Clay technology was implemented for remediation of a chlorinated-solvent source zone at Site 89, Camp Lejeune, NC. For remediation at Site 89, a volume of 22,900 m<sup>3</sup> of soil was treated to an average depth of 7.6 m by mixing with 2% ZVI and 3% bentonite (by dry weight). Compounds targeted for treatment included TeCA, TCE, and degradation products, consisting primarily of *c*DCE, *t*DCE, and VC.

Within one year after completion of mixing, site-wide average and median decreases in concentrations of total CVOCs in soil samples were 97% and >99%, respectively. The site-wide average and median reductions in concentrations of total CVOCs in groundwater were 81% and >99%, respectively. In several of the soil and groundwater monitoring locations, total CVOC concentration reductions of greater than 99.9% were apparent. In groundwater data, TeCA and TCE were largely reduced to detection limits within 4 and 12 months of treatment, respectively. Degradation products including *c*DCE, *t*DCE, and VC were observed. Concentrations of *c*DCE, *t*DCE, and VC were substantively reduced within one year of treatment in all but one monitoring well (MW-2A). In MW-2A,

formation of *c*DCE, and subsequently VC, was noted in the first year. However, concentrations of both compounds were largely reduced in an additional sample collected three years after mixing had been completed.

Due to the potential formation and subsequent removal of degradation products, a first-order reaction-network model was applied. TeCA and TCE were degraded rapidly (i.e., in the first one to four months after mixing) relative to the frequency of sampling events. As a result, an insufficient number of data points were available to calculate rate coefficients for TeCA and TCE. However, degradation rates for *c*DCE, *t*DCE, and VC were sufficient to allow calculation of the rate coefficients, which were determined to be  $0.028 \pm 0.011$ ,  $0.036 \pm 0.018$ , and  $0.029 \pm 0.016 \text{ d}^{-1}$ , respectively.

Pre- and post-mixing average hydraulic conductivity,  $K$ , values were  $1.7 \times 10^{-5}$  and  $5.2 \times 10^{-8} \text{ m}\cdot\text{s}^{-1}$ , respectively, indicating an average reduction in  $K$  of about 2.5 orders of magnitude. This reduction in  $K$  combined with reduced contaminant concentrations, due to ZVI-mediated degradation, is shown to result in a potentially significant reduction in the advective mass flux of contaminants emanating from the source zone. Thus, results of the ZVI-Clay remediation technology at Site 89 suggest that the technology has the potential for imparting substantial reduction in contaminant mass discharge rates from source zones contaminated with chlorinated solvents.

## 2.5 Attribution of Credit

This paper is dedicated to our now absent friends and colleagues, Stephanie O'Hannesin and Dave Gilbert. We also thank: DuPont for their support in development of ZVI-Clay; personnel from Camp Lejeune and Naval Facilities Engineering Command, Mid-Atlantic Division; and our reviewers.

## REFERENCES

- AGVIQ-CH2M HILL. 2010. Non-time-critical Removal Action Summary Report, Site 89, Operable Unit 16. Marine Corps Base Camp Lejeune, Jacksonville, North Carolina. Charlotte, NC: CH2M HILL.
- Arnold, W. A., and A. L. Roberts. 2000a. Inter- and intraspecies competitive effects in reactions of chlorinated ethylenes with zero-valent iron in column reactors. *Environmental Engineering Science* 17 (5):291-302.
- Arnold, W. A., and A. L. Roberts. 2000b. Pathways and kinetics of chlorinated ethylene and chlorinated acetylene reaction with Fe(0) particles. *Environmental Science & Technology* 34 (9):1794-1805.
- Arnold, W. A., P. Winget, and C. J. Cramer. 2002. Reductive dechlorination of 1,1,2,2-tetrachloroethane. *Environmental Science & Technology* 36 (16):3536-3541.
- Bi, E. P., J. F. Devlin, B. Huang, and R. Firdous. 2010. Transport and Kinetic Studies To Characterize Reactive and Nonreactive Sites on Granular Iron. *Environmental Science & Technology* 44 (14):5564-5569.
- Brooks, M. C., A. L. Wood, M. D. Annable, K. Hatfield, J. Cho, C. Holbert, R. S. C. Rao, C. G. Enfield, K. Lynch, and R. E. Smith. 2008. Changes in contaminant mass discharge from DNAPL source mass depletion: Evaluation at two field sites. *Journal of Contaminant Hydrology* 102 (1-2):140-153.
- Castelbaum, D., and C. D. Shackelford. 2009. Hydraulic conductivity of bentonite slurry mixed sands. *Journal of Geotechnical and Geoenvironmental Engineering* 135 (12):1941-1956.
- Chapman, S. W., and B. L. Parker. 2005. Plume persistence due to aquitard back diffusion following dense nonaqueous phase liquid source removal or isolation. *Water Resources Research* 41 (12):W12411.
- Day, S. R., S. F. O'Hannesin, and L. Marsden. 1999. Geotechnical techniques for the construction of reactive barriers. *Journal of Hazardous Materials* 67 (3):285-297.
- Day, S. R., and C. Ryan. 1995. Containment, stabilization and treatment of contaminated soils using in-situ soil mixing. In *Geoenvironment 2000: Characterization, Containment, Remediation, and Performance in Environmental Geotechnics, Vols 1 and 2*, edited by Y. B. Acar and D. E. Daniel. New York: ASCE.
- Devlin, J. F., and K. O. Allin. 2005. Major anion effects on the kinetics and reactivity of granular iron in glass-encased magnet batch reactor experiments. *Environmental Science & Technology* 39 (6):1868-1874.
- Farrell, J., N. Melitas, M. Kason, and T. Li. 2000. Electrochemical and column investigation of iron-mediated reductive dechlorination of trichloroethylene and perchloroethylene. *Environmental Science & Technology* 34 (12):2549-2556.
- Friis, A. K., H. J. Albrechtsen, G. Heron, and P. L. Bjerg. 2005. Redox processes and release of organic matter after thermal treatment of a TCE-contaminated aquifer. *Environmental Science & Technology* 39 (15):5787-5795.

- Gillham, R. W., and S. F. O'Hannesin. 1994. Enhanced degradation of halogenated aliphatics by zero-valent iron. *Ground Water* 32 (6):958-967.
- Grant, G. P., and B. H. Kueper. 2004. The influence of high initial concentration aqueous-phase TCE on the performance of iron wall systems. *Journal of Contaminant Hydrology* 74 (1-4):299-312.
- Guilbeault, M. A., B. L. Parker, and J. A. Cherry. 2005. Mass and flux distributions from DNAPL zones in sandy aquifers. *Ground Water* 43 (1):70-86.
- Jasperse, B. H., and C. R. Ryan. 1987. Geotech import - Deep soil mixing. *Civil Engineering* 57 (12):66-68.
- Jeen, S. W., R. W. Gillham, and A. Przepiora. 2011. Predictions of long-term performance of granular iron permeable reactive barriers: Field-scale evaluation. *Journal of Contaminant Hydrology* 123 (1-2):50-64.
- Johnson, T. L., M. M. Scherer, and P. G. Tratnyek. 1996. Kinetics of halogenated organic compound degradation by iron metal. *Environmental Science & Technology* 30 (8):2634-2640.
- Klausen, J., P. J. Vikesland, T. Kohn, D. R. Burris, W. P. Ball, and A. L. Roberts. 2003. Longevity of granular iron in groundwater treatment processes: Solution composition effects on reduction of organohalides and nitroaromatic compounds. *Environmental Science & Technology* 37 (6):1208-1218.
- Mackay, D. M., and J. A. Cherry. 1989. Groundwater contamination: Pump-and-treat remediation. *Environmental Science & Technology* 23 (6):630-636.
- McGuire, T. M., J. M. McDade, and C. J. Newell. 2006. Performance of DNAPL source depletion technologies at 59 chlorinated solvent-impacted sites. *Ground Water Monitoring and Remediation* 26 (1):73-84.
- NRC. 2005. *Contaminants in the subsurface source zone assessment and remediation*. Washington, DC: National Academies Press.
- Olson, M.R. 2005. In situ remediation via admixing zero valent iron and clay performance prediction. M.S. thesis, Department of Civil and Environmental Engineering, Colorado State University.
- Pankow, J.F., and J.A. Cherry. 1996. *Dense chlorinated solvents and other DNAPLs in groundwater: History, behavior, and remediation*. Portland, OR: Waterloo Press.
- Parker, L. V., and C. H. Clark. 2004. Study of five discrete-interval-type ground water sampling devices. *Ground Water Monitoring and Remediation* 24 (3):111-123.
- Phillips, D. H., T. Van Nooten, L. Bastiaens, M. I. Russell, K. Dickson, S. Plant, J. M. E. Ahad, T. Newton, T. Elliot, and R. M. Kalin. 2010. Ten year performance evaluation of a field-scale zero-valent iron permeable reactive barrier installed to remediate trichloroethene contaminated groundwater. *Environmental Science & Technology* 44 (10):3861-3869.

- Puls, R. W., D. W. Blowes, and R. W. Gillham. 1999. Long-term performance monitoring for a permeable reactive barrier at the US Coast Guard Support Center, Elizabeth City, North Carolina. *Journal of Hazardous Materials* 68 (1-2):109-124.
- Quinn, J., C. Geiger, C. Clausen, K. Brooks, C. Coon, S. O'Hara, T. Krug, D. Major, W. S. Yoon, A. Gavaskar, and T. Holdsworth. 2005. Field demonstration of DNAPL dehalogenation using emulsified zero-valent iron. *Environmental Science & Technology* 39 (5):1309-1318.
- Rabideau, A. J., P. L. Shen, and A. Khandelwal. 1999. Feasibility of amending slurry walls with zero-valent iron. *Journal of Geotechnical and Geoenvironmental Engineering* 125 (4):330-333.
- Reardon, E. J. 2005. Zerivalent irons: Styles of corrosion and inorganic control on hydrogen pressure buildup. *Environmental Science & Technology* 39 (18):7311-7317.
- Ritter, K., M. S. Odziemkowski, and R. W. Gillham. 2002. An in situ study of the role of surface films on granular iron in the permeable iron wall technology. *Journal of Contaminant Hydrology* 55 (1-2):87-111.
- Roberts, A. L., L. A. Totten, W. A. Arnold, D. R. Burris, and T. J. Campbell. 1996. Reductive elimination of chlorinated ethylenes by zero valent metals. *Environmental Science & Technology* 30 (8):2654-2659.
- Sale, T. C., J. A. Zimbron, and D. S. Dandy. 2008. Effects of reduced contaminant loading on downgradient water quality in an idealized two-layer granular porous media. *Journal of Contaminant Hydrology* 102 (1-2):72-85.
- Scherer, M. M., B. A. Balko, D. A. Gallagher, and P. G. Tratnyek. 1998. Correlation analysis of rate constants for dechlorination by zero-valent iron. *Environmental Science & Technology* 32 (19):3026-3033.
- Schwarzenbach, R. P., P. M. Gschwend, and D. M. Imboden. 2003. *Environmental Organic Chemistry*. 2nd ed. New York: Wiley.
- Shackelford, C. D., and T. C. Sale. 2011. Using the ZVI-clay technology for source zone remediation. *Geo-Strata* 15 (2):36-42.
- Shackelford, C. D., T. C. Sale, and M.R. Liberati. 2005. In-situ remediation of chlorinated solvents using zero valent iron and clay mixtures: A case history. In *Waste Containment and Remediation*, edited by A. Alshawabkeh, C. H. Benson, P. J. Culligan, J. C. Evans, B. A. Gross, D. Narejo, R. Reddy, C. D. Shackelford and J. G. Zornberg. Geotechnical Special Publication 142 (CD ROM), Reston, VA: ASCE.
- Shimotori, T., E. E. Nuxoll, E. L. Cussler, and W. A. Arnold. 2004. A polymer membrane containing Fe-0 as a contaminant barrier. *Environmental Science & Technology* 38 (7):2264-2270.
- Siegrist, R. L., K. S. Lowe, L. C. Murdoch, T. L. Case, and D. A. Pickering. 1999. In situ oxidation by fracture emplaced reactive solids. *Journal of Environmental Engineering* 125 (5):429-440.
- Siegrist, R. L., O. R. West, M. I. Morris, D. A. Pickering, D. W. Greene, C. A. Muhr, D. D. Davenport, and J. S. Gierke. 1995. In-situ mixed region vapor stripping in low-permeability media. 2. Full-scale field experiments. *Environmental Science & Technology* 29 (9):2198-2207.

Tratnyek, P. G., M. M. Scherer, B. L. Deng, and S. D. Hu. 2001. Effects of natural organic matter, anthropogenic surfactants, and model quinones on the reduction of contaminants by zero-valent iron. *Water Research* 35 (18):4435-4443.

USEPA. 2003. *The DNAPL remediation challenge: Is there a case for source depletion?* EPA/600/R-03/143. Cincinnati, OH: U.S. Environmental Protection Agency, National Risk Management Research Laboratory.

Wadley, S. L. S., R. W. Gillham, and L. Gui. 2005. Remediation of DNAPL source zones with granular iron: Laboratory and field tests. *Ground Water* 43 (1):9-18.

Zhang, W. X. 2003. Nanoscale iron particles for environmental remediation: An overview. *Journal of Nanoparticle Research* 5 (3-4):323-332.

## CHAPTER 3

### INITIAL RATE STUDIES EVALUATING REACTION KINETICS IN SYSTEMS CONTAINING ZERO VALENT IRON AND NAPL-PHASE TCE

#### *Synopsis of Chapter*

This research was conducted to improve our understanding of the interaction between granular-scale zero-valent iron (ZVI) and trichloroethene (TCE) in soil/water systems. Tasks included batch-reactor initial-rate studies and modeling. Initial rate studies were conducted to evaluate the TCE degradation rate across a range of initial TCE concentrations ( $C_{TCE}^0$ ), both above and below the solubility threshold ( $C_{TCE}^*$ ). The Michaelis-Menton (M-M) kinetic model provided a good fit of experimental data ( $r^2 = 0.998$ ) when the initial TCE concentration was below the solubility threshold ( $C_{TCE}^0 < C_{TCE}^*$ ). The M-M model fitting parameters were  $k_0 = 0.64 \text{ mmol}\cdot\text{L}^{-1}\cdot\text{d}^{-1}$  and  $K = 2.5 \text{ mmol}\cdot\text{L}^{-1}$ . When above the solubility threshold ( $C_{TCE}^0 > C_{TCE}^*$ ), Non-Aqueous Phase Liquid (NAPL)-phase TCE was present and the aqueous-phase TCE concentration remained fixed at solubility. Under such conditions, the degradation rate was observed to be independent of the amount of NAPL present in the system. However, a decline in the degradation rate by about 20% was noted as the initial TCE concentration increased across the solubility threshold. This decline suggests that NAPL has a minor inhibitory effect on the reactivity of ZVI, which may be explained by NAPL preferentially wetting the ZVI surface. In systems containing variable ZVI concentrations (with a fixed initial TCE concentration), the reaction rate was observed to increase linearly with an increase in the ZVI concentration. An iron-concentration-normalized rate constant was calculated to be  $0.0035 \text{ mmol}\cdot\text{g}^{-1}\cdot\text{d}^{-1}$ .

### 3.1 Introduction

Chlorinated solvents, a class of anthropogenic organic compounds such as trichloroethene (TCE), perchloroethene (PCE), were widely produced throughout the 20<sup>th</sup> century. Commercial production of chlorinated solvents declined substantially in the latter third of the 1900s as humans became increasingly aware of the potential for negative environmental impacts (Pankow and Cherry 1996). Subsequently, a substantial amount of research has been dedicated to the depletion of chlorinated solvents from subsurface environments.

Natural abiotic and biological degradation processes can contribute to removal of chlorinated solvents but may be slow, perhaps requiring decades to centuries, and in many cases result in incomplete dechlorination (EPA 2003; Stroo et al. 2012). Several technologies have been advanced to accelerate remediation and/or protect downstream receptors. A recent review article addresses established technologies as well as the current state of knowledge for remediation of chlorinated solvent source zones (Stroo et al. 2012). Several technologies are capable of achieving partial source removal; these include pump-and-treat, injection of reactive media, surfactant/cosolvent flushing, and *in situ* thermal treatment. While each of these is capable of removing a substantial amount of contaminant mass, complete source removal has rarely been achieved (Pankow and Cherry 1996; Stroo et al. 2012). The treatment limitations can primarily be linked to the heterogeneous nature of the subsurface (EPA 2003; Stroo et al. 2003). Advection-based treatments, including those involving fluid-flushing or transport of injected chemicals, are limited in their ability to impact contaminants in low-k zones. Moreover, after treatment application has stopped, back-diffusion of contaminants from low-permeability soil zones can sustain groundwater concentrations, thus limiting treatment effectiveness (Chapman and Parker 2005). The review authors (Stroo et al. 2012) indicated that “Back diffusion can limit performance of any technology based on advective transport (all technologies except excavation and [in situ thermal treatment]), as contaminants in less permeable zone may remain untreated.” Of the technologies discussed previously, only thermal technologies directly address contaminants in low-k zones. Thermal technologies can be effective in

some situations, but require a high energy input (Lemming et al. 2013) and overall performance can be limited at some sites, such as those of high groundwater velocity (Kingston et al. 2010).

Use of soil mixing for reagent delivery was not mentioned in the review, but as a delivery approach soil mixing has the potential to overcome the mass-transfer limitations cited by Stroo et al. (2012). Soil mixing effectively blends together the naturally-occurring interbedded low- and high-permeability soil zones, while treatment reagents are admixed with soils, *in situ* (i.e., without the need to bring soils to the surface). Thus, after mixing is completed, contrasting low- and high-permeability zones (theoretically) no longer exist. Rather, the entire source zone is transformed into a relatively homogeneous low-permeability zone with reactive media distributed throughout. DNAPL pools are also disrupted, with contaminants being re-distributed and brought into close proximity to reactive media.

Soil mixing provides a delivery approach in which any type of reactive media can be selected, as long as the selected media provides effective treatment with no inherent negative environmental impacts and is compatible with mixing equipment. For the model system presented herein, we have selected granular-scale (i.e., <1 mm) zero valent iron (ZVI) as a reactant. Soil mixing in a chlorinated solvent source zone can result in ZVI contact with relatively high contaminant concentrations, including non-aqueous phase liquids (NAPL). Although ZVI-mediated degradation of aqueous-phase chlorinated solvents is the subject of a vast body of literature (e.g., Gillham and O'Hannesin 1994; Johnson et al. 1996; Scherer et al. 1998; Puls et al. 1999; Wust et al. 1999; Arnold and Roberts 2000b; Farrell et al. 2000; Ritter et al. 2002; Klausen et al. 2003; Grant and Kueper 2004; Devlin and Allin 2005; Henderson and Demond 2007; Bi et al. 2010; Li and Benson 2010) studies addressing ZVI-mediated treatment of chlorinated-solvent NAPL are rather limited (Wadley et al. 2005; Berge and Ramsburg 2010; Taghavy et al. 2010; Fagerlund et al. 2012). Most of this research has evaluated injection of nano-scale ZVI. Use of soil mixing for delivery of ZVI and bentonite in chlorinated solvent source zones was applied in a field-scale demonstration at Canadian Forces Base Borden (Wadley et al. 2005) and in full-scale remediation of

chlorinated solvent source zones (Shackelford et al. 2005; Bozzini et al. 2006; Olson et al. 2012; U.S.EPA 2012).

For treatment of chlorinated solvent NAPL source zones, soil mixing with ZVI and bentonite has been demonstrated, but mechanistic understanding of the processes controlling treatment in systems comprising granular-scale ZVI, DNAPL, and soils is limited. Thus, the primary objective of the research presented herein is to address this knowledge gap. To achieve this objective, initial rate studies were conducted with variable initial TCE concentrations and ZVI amounts. Initial rate studies are an experimental approach used to determine reaction rate information by comparison of measured rate data across a range of initial reactant concentrations (Atkins 1994; Fogler 1999). Modeling of experimental data is conducted to further develop insights into treatment processes.

### **3.2 Methods and Materials**

To achieve experimental objectives, batch-reactor studies were conducted to evaluate the initial degradation rate of TCE in the presence of ZVI. Experiments were conducted in 20-mL glass headspace vials with PTFE®-lined septa and aluminum crimp-style caps. The vials were prepared with soil, aqueous solution, and ZVI particles. The experimental design consisted of 12 vial sets containing variable quantities of TCE and ZVI (Table 3-1). Initial TCE concentrations ranged from 6% to 350% of solubility; for those vial sets containing TCE above solubility, TCE was initially present in the NAPL phase. Vial sets were prepared in replicates of eight; vials were sacrificed over time to establish initial degradation rates.

**Table 3-1. Experimental design for batch-reactor kinetic experiments.**

Description	Target solubility multiplier	Total TCE ( $\mu\text{mol}$ )	TCE conc (mg/kg)	ZVI conc (g/L)	Aqueous solution (mL)	Porous media* (g)
C1	0.06	5.48	60	80	10	12
C2	0.12	11.0	120	80	10	12
C3	0.24	21.9	240	80	10	12
C4	0.48	43.8	480	80	10	12
C5	0.96	87.6	960	80	10	12
C6	2	183	2000	80	10	12
C7	3.5	319	3500	80	10	12
C8	5	456	5000	80	10	12
C4-control	0.48	43.8	480	0	10	12
C7-control	3.5	319	3500	0	10	12
C7-low ZVI	3.5	319	3500	25	10	12
C7-high ZVI	3.5	319	3500	250	10	12

\*Porous media consisted of 4% kaolin in fine-grained silica sand.

### 3.2.1 Materials

Porous media used for the degradation studies consisted of uniformly-graded fine-grained F-95 sand (US Silica; Frederick, MD) and B-80 kaolin clay (Thiele Kaolin; Sandersville, GA). Granular ZVI consisted of 50-70 mesh Iron Filings (Fisher Scientific; Waltham, MA). Granular ZVI was surface-activated prior to use by washing in 1M HCl for two minutes; after washing, ZVI was rinsed in deaired/deionized water, rinsed in de-aired acetone, and then dried in an anaerobic chamber (approximately 1% H<sub>2</sub> with a balance of N<sub>2</sub>). Experiments were commenced within one day of acid-washing the ZVI. The aqueous solutions used for the studies consisted of 10mM 1,4-piperazinediethanesulfonic acid (PIPES buffer) dipotassium salt (MP Biomedicals; Santa Ana, CA) and 100 mM NaCl, reduced to pH 7 by titrating with 1M HCl. The contaminant used in the studies consisted of neat TCE (Alfa Aesar; Ward Hill, MA).

Calibration stock solutions for TCE, *cis*-1,2-dichloroethene (*c*DCE; manufactured by Acros Organics; Waltham, MA), *trans*-1,2-dichloroethene (*t*DCE; Alfa Aesar), 1,1-dichloroethene (11-DCE; Alfa Aesar) were prepared by dissolving the neat compounds in HPLC-grade methanol (Burdick & Jackson; Morris Plains, NJ). A 100 ppm standard of VC in methanol was obtained from Ultra Scientific (North Kingstown, RI). For low-molecular-weight degradation products ethane, ethene, and acetylene, gas-cylinders of the neat compounds were provided by AirGas (Radnor, PA).

### 3.2.2 Experimental Methods

All vials contained 12 g of porous media (4% kaolin in sand) and 10 mL of water. Vial sets C1 to C5 (including C4-Control) contained TCE at levels below aqueous-phase solubility. For these vial sets, aqueous phase TCE solutions were prepared prior to filling the vials. TCE solutions were prepared by adding 150 mL of the buffer solution to a 200-mL glass bottle and spiking the solution with the proper amount of neat TCE. The bottles were mixed end-over-end for at least 18 hours to ensure complete dissolution of the TCE. Vial sets C6 to C8 (including C7 vial sets with variable ZVI amounts) contained TCE at levels above solubility. For these vial sets, neat TCE was injected directly into individual vials, as described below.

For loading of the vials, dry porous media and ZVI were weighed out and added to individual vials. Vials were then placed in an anaerobic chamber. For low-concentration vial sets, 10 mL of the TCE-spiked solution was added to each vial using a glass syringe and stainless-steel needle; to avoid volatilization losses, vials were sealed immediately after filling with the aqueous solution. For high-concentration vial sets, 10 mL of clean water was injected into each vial; a prescribed amount of neat TCE was then added to each vial using a 100- $\mu$ L glass gas-tight syringe; vials were crimp-sealed immediately after spiking. Once sealed, vials were removed from the anaerobic chamber and placed on a vortex mixer for about 30 seconds to disperse vial contents. Vials were tumbled end-over-end at 12 rotations per minute until analysis to facilitate equilibrium between all phases present in the vial.

### 3.2.3 Analysis

To determine reaction rates, vials were sacrificed for analysis at six times. At one time for each vial set, triplicate analysis was conducted. Vials were analyzed for TCE and degradation products including *c*DCE, *t*DCE, 1,1-DCE, ethene, ethane, and acetylene. Analysis was conducted directly on a headspace autosampler. Using this method, no extraction was required and vials were analyzed without any sample exposure to the atmosphere. Instrumentation used to conduct the analysis included a Tekmar 7000 headspace autosampler and an Agilent 6890 gas chromatograph with a flame ionization detector. The GC was equipped with a Restek Rt-Q-Bond (30 m × 0.32 mm × 10 μm) column. The headspace autosampler protocol consisted of a 5 minute equilibration period at 40°C. Samples were injected at a 50:1 split ratio. To analyze for TCE and related dechlorination products, the GC/FID method included both temperature and flow ramping to optimize separation of highly-volatile degradation products (ethane, ethene, and acetylene) while minimizing the total run time needed for elution of heavier compounds such as TCE. The flow rate was held at 1 mL·min<sup>-1</sup> for 5.5 min, ramped at 12 mL·min<sup>-2</sup> to 4 mL·min<sup>-1</sup>, and held at 4 mL·min<sup>-1</sup> for the remainder of the run. The temperature was held at 45°C for 5 min and ramped at 20°C·min<sup>-1</sup> to 250°C.

Calibration standards were prepared for chlorinated and non-chlorinated compounds. For all calibration standards, a series of headspace vials were prepared with 10 mL of the PIPES buffer solution and 12 g of the soil/kaolin mixture, then crimp-sealed with PTFE-lined septa caps. Target compounds were spiked into the vials through the septa caps using glass gas-tight syringes. For the chlorinated compounds, stock solutions were prepared at a range of concentrations in methanol; the stock solutions were injected into the headspace vials. For low-molecular weight degradation products ethane, ethene, and acetylene, pure gas-phase standards were injected into the headspace vials. After injection, vials were tumbled end-over-end for approximately 18 hours and then analyzed using the previously described headspace analytical method. Calibration curves were generated for each compound by plotting the instrument response versus the total moles present in the vial.

### 3.2.4 Data Analysis and Statistics

TCE and several of the degradation products, which included DCE isomers, VC, ethane, ethene, and acetylene, were identified in GC chromatograms based on their retention times and were quantified based on linear calibration factors. Additional peaks were observed in the GC chromatograms, representing unrecognized compounds; these compounds are herein lumped together as compound *U*. To complete the mass balance, these peaks were quantified using the average value of the GC response factors for the eight known compounds, consisting of TCE and the degradation products listed previously.

TCE degradation rates and confidence intervals for each vial set (i.e., for each treatment condition) were calculated by linear regression of total degradation product concentration ( $\mu\text{mol}\cdot\text{L}^{-1}$ ) versus time (d). Total degradation products were calculated as the sum of the molar concentration present for all known (DCE isomers, VC, ethene, ethane, and acetylene) and unknown (*U*) compounds. Each vial set consisted of eight vials, which were sacrificed at six times for analysis, one time in triplicate. For linear regression, each of the triplicate samples was treated as an individual sample; thus, linear regression was based on eight independent samples.

Statistical comparison of degradation rates under differing treatment conditions was conducted using the Student's T-test. To conduct these tests, a degradation rate was calculated for each vial by dividing the total degradation products by the sampling time, thus providing a population of eight data points for each vial set. The data-point populations for different treatment conditions were compared using standard T-test methods.

## 3.3 Mathematical Modeling

ZVI-Clay soil mixing applications can result in a wide range of initial contaminant concentrations. In systems where the total contaminant mass present before mixing exceeds the solubility threshold (i.e., the capacity of the aqueous and sorbed phases to store the contaminant), NAPL will

remain in the system after mixing. Under such conditions, the aqueous phase concentration remains at solubility as long as NAPL remains present; assuming NAPL dissolution is rapid relative to degradation, the concentration remains at solubility even as degradation proceeds. Conversely, where the initial TCE mass is less than the solubility threshold, no NAPL will be present after mixing. Where such is the case, any aqueous phase concentration up to the solubility limit may be encountered. Thus, the kinetic model applied must account for reaction rates encountered over the entire range of possible concentrations.

As a first approximation, a pseudo-first order kinetic model has been used (Gillham and O'Hannesin 1994; Matheson and Tratnyek 1994; Orth and Gillham 1996; Wadley et al. 2005; Song and Carraway 2006; Olson et al. 2012):

$$R = -k_1 C \quad (1)$$

where  $R$  ( $\text{mol}\cdot\text{L}^{-1}\text{d}^{-1}$ ) is the reaction rate, or the change in total TCE moles per volume of water, over time;  $k_1$  ( $\text{d}^{-1}$ ) is the first-order rate coefficient; and  $C$  ( $\text{mol}\cdot\text{L}^{-1}$ ) is the aqueous-phase contaminant concentration. The pseudo-first order model predicts a linear relationship between  $R$  and  $C$ . Limitations of this approach have been observed in systems of highly-variable initial concentrations both in published research (Johnson et al. 1996; Wust et al. 1999; Arnold and Roberts 2000a) and in ZVI-Clay treatability studies conducted by Colorado State University (unpublished), wherein  $R$  has been shown to approach a zero-order relationship with  $C$  at elevated concentrations, in particular at concentrations above the solubility threshold.

The Michaelis-Menton (M-M) kinetic model has been used to describe ZVI-mediated degradation of TCE across a range of aqueous phase concentrations. This model is based on the following assumptions: (a) degradation is first order in the surface-sorbed reactant concentration, (b) the concentration of reactive surface sites is small compared to the reactant concentration, and (c) the

aqueous- and sorbed-phase reactant concentrations reach rapid equilibrium. A general form of the M-M model is as follows (Johnson and Goody 2011):

$$R = -\frac{V_{max} C}{K + C} \quad (2)$$

where  $V_{max}$  ( $\text{mol}\cdot\text{L}^{-1}\text{d}^{-1}$ ) is the maximum degradation rate,  $C$  ( $\text{mol}\cdot\text{L}^{-1}$ ) is the contaminant concentration, and  $K$  ( $\text{mol}\cdot\text{L}^{-1}$ ) is a fitting parameter that corresponds to the concentration at which  $R$  is equal to half of  $V_{max}$ . In the context of ZVI-mediated degradation of TCE, the model can be written as follows (after Wust et al. 1999):

$$R = -\frac{k_a \rho_{ZVI} C_{TCE}}{K + C_{TCE}} \quad (3)$$

where  $k_a$  ( $\text{mol}\cdot\text{m}^{-2}\text{d}^{-1}$ ) is the degradation rate coefficient,  $\rho_{ZVI}$  ( $\text{m}^2\text{L}^{-1}$ ) is the ZVI surface area per volume of water, and  $C_{TCE}$  ( $\text{mol}\cdot\text{L}^{-1}$ ) is the aqueous-phase concentration of TCE. This model suggests that  $R$  is proportional to  $\rho_{ZVI}$ . Furthermore, when  $C_{TCE}$  is large compared to  $K$ , the rate approaches zero-order with a rate of  $k_a\cdot\rho_{ZVI}$ ; when  $C_{TCE}$  is small compared to  $K$ , the rate approaches first-order with a rate coefficient of  $k_a\cdot\rho_{ZVI}\cdot K^{-1}$ . Where  $\rho_{ZVI}$  is constant, Equation 3 can be written as:

$$R = -\frac{k_0 C_{TCE}}{K + C_{TCE}} \quad (4)$$

where  $k_0$  ( $\text{mol}\cdot\text{L}^{-1}\text{d}^{-1}$ ) is a 0-order degradation rate, corresponding to the maximum degradation rate. By comparison to Equation 2,  $k_0$  is analogous to  $V_{max}$ . Equation 4 can be rearranged as follows:

$$-\frac{1}{R} = \left(\frac{k_0}{K}\right)\frac{1}{C_{TCE}} + \frac{1}{k_0} \quad (5)$$

From Equation 5, values for the parameters  $k_0$  and  $K$  can be determined from initial degradation rates measured at a range of initial concentrations,  $C_{TCE}^0$ , and conducting linear regression of a plot of  $-1/R$  versus  $1/C_{TCE}^0$ .

Where NAPL is present,  $C_{TCE}$  is no longer variable but is fixed at the solubility concentration,  $C_{TCE}^*$ . Equation 3 is then written as follows:

$$R = -\frac{k_a \rho_{ZVI} C_{TCE}^*}{K + C_{TCE}^*} \quad (6)$$

This implies that the TCE degradation rate is independent of the amount of TCE in the system, where NAPL is present. If  $K \ll C_{TCE}^*$ , Equation 6 can be simplified as follows:

$$R = -k_a \rho_{ZVI} \quad (7)$$

If  $\rho_{ZVI}$  can be assumed to be constant, this can be further simplified as:

$$R = -k_0 \quad (8)$$

This model assumes that the presence of NAPL does not interfere with ZVI reactivity.

### 3.4 Results and Discussion

To achieve experimental objectives, the initial-rate experimental approach was used to evaluate TCE degradation rates as a function of initial TCE concentration and ZVI concentration. This section presents results of the initial rate studies and model-fitting of experimental data.

#### 3.4.1 TCE Degradation and Product Formation

For reaction vials containing TCE below solubility (vial sets C1 to C5), headspace TCE concentrations declined concurrent with formation of degradation products (Figure 3-1). In the relatively short duration of the experiment, only small fractions (20 to 60%) of total initial TCE were degraded. However, formation of degradation products provides evidence that degradation of TCE did indeed occur. The quantity of degradation products increases with initial TCE concentration. None of the degradation products were detected in the no-ZVI control.

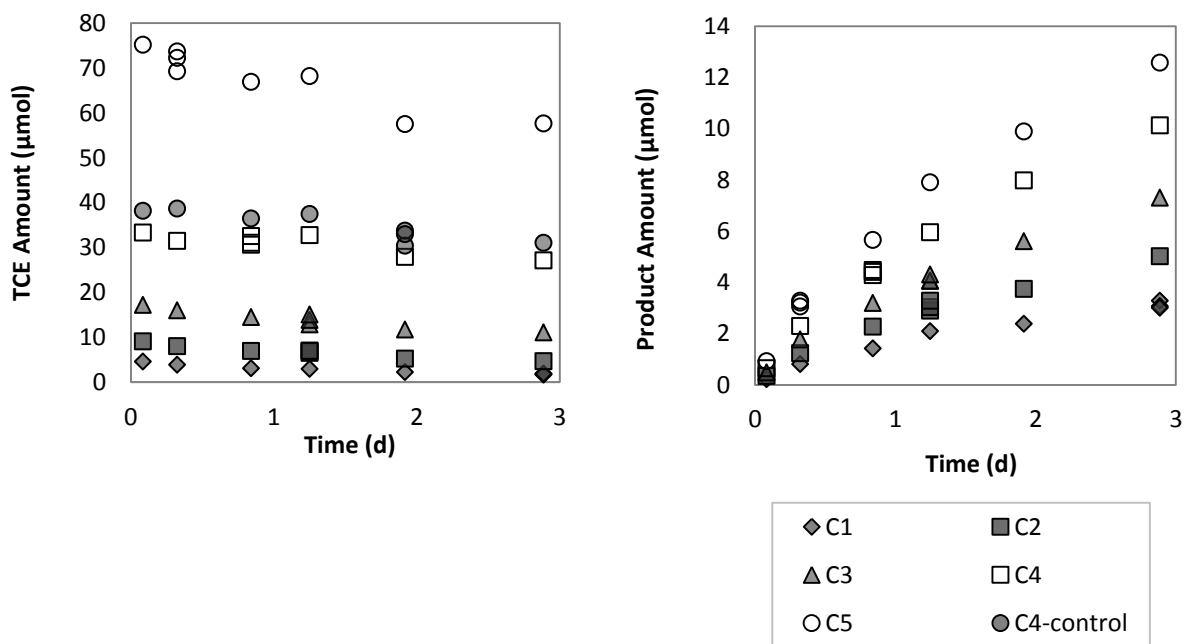


Figure 3-1. TCE amount (left) and total degradation products (right) versus time in vial sets C1 to C5, which initially contained TCE at levels below the solubility threshold. Each of the triplicate sample data points are shown.

For reaction vials containing TCE above solubility (vial sets C6 to C8), NAPL is present and the aqueous phase TCE concentration is assumed to be fixed at solubility. The headspace is assumed to be in equilibrium with the aqueous phase; therefore, the headspace TCE concentration would also be constant, regardless of the amount of NAPL present in the vials (that is, the quantity of NAPL-phase TCE would not be directly apparent in the headspace analytical method used for this study; nor would sorbed-phase TCE). Experimental data confirm that TCE concentrations were constant in vials with variable amounts of NAPL; however, total degradation product levels increased with time (Figure 3-2). In time 0 samples, TCE headspace concentrations exceeded the theoretical maximum. This may be attributed to the fact that vials had a relatively short time (~1 hour) to equilibrate, allowing NAPL to directly impact the headspace. The highest level of degradation products was observed in vial set C7 with an elevated ZVI concentration

(250 g·L<sup>-1</sup>). Conversely, the lowest level of degradation product formation was observed in vial set C7 with a low ZVI concentration (25 g·L<sup>-1</sup>). The level of product formation in vial sets C6, C7, and C8 with similar iron concentrations (80 g·L<sup>-1</sup>) appeared to be of similar in magnitude. Additional discussion and statistical analysis is presented in the subsequent reaction-rate analysis.

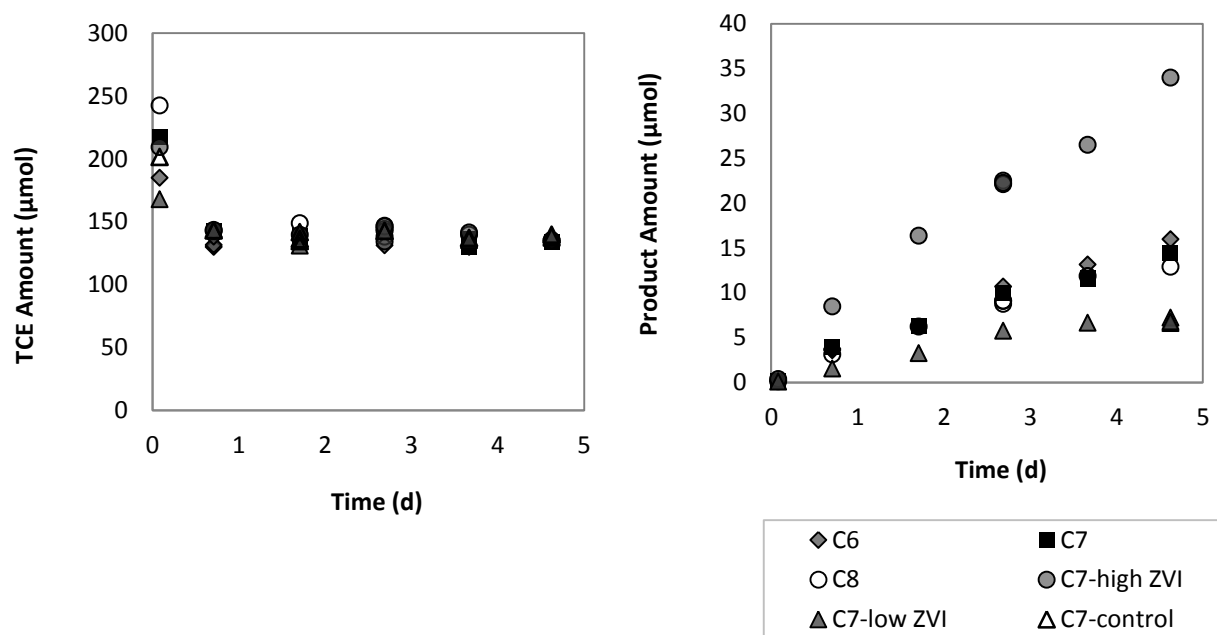


Figure 3-2. TCE amount (left) and total degradation products (right) versus time in vial sets C6 to C8, which initially contained TCE above the solubility threshold. Note that the TCE amount excludes NAPL-phase and sorbed-phase TCE.

### 3.4.2 Degradation Rate

The TCE degradation rate was calculated for all vial sets based on the quantity of degradation products formed versus time. Rate calculations are based on degradation product data, rather than TCE depletion data, for two reasons: (1) TCE concentrations were constant in the vials containing TCE above the solubility threshold, where NAPL maintained aqueous-phase TCE concentrations at the solubility limit, and (2) degradation products provide a conservative estimate of the TCE degradation rate as

volatilization losses cannot be misinterpreted as degradation. TCE degradation rates were calculated by conducting linear regression of product-versus-time data.

Results of the study (Figure 3-3) show that at initial TCE levels below the solubility threshold, the initial degradation rate increases with initial concentration. Above the solubility threshold, the TCE degradation rate no longer increases; in fact, the TCE degradation rate appears to decrease by about 20%. Student's T-test analysis was conducted to compare degradation rates in vial sets near or above the solubility threshold (C5, C6, C7, and C8). Degradation rates in the three vial sets C6, C7, and C8, which contained TCE above solubility and a ZVI concentration of  $80 \text{ g}\cdot\text{L}^{-1}$ , were statistically similar (P-values ranged from 0.17 to 0.68). When compared to vial set C5, each was significantly different (P-values were less than 0.003).

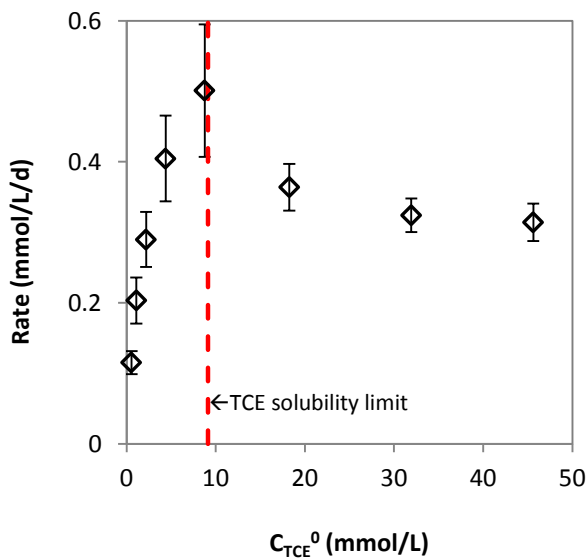


Figure 3-3. TCE degradation rate versus initial TCE concentration (total amount of TCE per volume of water). Data is shown for vials containing ZVI at a concentration (aqueous phase basis) of  $80 \text{ g/L}$ . The vertical dashed line indicates the TCE solubility limit. Error bars indicated 95% confidence intervals for the rate values, calculated from linear regression of experimental data.

### 3.4.3 Model Fitting

Model fitting parameters were calculated by linear regression of  $1/R$  versus  $1/C_{TCE}^0$  (per Equation 5). Following this method, the fitting parameter values are as follows:  $k_0 = 0.64 \text{ mmol}\cdot\text{L}^{-1}\text{d}^{-1}$  and  $K = 2.5 \text{ mmol}\cdot\text{L}^{-1}$ . Figure 3-4 shows calculated rate values for C1 to C5 (vials sets where initial TCE was less than solubility) compared to model output. The model provides an excellent fit of experimental data ( $r^2 = 0.998$ ). This suggests that the Michaelis-Menton type kinetics adequately describe degradation kinetics in the experimental system at initial TCE concentrations below the NAPL threshold.

Equation 6 predicts that the TCE degradation rate will reach a maximum value at the solubility limit and will remain constant at higher TCE levels, regardless of the amount of NAPL in the system. As shown in Figure 3-3, in the three vial sets containing TCE at levels above the solubility threshold (C6, C7, and C8), the observed TCE degradation rate remains statistically similar as the initial TCE amount increases; this agrees with the model prediction. However, the degradation rates in C6, C7 and C8 are statistically lower than the degradation rate in the vial set with TCE just below the solubility threshold (C5). This decline in the reaction rate as initial TCE amount increases past the solubility threshold is not predicted by the proposed model. This suggests that the presence of NAPL may have an inhibitory effect on the TCE degradation rate. Although the cause of this is not clear given existing data, we can speculate that reactive sites on the ZVI surface may be saturated or otherwise inhibited by the presence of NAPL.

As discussed previously in the Mathematical Modeling section, Equation 7 was proposed as a simplification to Equation 6, based on the assumption that  $K \ll C_{TCE}^*$ . From this experimental data,  $K = 2.5 \text{ mmol}\cdot\text{L}^{-1}$ , as compared to a  $C_{TCE}^*$  value of  $9.1 \text{ mmol}\cdot\text{L}^{-1}$ . This suggests that  $K$ , at approximately 27% of  $C_{TCE}^*$ , is not trivial. Thus, under the conditions applied in this experiment, Equation 6 should be used instead of Equation 7 when NAPL is present.

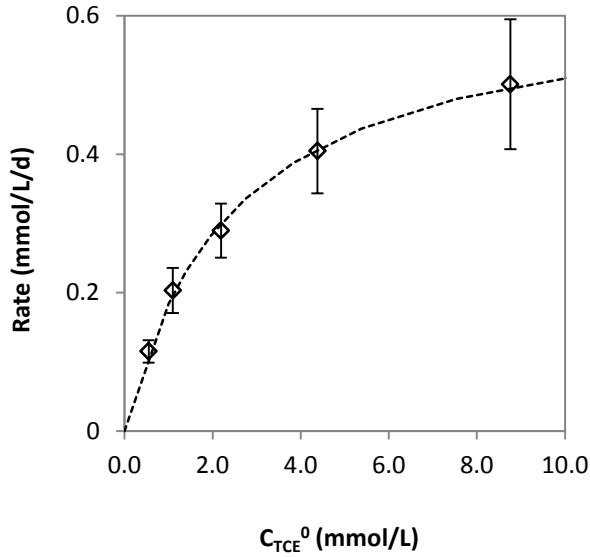


Figure 3-4. TCE degradation rate versus initial TCE concentration (total amount of TCE per volume of water) for experimental data ( $\diamond$ ) and model output (-----).

#### 3.4.4 Degradation Rate versus ZVI Amount

A second experimental variable was the ZVI amount. At an initial TCE concentration of 32  $\text{mmol}\cdot\text{L}^{-1}$  ( $3.5 \times$  the NAPL threshold), three ZVI concentrations ( $\rho_{ZVI}$ ) were evaluated: 25, 80 and 250  $\text{g}\cdot\text{L}^{-1}$ . A plot of the TCE degradation rate (calculated from the product formation rate) versus  $\rho_{ZVI}$  (Figure 3-5) shows that a linear relationship exists between  $R$  and  $\rho_{ZVI}$  ( $r^2 = 0.999$ ), as predicted by Equation 6. The slope of the line, which corresponds to  $k_a$  in Equation 6, is  $0.0027 \pm 0.0007 \text{ mmol}\cdot\text{g}^{-1}\text{d}^{-1}$  and the intercept is not statistically different from 0 ( $0.097 \pm 0.11 \text{ mmol}\cdot\text{d}^{-1}$ ; P-value = 0.056).

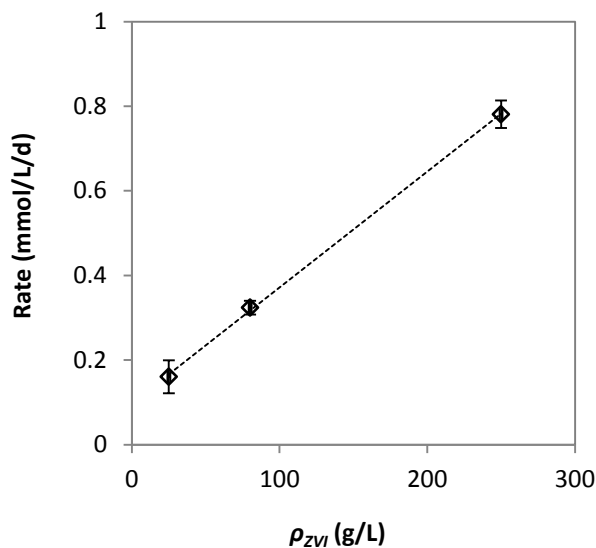


Figure 3-5. TCE degradation rate versus ZVI concentration (aqueous phase basis) for experimental data (  $\diamond$  ) and model output ( - - - - - ). Data is shown for vials containing TCE at a concentration (amount of TCE per volume of water) of 32 mmol/L, at 3.5 $\times$  the solubility of TCE.

### 3.5 Conclusions and Recommendations for Future Work

This research provides novel insights into the interaction between ZVI and TCE under a range of concentrations, both above and below the solubility threshold. At TCE concentrations below the solubility threshold, the M-M kinetic model provided a good fit ( $r^2 = 0.998$ ) of experimental data. Where NAPL was present, the aqueous-phase TCE concentration remained fixed at solubility, and the measured degradation rates were statistically similar in systems of variable TCE concentrations. This indicates that the aqueous phase concentration, rather than the amount of NAPL present in the system, governs the degradation rate. However, a decline in the degradation rate by about 20% was noted as TCE concentrations crossed the solubility threshold. This decline suggests that NAPL may have an inhibitory effect on the reactivity of ZVI. A possible explanation for this inhibition is that NAPL preferentially wets the ZVI surface, thus blocking reactive sites (this hypothesis has not been tested).

In addition to variable TCE concentrations, experiments were conducted with variable ZVI concentrations at a fixed initial TCE concentration. In these experiments, the reaction rate was observed to vary linearly with changes in ZVI concentration. This observation agrees with the model for a system containing TCE-NAPL (Equation 6). An iron-concentration-normalized rate constant was calculated to be  $0.0035 \text{ mmol}\cdot\text{g}^{-1}\cdot\text{d}^{-1}$ . This rate constant can be used to translate results from a system containing a given ZVI concentration to systems of alternative ZVI concentrations.

The experiments were conducted under idealized conditions. For example, the media used in these studies was selected such that sorption was assumed to be negligible. Also, the reactors were mixed continuously during the reactive portion of the experiment; under field conditions, mixing occurs only at the time of implementation. Thus, mass transfer limitations that may occur under field conditions were excluded from this experiment. The objectives of this experiment were to evaluate the interaction between TCE and ZVI; including the role of mass transfer was outside of these experimental objectives but is recommended for future work.

An additional area of recommended future work involves detailed analysis of degradation pathways. Pathways would help our understanding of mechanisms; a comparison of pathways and mechanisms in systems with and without NAPL would be beneficial for predicting treatment in field-scale applications. Although pathway analysis was not conducted as part of this research, the analytical method provided detailed degradation product data. This includes several unknown peaks in the GC chromatogram. Existing experimental data can be further evaluated to provide information on degradation pathways and kinetics. A possible method to identify the unknown peaks will be to use a Mass Spectroscopic (MS) detector. The GC/MS may be able to identify peaks that are not included on the list of routine analytes in the laboratory.

## REFERENCES

- Arnold, W. A., and A. L. Roberts. 2000a. Inter- and intraspecies competitive effects in reactions of chlorinated ethylenes with zero-valent iron in column reactors. *Environmental Engineering Science* 17 (5):291-302.
- Arnold, W. A., and A. L. Roberts. 2000b. Pathways and kinetics of chlorinated ethylene and chlorinated acetylene reaction with Fe(0) particles. *Environmental Science & Technology* 34 (9):1794-1805.
- Atkins, P. W. 1994. *Physical chemistry*. New York: W.H. Freeman.
- Berge, N. D., and C. A. Ramsburg. 2010. Iron-mediated trichloroethene reduction within nonaqueous phase liquid. *Journal of Contaminant Hydrology* 118 (3-4):105-116.
- Bi, E. P., J. F. Devlin, B. Huang, and R. Firdous. 2010. Transport and Kinetic Studies To Characterize Reactive and Nonreactive Sites on Granular Iron. *Environmental Science & Technology* 44 (14):5564-5569.
- Bozzini, C., T. Simpkin, T. Sale, D. Hood, and B. Lowder. 2006. DNAPL Remediation at Camp Lejeune using ZVI-Clay Soil Mixing. In *Fifth Battelle Conference on Remediation of Chlorinated and Recalcitrant Compounds*. Monterrey, CA.
- Chapman, S. W., and B. L. Parker. 2005. Plume persistence due to aquitard back diffusion following dense nonaqueous phase liquid source removal or isolation. *Water Resources Research* 41 (12):W12411.
- Devlin, J. F., and K. O. Allin. 2005. Major anion effects on the kinetics and reactivity of granular iron in glass-encased magnet batch reactor experiments. *Environmental Science & Technology* 39 (6):1868-1874.
- EPA. 2003. *The DNAPL remediation challenge: Is there a case for source depletion?* Edited by M. C. Kavanaugh and P. S. C. Rao. Cincinnati, OH: U.S. Environmental Protection Agency, National Risk Management Research Laboratory.
- Fagerlund, F., T. H. Illangasekare, T. Phenrat, H. J. Kim, and G. V. Lowry. 2012. PCE dissolution and simultaneous dechlorination by nanoscale zero-valent iron particles in a DNAPL source zone. *Journal of Contaminant Hydrology* 131 (1-4):9-28.
- Farrell, J., N. Melitas, M. Kason, and T. Li. 2000. Electrochemical and column investigation of iron-mediated reductive dechlorination of trichloroethylene and perchloroethylene. *Environmental Science & Technology* 34 (12):2549-2556.
- Fogler, H. Scott. 1999. *Elements of chemical reaction engineering, Prentice-Hall international series in the physical and chemical engineering sciences*. Upper Saddle River, N.J.: Prentice Hall PTR.
- Gillham, R. W., and S. F. O'Hannesin. 1994. Enhanced degradation of halogenated aliphatics by zero-valent iron. *Ground Water* 32 (6):958-967.

- Grant, G. P., and B. H. Kueper. 2004. The influence of high initial concentration aqueous-phase TCE on the performance of iron wall systems. *Journal of Contaminant Hydrology* 74 (1-4):299-312.
- Henderson, A. D., and A. H. Demond. 2007. Long-term performance of zero-valent iron permeable reactive barriers: A critical review. *Environmental Engineering Science* 24 (4):401-423.
- Johnson, K. A., and R. S. Goody. 2011. The Original Michaelis Constant: Translation of the 1913 Michaelis-Menten Paper. *Biochemistry* 50 (39):8264-8269.
- Johnson, T. L., M. M. Scherer, and P. G. Tratnyek. 1996. Kinetics of halogenated organic compound degradation by iron metal. *Environmental Science & Technology* 30 (8):2634-2640.
- Kingston, J. L. T., P. R. Dahlen, and P. C. Johnson. 2010. State-of-the-practice review of in situ thermal technologies. *Ground Water Monitoring and Remediation* 30 (4):64-72.
- Klausen, J., P. J. Vikesland, T. Kohn, D. R. Burris, W. P. Ball, and A. L. Roberts. 2003. Longevity of granular iron in groundwater treatment processes: Solution composition effects on reduction of organohalides and nitroaromatic compounds. *Environmental Science & Technology* 37 (6):1208-1218.
- Lemming, G., S. G. Nielsen, K. Weber, G. Heron, R. S. Baker, J. A. Falkenberg, M. Terkelsen, C. B. Jensen, and P. L. Bjerg. 2013. Optimizing the Environmental Performance of In Situ Thermal Remediation Technologies Using Life Cycle Assessment. *Ground Water Monitoring and Remediation* 33 (3):38-51.
- Li, L., and C. H. Benson. 2010. Evaluation of five strategies to limit the impact of fouling in permeable reactive barriers. *Journal of Hazardous Materials* 181 (1-3):170-180.
- Matheson, L. J., and P. G. Tratnyek. 1994. Reductive Dehalogenation of Chlorinated Methanes by Iron Metal. *Environmental Science & Technology* 28 (12):2045-2053.
- Olson, Mitchell R., Thomas C. Sale, Charles D. Shackelford, Christopher Bozzini, and Jessica Skeean. 2012. Chlorinated Solvent Source-Zone Remediation via ZVI-Clay Soil Mixing: 1-Year Results. *Ground Water Monitoring & Remediation* 32 (3):63-74.
- Orth, W. S., and R. W. Gillham. 1996. Dechlorination of trichloroethene in aqueous solution using Fe-O. *Environmental Science & Technology* 30 (1):66-71.
- Pankow, J.F., and J.A. Cherry. 1996. *Dense chlorinated solvents and other DNAPLs in groundwater: History, behavior, and remediation*. Portland, OR: Waterloo Press.
- Puls, R. W., D. W. Blowes, and R. W. Gillham. 1999. Long-term performance monitoring for a permeable reactive barrier at the US Coast Guard Support Center, Elizabeth City, North Carolina. *Journal of Hazardous Materials* 68 (1-2):109-124.
- Ritter, K., M. S. Odziemkowski, and R. W. Gillham. 2002. An in situ study of the role of surface films on granular iron in the permeable iron wall technology. *Journal of Contaminant Hydrology* 55 (1-2):87-111.

Scherer, M. M., B. A. Balko, D. A. Gallagher, and P. G. Tratnyek. 1998. Correlation analysis of rate constants for dechlorination by zero-valent iron. *Environmental Science & Technology* 32 (19):3026-3033.

Shackelford, C. D., T. C. Sale, and M.R. Liberati. 2005. In-situ remediation of chlorinated solvents using zero valent iron and clay mixtures: A case history. In *Waste Containment and Remediation*, edited by A. Alshawabkeh, C. H. Benson, P. J. Culligan, J. C. Evans, B. A. Gross, D. Narejo, R. Reddy, C. D. Shackelford and J. G. Zornberg. Geotechnical Special Publication 142 (CD ROM), Reston, VA: ASCE.

Song, H., and E. R. Carraway. 2006. Reduction of chlorinated methanes by nano-sized zero-valent iron. Kinetics, pathways, and effect of reaction conditions. *Environmental Engineering Science* 23 (2):272-284.

Stroo, H. F., A. Leeson, J. A. Marqusee, P. C. Johnson, C. H. Ward, M. C. Kavanaugh, T. C. Sale, C. J. Newell, K. D. Pennell, C. A. Lebron, and M. Unger. 2012. Chlorinated Ethene Source Remediation: Lessons Learned. *Environmental Science & Technology* 46 (12):6438-6447.

Stroo, H. F., M. Unger, C. H. Ward, M. C. Kavanaugh, C. Vogel, A. Leeson, J. A. Marqusee, and B. P. Smith. 2003. Remediating chlorinated solvent source zones. *Environmental Science & Technology* 37 (11):224A-230A.

Taghavy, A., J. Costanza, K. D. Pennell, and L. M. Abriola. 2010. Effectiveness of nanoscale zero-valent iron for treatment of a PCE-DNAPL source zone. *Journal of Contaminant Hydrology* 118 (3-4):128-142.

U.S.EPA. 2012. Fourth Five-Year Review Report fo Outboard Marine Corporation Superfund Site. Chicago, IL: U.S.EPA Region 5.

Wadley, S. L. S., R. W. Gillham, and L. Gui. 2005. Remediation of DNAPL source zones with granular iron: Laboratory and field tests. *Ground Water* 43 (1):9-18.

Wust, W. F., R. Kober, O. Schlicker, and A. Dahmke. 1999. Combined zero- and first-order kinetic model of the degradation of TCE and cis-DCE with commercial iron. *Environmental Science & Technology* 33 (23):4304-4309.

## CHAPTER 4

### HYDRAULIC IMPLICATIONS OF BENTONITE ADDITION DURING ZVI-CLAY SOIL MIXING

#### *Synopsis of Chapter*

ZVI-Clay is a remediation technology that uses soil mixing techniques to deliver zero valent iron (ZVI) and bentonite (Clay) into chlorinated solvent source zones. ZVI-Clay applications use bentonite in smaller amounts (1 to 3%, dry soil basis) than those typically used for contaminant stabilization applications (>5%). Laboratory studies were conducted to evaluate the hydraulic conductivity,  $K$  ( $\text{m}\cdot\text{s}^{-1}$ ), in soils mixed with small amounts of bentonite amounts ranging from 0.5 to 4% (dry soil basis). Two soil types were evaluated: a well-sorted fine sand (initial  $K = 10^{-4} \text{ m}\cdot\text{s}^{-1}$ ) and a moderately-sorted fine sand with silt (initial  $K = 10^{-8} \text{ m}\cdot\text{s}^{-1}$ ). In the fine sand,  $K$  was reduced by about a factor of 10 for each percent bentonite added to the soils. In the silty sand, only minor reductions in  $K$  were observed with addition of up to 4% bentonite. Flow modeling was conducted using MODFLOW to evaluate impacts of reduction in  $K$  on site-scale groundwater flow patterns within and in the region of the treated soil body. Results indicate that impacts on regional flow patterns (i.e., outside of the treated soil body) are largely independent of the flow reduction within the treated soils, given a reduction in  $K$  by at least an order of magnitude. Taken together, results of laboratory testing and flow modeling indicate that the amount of bentonite added to transmissive soils can have a substantial impact on residence time within treated soils.

## 4.1 Introduction

ZVI-Clay is an emerging technology for remediation of chlorinated solvent source zones that involves soil mixing of zero-valent iron (ZVI) and bentonite (clay). Implementation of this technology utilizes soil mixing equipment to achieve homogenization of soils and uniform delivery of reactive media. Within the treated soils, the presence of ZVI and bentonite serves two primary treatment benefits. First, anaerobic corrosion of ZVI in the presence of many of the common chlorinated solvents, such as trichloroethene (TCE) and tetrachloroethene (PCE), drives reductive dechlorination (Gillham and O'Hannesin 1994). Second, inclusion of bentonite reduces the hydraulic conductivity,  $K$  ( $\text{m}\cdot\text{s}^{-1}$ ), of the treated soils (Olson et al. 2012). Secondary benefits of bentonite include reduction in the mechanical energy required for mixing and facilitating a uniform delivery of ZVI (Wadley et al. 2005).

Extensive research has been conducted on hydraulic conductivity of porous media admixed with bentonite. Primarily, this research has addressed hydraulic containment structures such as vertical cutoff walls (Yeo et al. 2005) or horizontal liners to waste contaminant systems (Kenney et al. 1992; Shackelford and Moore 2013). In such applications, bentonite is typically mixed with soils at levels of 5% (by weight) or greater, with target  $K$  values of less than  $10^{-9} \text{ m}\cdot\text{s}^{-1}$ . In vertical cut-off walls, such  $K$ -values (combined with a low hydraulic gradient) can provide long-term isolation of a contamination source by reducing advective discharge to a level where diffusion becomes the predominant transport mechanism (Shackelford 1990) and solute transport rates are restricted (Yeo et al. 2005). In ZVI-Clay systems, the reduction in  $K$  is coupled with ZVI-mediated degradation. As such, the objective of including bentonite in ZVI-Clay applications is not permanent isolation of a source, but rather to enhance the benefits of ZVI-mediated degradation by reducing the groundwater flow so as to extend the residence time of contaminants within the system. Thus, achieving  $K$  values of less than  $10^{-9} \text{ m}\cdot\text{s}^{-1}$  may not be necessary in soils treated with ZVI-Clay; a reduction in  $K$  by a lesser amount may be sufficient to extend the residence time such that most of the contaminant mass will be susceptible to ZVI-mediated degradation.

Typical ZVI-Clay applications have involved admixing soils with 1 to 3% bentonite. Castelbaum and Shackelford (2009) reported results of laboratory column studies in which uniform fine-grained sands were mixed with 0.6 to 8% bentonite. Reported  $K$ -values declined from about  $10^{-4} \text{ m}\cdot\text{s}^{-1}$  in unmixed sands to about  $10^{-8} \text{ m}\cdot\text{s}^{-1}$  at bentonite contents of greater than 3%. Bozzini et al. (2006) presented a case-study of a field application in which about  $5000 \text{ m}^3$  of soil were treated with 2% ZVI and 1% bentonite. Post-mixing  $K$  values were reported as  $5 \times 10^{-6} \text{ m}\cdot\text{s}^{-1}$  within the treated soil body, compared to  $K$ -values of  $4 \times 10^{-5}$  and  $2 \times 10^{-4} \text{ m}\cdot\text{s}^{-1}$  in wells located adjacent to the treated soil body, which indicates a reduction by about an order of magnitude. Olson et al. (2012) discussed a field application in which  $23,000 \text{ m}^3$  of soil were admixed with 2% ZVI and 3% bentonite. In seven monitoring wells located within the treated soil region, average pre- and post-mixing  $K$  values were  $1.7 \times 10^{-5}$  and  $5.2 \times 10^{-8} \text{ m}\cdot\text{s}^{-1}$ , respectively. This indicates a reduction of about 2.5 orders of magnitude. These results suggest that the  $K$  of treated soils can be controlled, to some extent, via the amount of bentonite added. However, only limited information has appeared in the literature on the ability to control  $K$  values in soils mixed with low amounts (i.e., < 5%) of bentonite and subsequent impacts on regional water flow patterns.

This research has two primary objectives: (a) evaluation of hydraulic conductivity as a function of bentonite content in mixed soils with bentonite content of less than 5% and (b) modeling groundwater flow through a treated soil zone as a function of  $K$  reduction. In support of this objective, laboratory experiments were conducted to evaluate  $K$  values in two field-collected soil specimens admixed with varying amounts of bentonite, ranging from 0.5 to 4%. In addition, MODFLOW groundwater flow modeling was conducted in the region of a treated source zone. MODFLOW modeling was conducted under steady-state conditions; drainage of excess water that may be delivered during mixing was not considered in the present model.

## 4.2 Methods and Materials

Laboratory column studies were conducted to evaluate hydraulic conductivity,  $K$  ( $\text{m}\cdot\text{s}^{-1}$ ), in two soil types as a function of bentonite content. This section describes methods and materials used for  $K$  testing.

### 4.2.1 Materials

Testing of  $K$  as a function of bentonite content was conducted using two field-collected soils: a well-sorted fine-grained sand that contained 4.3% silt (fine sand) and a moderately-sorted fine-grained sand that contained 32% silt (silty sand). Particle size distribution curves are shown (Figure 4-1). Black Hills Bond unmodified sodium bentonite was supplied by Black Hills Bentonite (Mills, WY). Water used for the studies consisted of tap water (City of Fort Collins), de-aired under a vacuum of 25 inches of mercury.

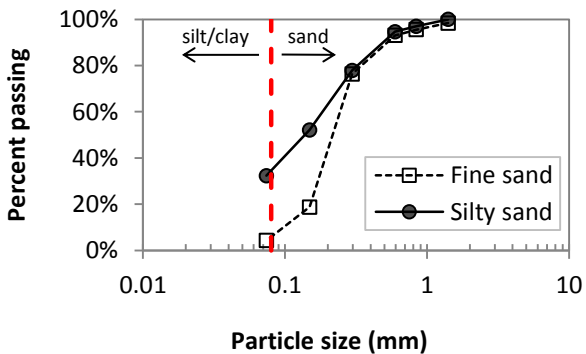


Figure 4-1. Particle size distribution curve for both types of porous media.

#### 4.2.2 K-Testing

Testing of hydraulic conductivity,  $K$  ( $\text{m}\cdot\text{s}^{-1}$ ), as a function of bentonite content in two media types was conducted in acrylic-walled permeameter cells which measured 5-cm in I.D. and 15 cm in length. Media types consisted of a fine sand and silty sand. The fine sand was tested with bentonite contents of 0, 0.5, 0.75, 1, 2, 3, and 4% (dry soil basis). The silty sand was tested with 0, 1, 2, and 4% bentonite.

Different methods for specimen preparation and testing were used for low- $K$  mixtures ( $K < 10^{-5}$   $\text{m}\cdot\text{s}^{-1}$ ) and high- $K$  mixtures ( $K > 10^{-5}$   $\text{m}\cdot\text{s}^{-1}$ ). High- $K$  samples consisted of fine sands with low bentonite content ( $\leq 1\%$ ). Low- $K$  samples consisted of fine sands with higher bentonite contents ( $>1\%$ ) and silty sands with any of the tested bentonite contents (0 to 4%). For specimen preparation of high- $K$  mixtures, sand/bentonite mixtures were loaded, dry, into the permeameter cells and then saturated with water by filling the cells from the bottom upward. Low- $K$  mixtures could not be filled with water from the bottom up, as the higher resistance to water permeation may lead to formation of fissures and, subsequently, preferential flow paths. As such, high-bentonite sands were hand-mixed with water in plastic zip-lock bags; the water-saturated materials were then extruded into the permeameter cells. For both low- $K$  and high- $K$  samples, two permeameter cells were initially stacked to a height of 30 cm and filled with specimen. After a period of several days for consolidation, the upper 15 cm of sample was discarded and the more highly-consolidated lower 15 cm was used for  $K$  testing.

Measurement of  $K$  also involved different techniques for low- $K$  and high- $K$  samples. For high- $K$  samples, constant flow techniques were used for analysis. Water was pumped through the columns at a series of six fixed flow rates,  $Q$  ( $\text{mL}\cdot\text{min}^{-1}$ ), ranging from 0.41 to 4.7  $\text{mL}\cdot\text{min}^{-1}$  (corresponding to Darcy flux,  $q$  ( $\text{m}\cdot\text{d}^{-1}$ ), values of 3.0 to 3.5  $\text{m}\cdot\text{d}^{-1}$ ). The pressure drop,  $\Delta h$  (cm water), across the samples was logged automatically using Solinst (Georgetown, ON) Model 3001 Leveloggers. For the constant-flow studies, estimated  $K$  values were obtained by plotting  $\Delta h$  vs.  $q$ . For low- $K$  sample specimens, falling head techniques were used for analysis. The falling head reservoir was filled to a level such that the initial

pressure drop across the samples was approximately 1 m of water. The declining values of  $\Delta h$  over time were automatically logged using Solinst Levelloggers. For the falling-head studies, estimated  $K$  values for the samples were obtained using the following equation:

$$K = \frac{aL}{At} \ln\left(\frac{h_0}{h_t}\right) \quad (1)$$

where  $a$  ( $\text{m}^2$ ) is the cross-sectional area of the falling-head reservoir,  $A$  ( $\text{m}^2$ ) is the cross-sectional area of the specimen,  $L$  (m) is the length of the specimen,  $t$  (d) is the time,  $h_0$  (m) is the initial head drop across the specimen and  $h_t$  (m) is the head drop across the specimen at time  $t$ . The value of  $K$  was determined by linear regression of a plot of  $\ln(h_0/h_t)$  versus  $At/aL$ .

Water content and density of the bentonite-mixed sands were calculated after conductivity testing by weighing the column contents, drying at  $60^\circ\text{C}$ , and re-weighing the dried samples.

#### 4.2.3 Groundwater Flow Modeling

Groundwater flow modeling in the region of bentonite-mixed soils was conducted based on a ZVI-Clay field application at Site 89, Marine Corps Base Camp Lejeune, North Carolina, USA (Olson et al. 2012). The primary contaminants of concern at Site 89 included trichloroethene (TCE) and 1,1,2,2-tetrachloroethane (TeCA). The ZVI-Clay technology was implemented at Site 89 in May through August 2009, when approximately  $23,000 \text{ m}^3$  of soils were admixed with 2% ZVI and 3% bentonite. A detailed description of implementation and treatment performance was published by Olson et al. (2012). The treated soils at Site 89 consisted of three treatment zones (Figure 4-2), which were selected based on initial contamination locations. The modeling conducted herein is based on Zone 3, which consisted of a 14- by 12-m rectangle. Groundwater flow in the region occurred primarily in a north-south direction with a regional gradient of 0.02.

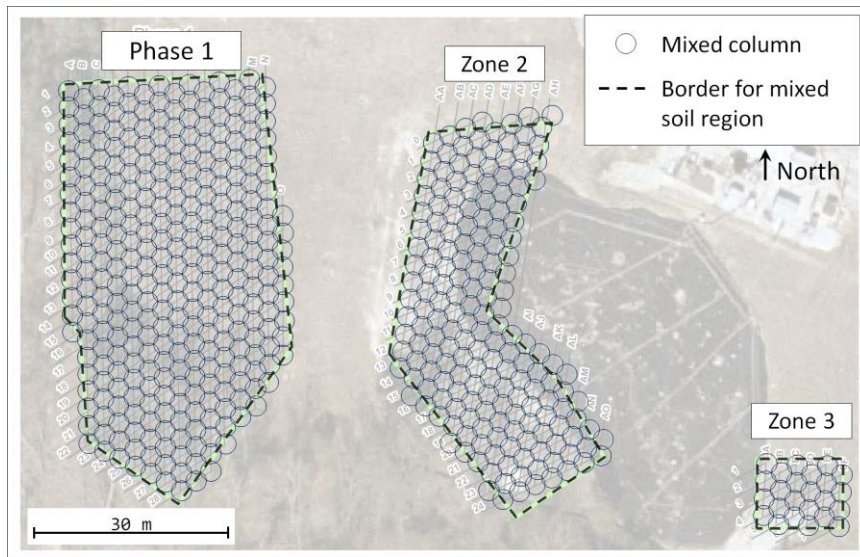


Figure 4-2. Treatment zones at Site 89, Camp Lejeune, NC (after Olson et al. 2012).

Groundwater flow modeling was conducted using Visual MODFLOW software version 4.1. The MODFLOW 2000 numeric engine was selected. Contaminant transport simulation was not included, as the objective of this modeling involved characterization of groundwater flow in the region of bentonite-mixed soils. Figure 4-3 shows the model domain, which consisted of an 80-m by 80-m region that was discretized into 80 rows and 80 columns. Isotropic conditions were assumed (vertical flow was not included in the model system). The treated soil zone, measuring 14-m ( $x$ -axis) by 12-m ( $y$ -axis) (the approximate dimensions of Zone 3 at Site 89), was located approximately in the center of the model domain.

Two hydraulic conductivity zones were assigned: one  $K$ -value was assigned to the treated soil zone and the other (background)  $K$ -value was assigned to all of the remaining cells. The background  $K$  was selected as  $1 \times 10^{-4} \text{ m}\cdot\text{s}^{-1}$ . Treated-zone  $K$ -values were selected by reducing the background  $K$  by factors of 10. The regional hydraulic gradient was fixed by applying fixed-head boundary conditions. Constant hydraulic head values of 20 m and 18.4 m were applied at the northern ( $y = 80 \text{ m}$ ) and southern

ends ( $y = 0$  m), respectively, of the model domain. Particle tracking was used to generate flow lines and to evaluate transport distances.

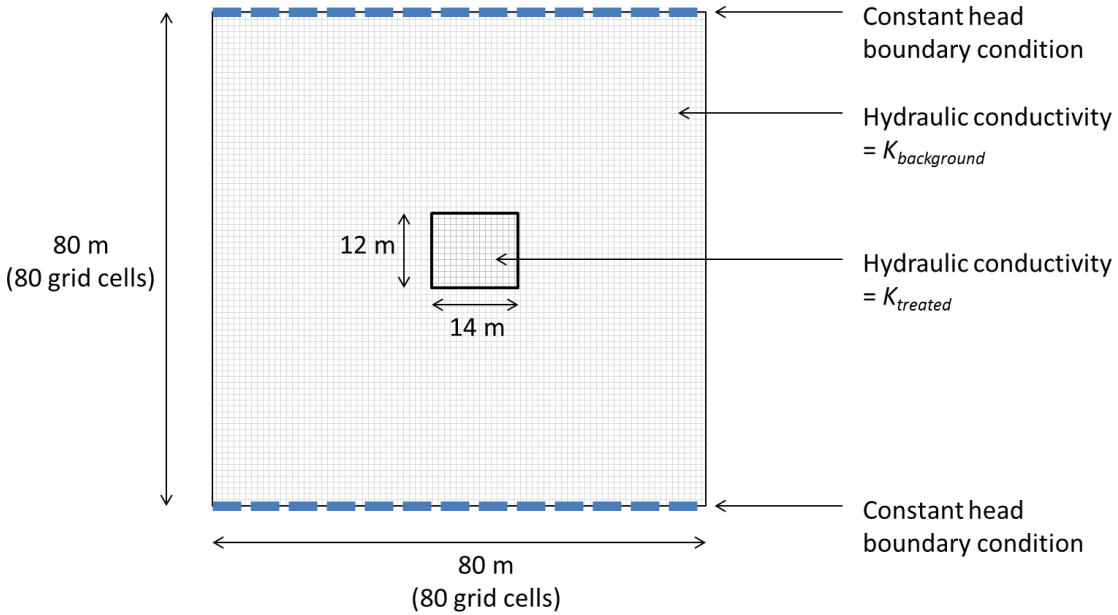


Figure 4-3. Illustration of model input domain and parameters. The grid cells are uniformly spaced throughout the model domain (the gridlines shown are not to scale).

### 4.3 Results

#### 4.3.1 K Testing

Figure 4-4 shows resulting of  $K$  testing, which was conducted on two soil types, a fine-grained sand and a silty-sand, with bentonite amounts ranging from 0 to 4%. The baseline (no bentonite) hydraulic conductivities of the two media types varied substantially:  $10^{-4}$  and  $10^{-8}$   $\text{m}\cdot\text{s}^{-1}$  for the fine-sand and silty-sand, respectively. In the fine-sand, mixing with less than 1% bentonite resulted in a decline in  $K$  by less than an order of magnitude, but  $K$  values exhibited a declining trend with an increase in

bentonite content. When mixed with bentonite amounts of 1 to 4%,  $K$ -values are reduced by about an order of magnitude for each 1% bentonite added (as a first approximation).

In the silt media, which had a much lower initial (untreated)  $K$ , bentonite content had only minor impacts on  $K$ . Although the general trend in the silt media was for  $K$  to decline with each additional percent bentonite, addition of up to 4% bentonite resulted in less than an order of magnitude reduction in  $K$ .

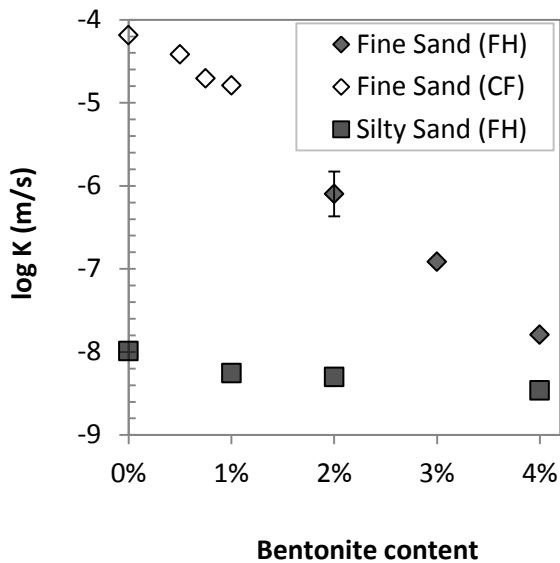


Figure 4-4.  $K$  versus bentonite content for two soil types. FH refers to values obtained using falling-head test methods; CF refers to values obtained using constant flow methods. Error bars indicate the 95% confidence interval for the mean, calculated based on triplicate analysis of the sand media at a BC of 2%.

#### 4.3.2 Groundwater Flow Modeling

Figure 4-5 to Figure 4-8 show modeled impacts on regional groundwater flow in the vicinity of a treated soil body, over a range of treated-zone  $K$ -values. Regional groundwater flow patterns are shown for systems with no flow reduction (Figure 4-5) and where treated zone  $K$ -values are reduced by factors of 10 (Figure 4-6), 100 (Figure 4-7), and 10,000 (Figure 4-8). The flow lines shown in Figure 4-5 to

Figure 4-8 were generated using particle tracking in MODFLOW. In each figure, particle tracking was conducted at three locations: (1) at the upper boundary of the model, (2) up-gradient of the treated soil zone, and (3) in the center of the treated soil zone.

Flow-lines generated from the particles placed at the upper boundary indicate regional flow patterns. Particles upgradient of the treated zone indicate the tendency of clean groundwater to enter to treated soil zone. Particles originating within the treated zone indicate the rate of flow occurring within the treated soil zone. In Figure 4-5 to Figure 4-8, the distance between arrows indicated the distance a conservative (non-reactive) particle would travel over 10 days. The length of flow lines (i.e., simulation time) is indicated in the caption of each figure.

Approximations for the treated-zone transit time can be estimated from the flow lines in Figure 4-5 to Figure 4-8. The average transit time is estimated as the time for a particle to travel half of the treated-zone length in the direction parallel to regional groundwater flow. With no flow reduction, the transit time is about 5 days. With treated-zone flow reductions by factors of 10, 100, and 10,000 the transit times are about 30 days, 220 days (0.6 years), and 22,000 days (60 years), respectively.

Figure 4-9 to Figure 4-12 show flow patterns for particles placed immediately up-gradient of the treated soil zone for systems with no flow reduction (Figure 4-9) and where treated zone  $K$ -values are reduced by factors of 10 (Figure 4-10), 100 (Figure 4-11), and 10,000 (Figure 4-12). The distance between arrows indicates the distance a particle would travel over 10 days and the length of flow lines (simulation time) is given in the caption for each figure. These results are indicative of the amount of water flowing into the soil body after treatment is applied. With a flow reduction of 10 $\times$  and 100 $\times$ , groundwater entry becomes increasingly restricted; with a flow reduction of 10,000 $\times$ , little to no groundwater enters the treated soil zone.

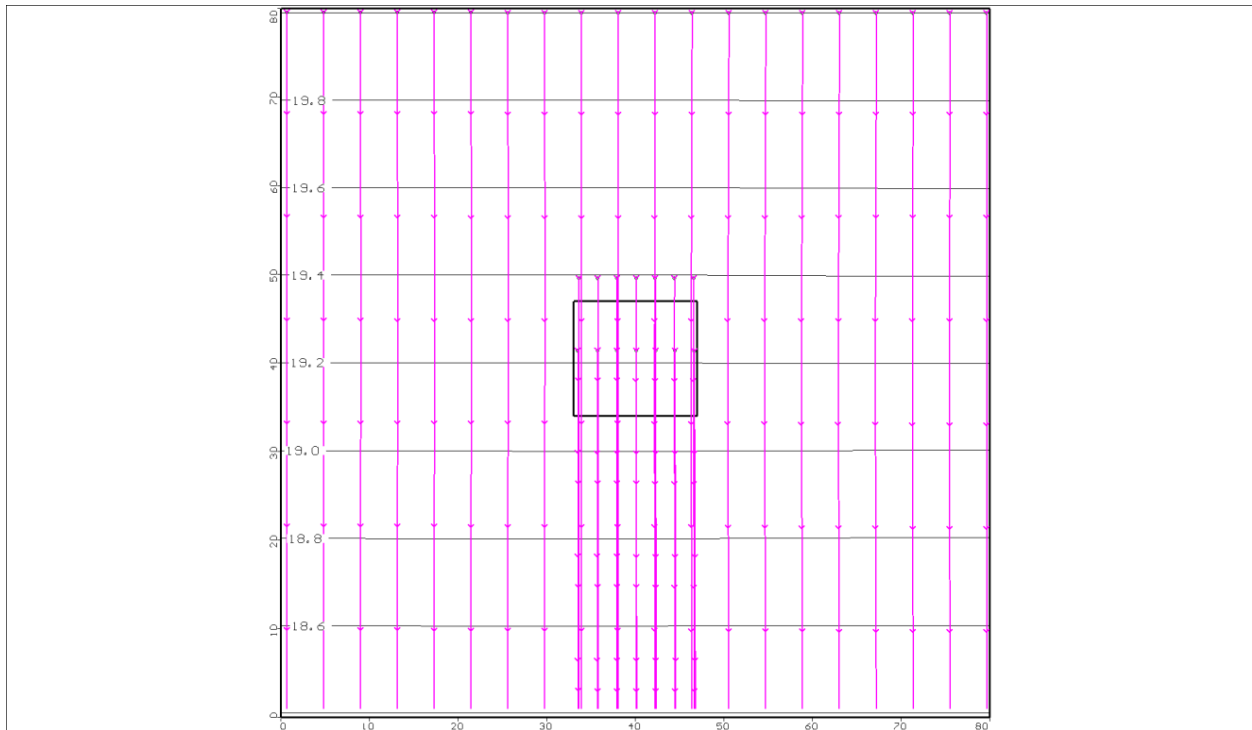


Figure 4-5. Regional flow diagram where  $K_{treated} = 10^{-4} \text{ m}\cdot\text{s}^{-1}$ , no reduction from  $K_{background}$ . The distance between flow markers represents the flow distance over 10 days. The simulation was run for 180 d (0.5 yr).

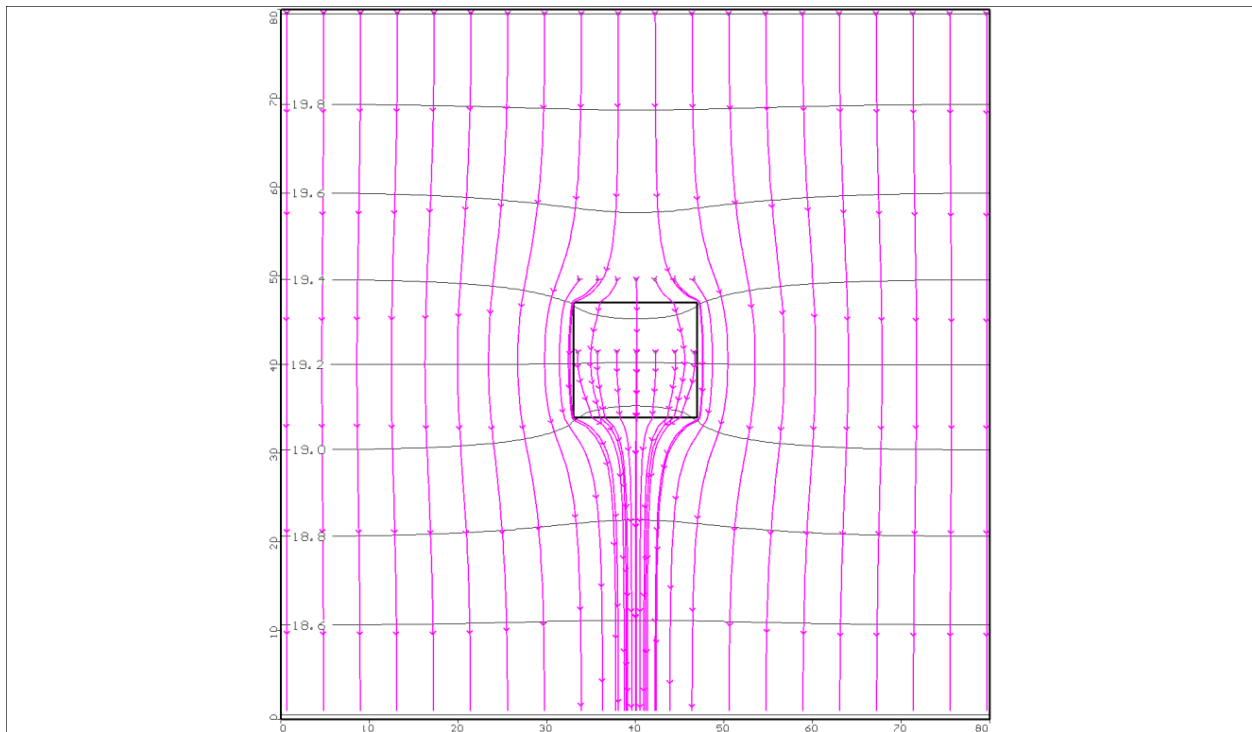


Figure 4-6. Regional flow diagram where  $K_{treated} = 10^{-5} \text{ m}\cdot\text{s}^{-1}$ , a reduction from  $K_{background}$  by a factor of 10. The distance between flow markers represents the flow distance over 10 days. The simulation was run for 180 d (0.5 yr).

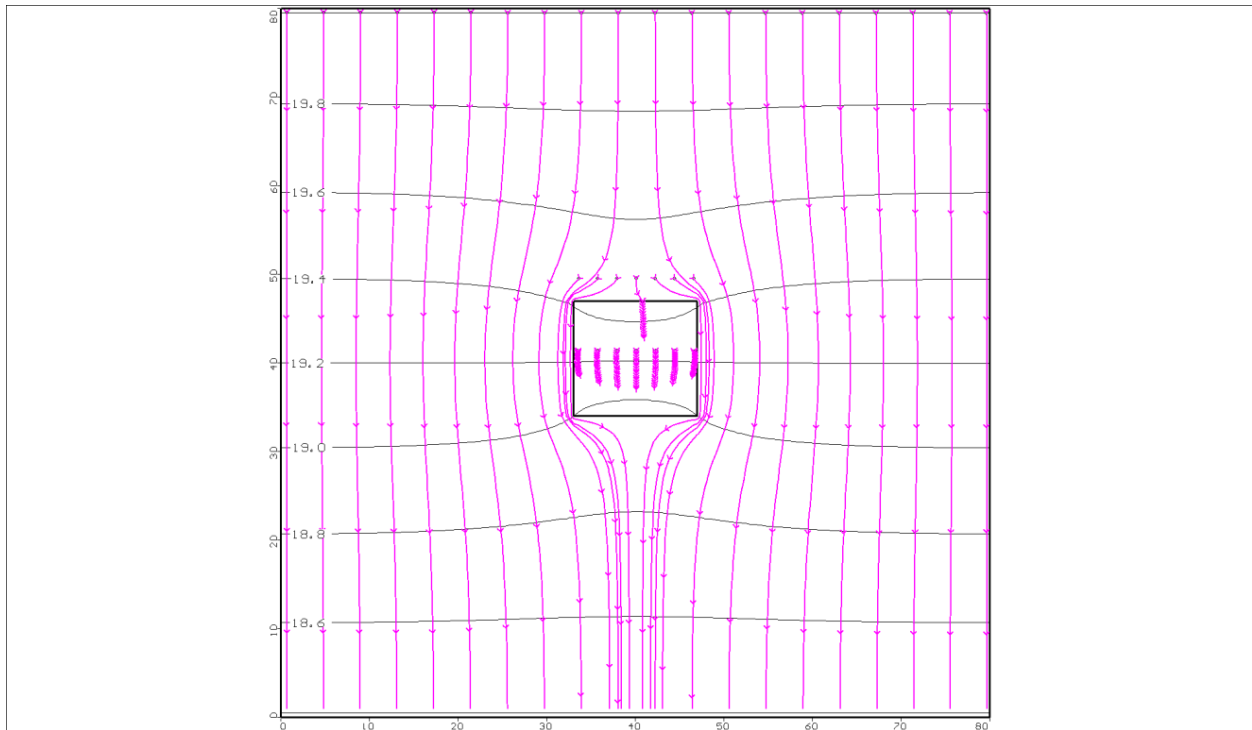


Figure 4-7. Regional flow diagram where  $K_{treated} = 10^{-6} \text{ m}\cdot\text{s}^{-1}$ , a reduction from  $K_{background}$  by a factor of 100. The distance between flow markers represents the flow distance over 10 days. The simulation was run for 180 d (0.5 yr).

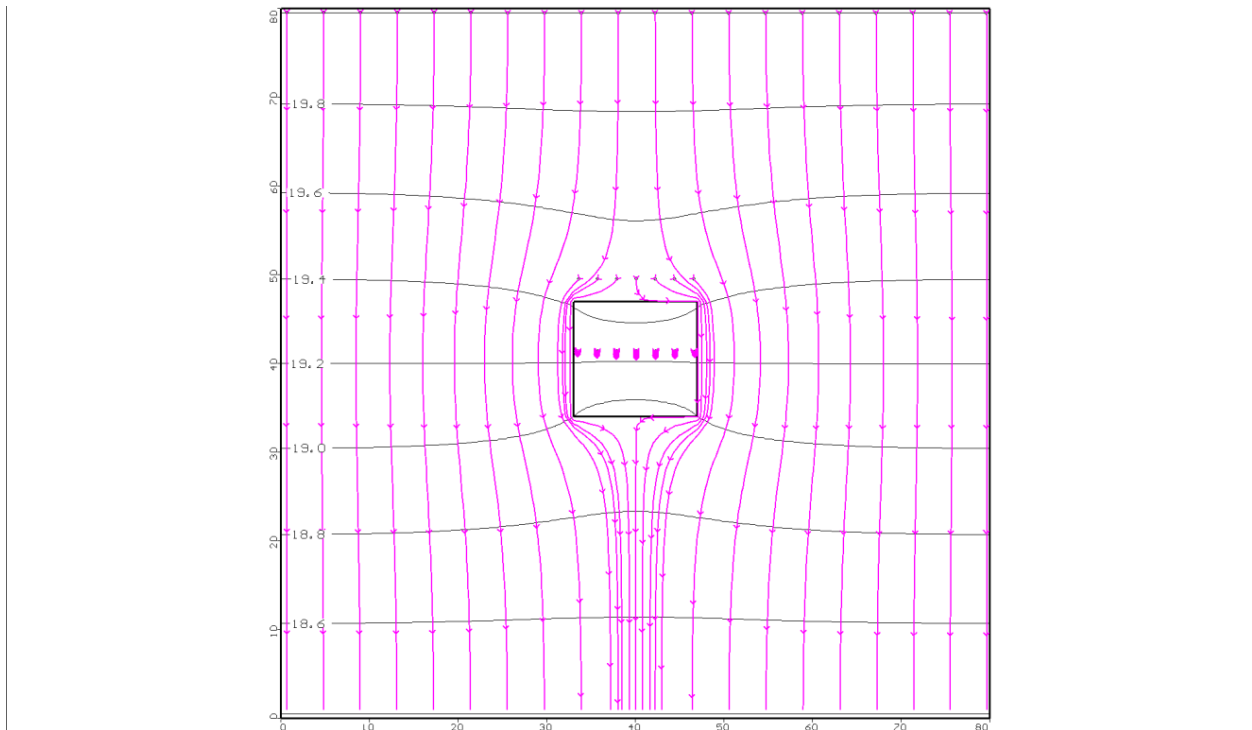


Figure 4-8. Regional flow diagram where  $K_{treated} = 10^{-8} \text{ m}\cdot\text{s}^{-1}$ , a reduction from  $K_{background}$  by a factor of 10,000. The distance between flow markers represents the flow distance over 10 days. The simulation was run for 3650 d (10 yr).

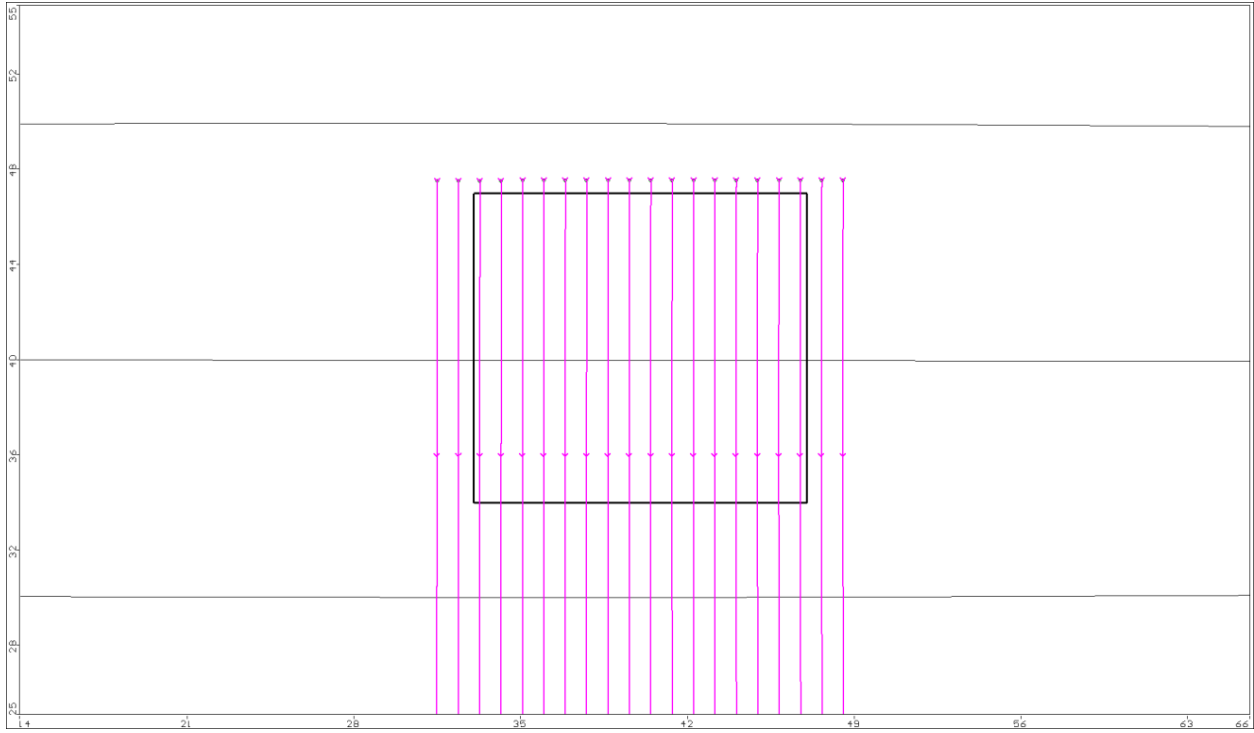


Figure 4-9. Source zone flow diagram where  $K_{treated} = 10^{-4} \text{ m}\cdot\text{s}^{-1}$ , no reduction from  $K_{background}$ . The distance between flow markers represents the flow distance over 10 days.

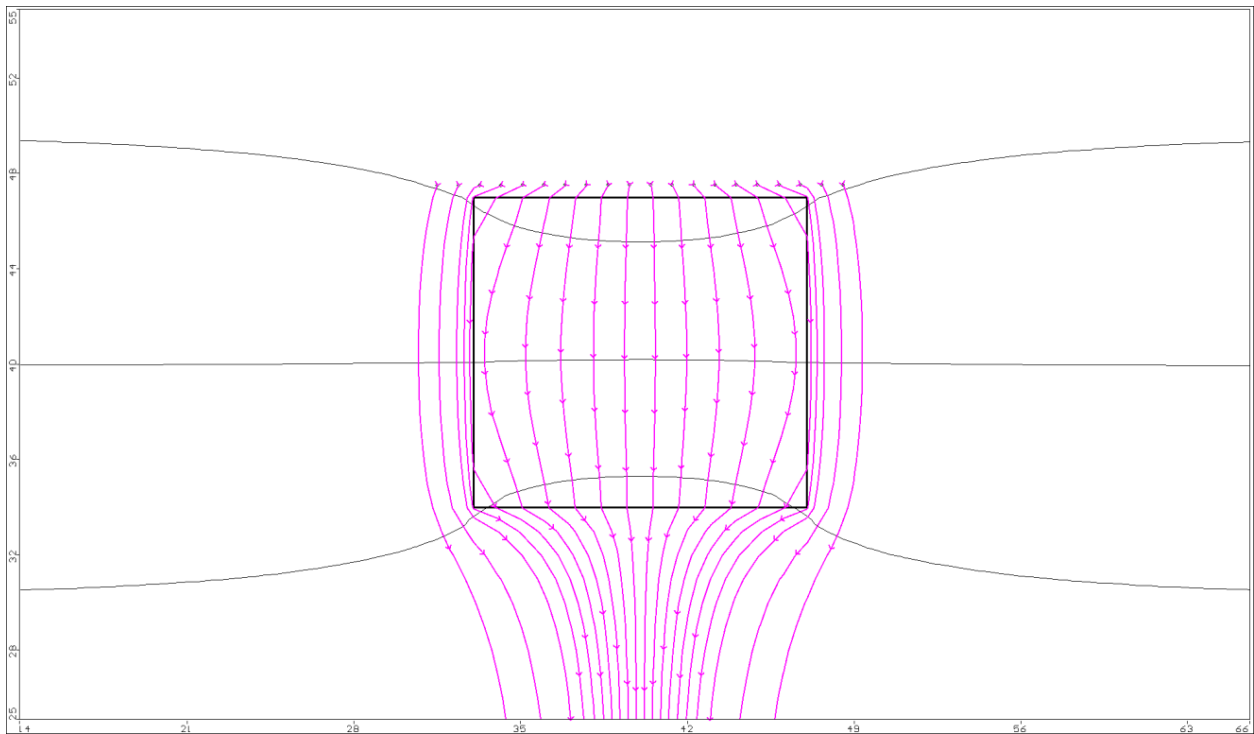


Figure 4-10. Source zone flow diagram where  $K_{treated} = 10^{-5} \text{ m}\cdot\text{s}^{-1}$ , a reduction from  $K_{background}$  by a factor of 10. The distance between flow markers represents the flow distance over 10 days. The simulation was run for a period of 365 days.

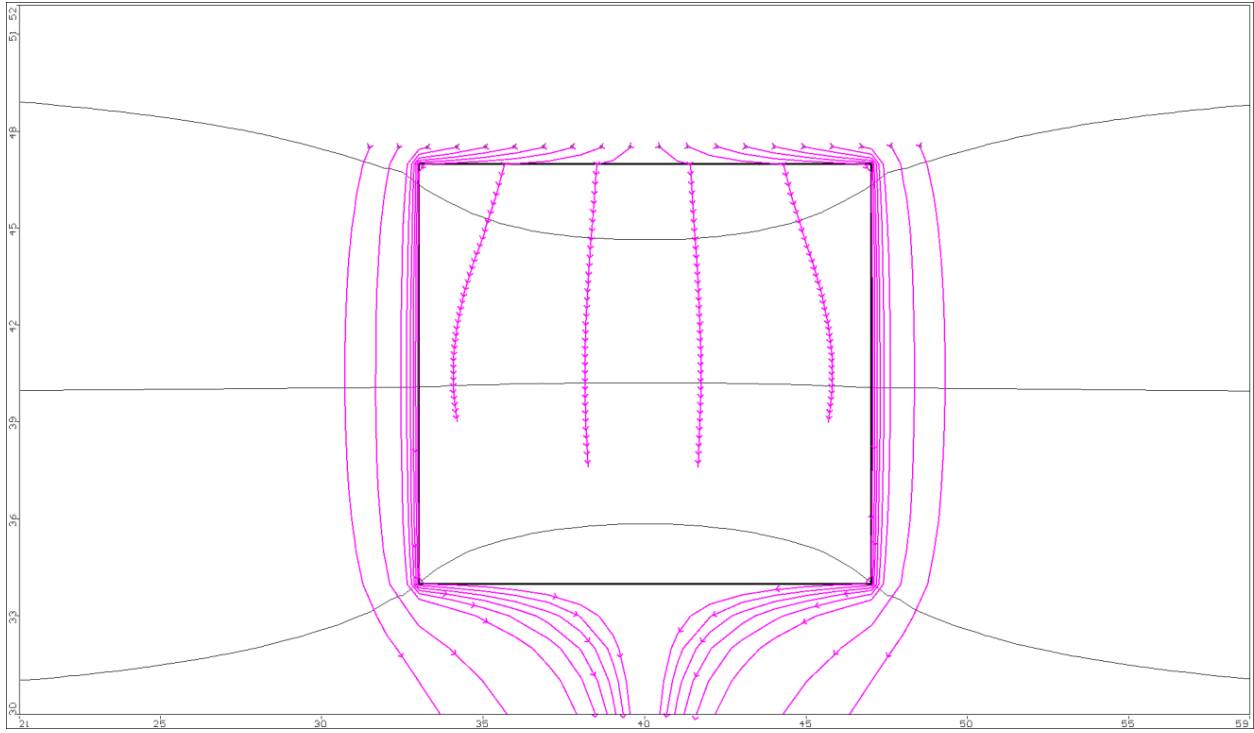


Figure 4-11. Source zone flow diagram where  $K_{treated} = 10^{-6} \text{ m}\cdot\text{s}^{-1}$ , a reduction from  $K_{background}$  by a factor of 100. The distance between flow markers represents the flow distance over 10 days. The simulation was run for a period of 365 days.

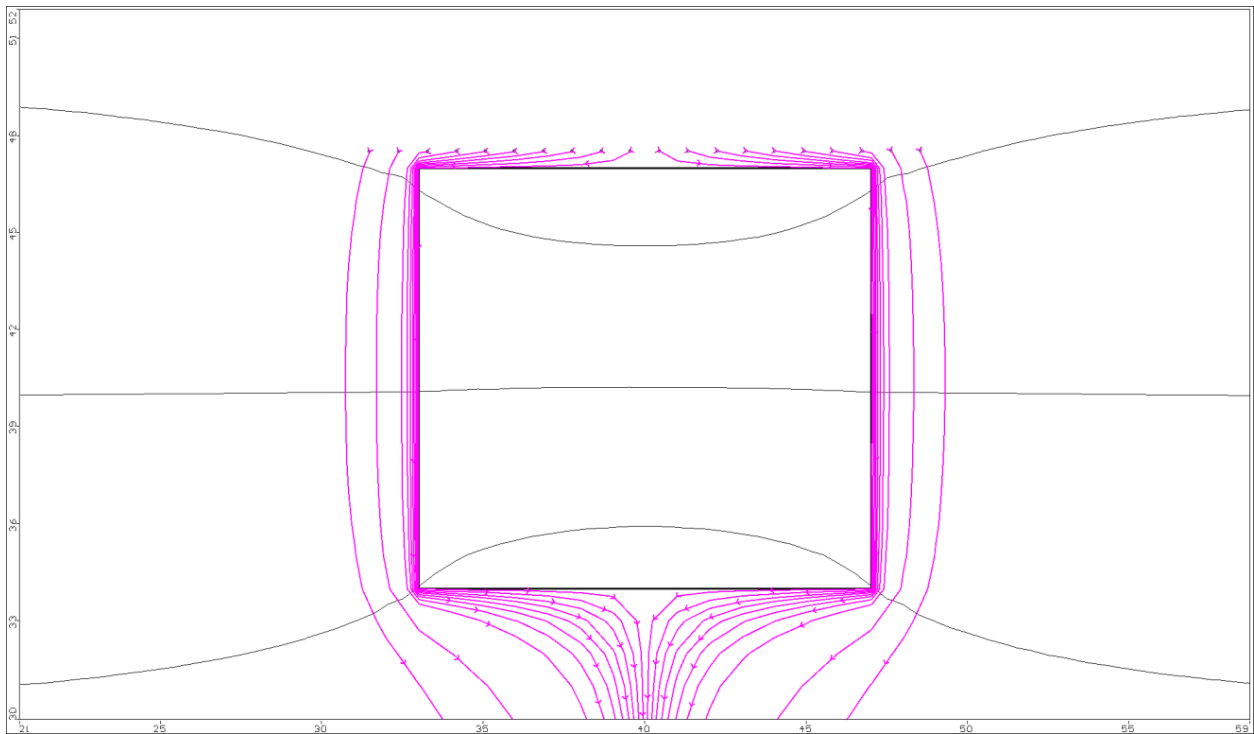


Figure 4-12. Source zone flow diagram where  $K_{treated} = 10^{-8} \text{ m}\cdot\text{s}^{-1}$ , a reduction from  $K_{background}$  by a factor of 10,000. The distance between flow markers represents the flow distance over 10 days. The simulation was run for a period of 365 days.

### 4.3.3 Comparison to Work by Others

Measurement of  $K$  in bentonite-mixed sands has been evaluated (Castelbaum and Shackelford 2009). In sands mixed with less than 4% bentonite, trends in  $K$  versus bentonite content reported by Castelbaum et al., conducted using a well-sorted fine-grained sand (grade F58 Ottawa sand), were similar to those observed in the present study. Observations included the following: (a) highly variable  $K$ -values ranging from  $10^{-5}$  to  $10^{-8}$   $\text{m}\cdot\text{s}^{-1}$  were observed in systems where  $\text{BC} < 2\%$ , (b) relatively steady  $K$ -values of  $<10^{-8}$   $\text{m}\cdot\text{s}^{-1}$  were observed in systems where  $\text{BC} > 2\%$ , and (c) non-uniform distribution of bentonite was reported in systems where  $\text{BC} < 3\%$ . Thus, the trend in  $K$ -reduction with increasing bentonite content is apparent, but is much more variable than that observed in the present experiment. A possible cause for the differing results may be related to the different types of porous media used in the two experiments; the uniform fine-grained sand used by Castelbaum et al. may not have supported a uniform distribution of bentonite as well as the poorly-sorted field sand sample in the present experiment. A more regular distribution of bentonite would likely result in a more consistent trend in  $K$  versus  $\text{BC}$ .

In field applications, mixing of media of moderately high pre-mixing  $K$  values with a  $\text{BC}$  of 1% resulted in a reduction in  $K$  by about 1 order of magnitude (Bozzini et al. 2006) and mixing with 3% bentonite resulted in reported reductions in  $K$  by about 2.5 orders of magnitude (Olson et al. 2012). Both of these field results are consistent with the empirical observation that  $K$  is reduced by about an order of magnitude for each percent bentonite added, under certain conditions (i.e.,  $\text{BC} < 4\%$  in media of moderately high initial conductivity).

## 4.4 Conclusions

This work has shown that post-mixing  $K$  values can be engineered, to an extent, by the amount of bentonite added. In a fine-sand media of moderately high  $K$  (pre-mixing),  $K$  is reduced by approximately

a factor of 10 for each percent bentonite added. However, in silty-sand media with a low initial  $K$ -value ( $10^{-6} \text{ m}\cdot\text{s}^{-1}$ ), only minor impacts to  $K$  are achieved at  $\text{BC} < 4\%$ .

Groundwater flow modeling indicates that the impacts on regional groundwater flow patterns are similar when  $K$  in the treated-zone is reduced by factors of 10 to 10,000; groundwater flow pathlines tend to diverge around the treated soil body. The primary impact of  $K$  reduction occurs within treated soils.

In the context of ZVI-Clay field applications, the objective is to extend the residence time so as to maximize the impact of ZVI-mediated degradation of contaminants. By analyzing the flow pathlines, we see that reduction in  $K$  by factors of 10, 100, and 10,000 result in treated-zone average transit times on the order of 0.1, 1, and 100 years, respectively. Results of this work indicate that inclusion of bentonite can have a substantial impact on the contaminant residence time within the treated soil zone when applied to soils of moderately high initial hydraulic conductivity.

## REFERENCES

- Bozzini, C., T. Simpkin, T. Sale, D. Hood, and B. Lowder. 2006. DNAPL Remediation at Camp Lejeune using ZVI-Clay Soil Mixing. In *Fifth Battelle Conference on Remediation of Chlorinated and Recalcitrant Compounds*. Monterrey, CA.
- Castelbaum, D., and C. D. Shackelford. 2009. Hydraulic conductivity of bentonite slurry mixed sands. *Journal of Geotechnical and Geoenvironmental Engineering* 135 (12):1941-1956.
- Gillham, R. W., and S. F. O'Hannesin. 1994. Enhanced degradation of halogenated aliphatics by zero-valent iron. *Ground Water* 32 (6):958-967.
- Kenney, T. C., W. A. Vanveen, M. A. Swallow, and M. A. Sungaila. 1992. Hydraulic Conductivity of Compacted Bentonite Sand Mixtures. *Canadian Geotechnical Journal* 29 (3):364-374.
- Olson, Mitchell R., Thomas C. Sale, Charles D. Shackelford, Christopher Bozzini, and Jessica Skeeane. 2012. Chlorinated Solvent Source-Zone Remediation via ZVI-Clay Soil Mixing: 1-Year Results. *Ground Water Monitoring & Remediation* 32 (3):63-74.
- Shackelford, C. D. 1990. Transit-Time Design of Earthen Barriers. *Engineering Geology* 29 (1):79-94.
- Shackelford, C. D., and S. M. Moore. 2013. Fickian diffusion of radionuclides for engineered containment barriers: Diffusion coefficients, porosities, and complicating issues. *Engineering Geology* 152 (1):133-147.
- Wadley, S. L. S., R. W. Gillham, and L. Gui. 2005. Remediation of DNAPL source zones with granular iron: Laboratory and field tests. *Ground Water* 43 (1):9-18.
- Yeo, S. S., C. D. Shackelford, and J. C. Evans. 2005. Membrane behavior of model soil-bentonite backfills. *Journal of Geotechnical and Geoenvironmental Engineering* 131 (4):418-429.

## CHAPTER 5

### DISSOLUTION, TRANSPORT, AND DEGRADATION OF TCE NAPL IN SOILS MIXED WITH ZVI AND BENTONITE: COLUMN STUDIES AND MODELING

#### *Synopsis of Chapter*

Zero valent iron (ZVI)-mediated degradation of chlorinated solvents in groundwater has been the subject of much research. In comparison, research into the interaction between ZVI and Non-Aqueous Phase Liquid (NAPL)-phase chlorinated solvents is rather limited. Specifically, the use of soil mixing to deliver ZVI into a NAPL source zone has not been thoroughly evaluated in the literature. To address this knowledge gap, the research presented herein was designed to evaluate remediation of NAPL source zones using soil mixing for delivery of zero valent iron (ZVI) and bentonite clay. This paper presents laboratory studies and mathematical modeling of TCE NAPL dissolution and subsequent degradation in homogeneous systems. An equilibrium modeling approach was adopted to describe dissolution of NAPL; a PDE was developed accordingly and an analytical solution for NAPL dissolution was obtained. Numerical methods were used to solve the reactive-transport PDEs for TCE and related degradation products. Established ZVI-mediated TCE degradation pathways, including hydrogenolysis, hydrolysis, and  $\beta$ -elimination steps, are included in the model. Laboratory column studies were conducted at two flow rates to test the model and provide estimates for model input parameters. Finally, the model is used to predict field-scale performance of a ZVI-Clay remedy in a homogeneous 10-m long source zone. Model output demonstrates the benefits of coupling groundwater flow reduction with degradation to maximize performance.

## 5.1 Introduction

Soil mixing is an *in situ* remediation approach that is designed to reduce the mobility, bioavailability, and/or concentrations of contaminants in treated soils. Since the introduction of soil mixing in the United States in the 1980s (Jasperse and Ryan 1987), the technique has seen wide use. Typical soil mixing applications have involved solidification/stabilization by admixing impacted soils with cement and bentonite (Paria and Yuet 2006). Subsequently, soil mixing has been enhanced to facilitate removal or destruction of contaminant mass (Day and Ryan 1995). For example, soil mixing has been coupled with steam injection to deplete volatile organic compounds (Siegrist et al. 1995). In addition, soil mixing has been used for delivery of reagents designed to degrade or sequester contaminants in treated soils. Such reagents include sorptive media such as activated carbon (Zimmerman et al. 2004), chemical oxidants (Siegrist et al. 2011), and chemical reductants (Wadley et al. 2005). Soil mixing is a robust delivery approach, in that practitioners can select reagents based on contaminants and site-specific remediation objectives.

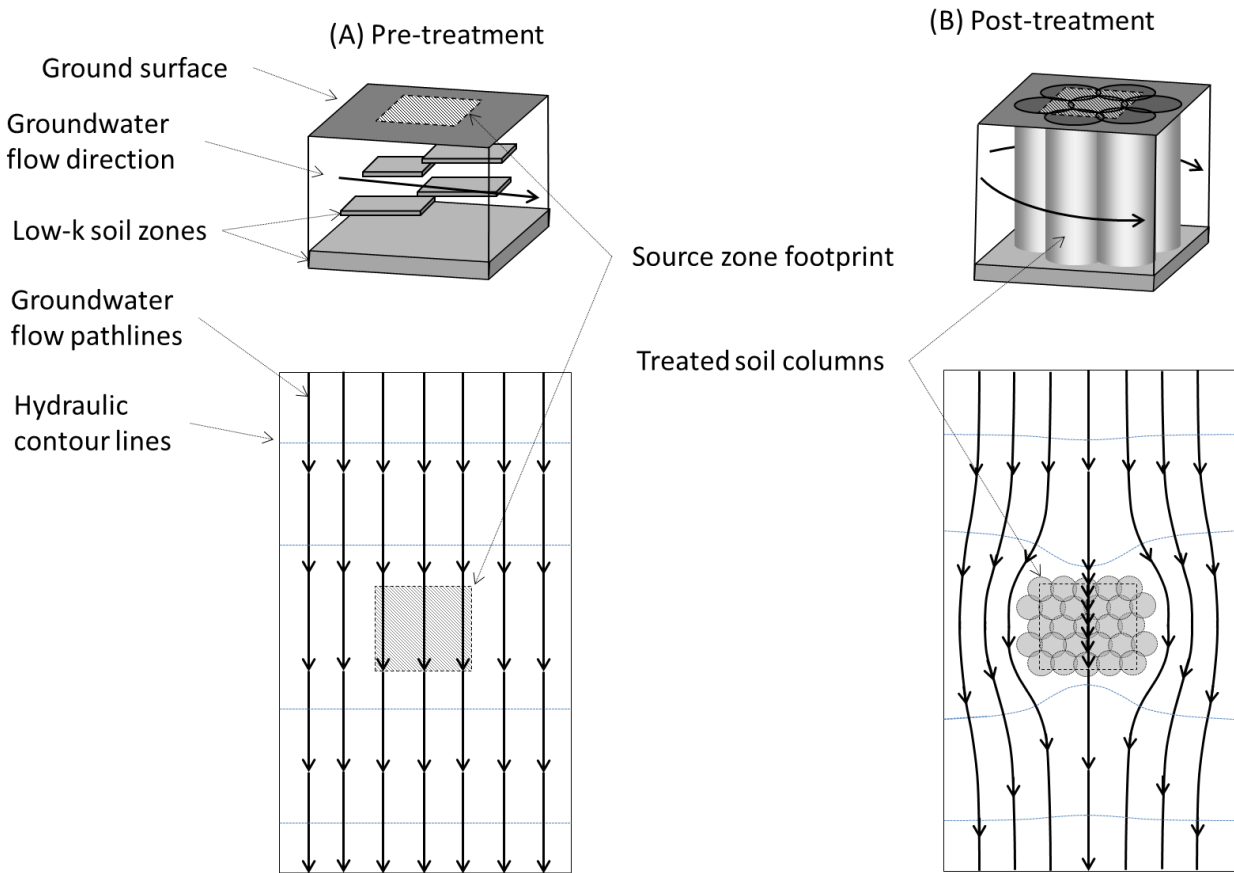
Soil mixing is particularly well-suited for remediation of soils impacted by dense non-aqueous phase liquids (DNAPLs) including trichloroethene (TCE) and perchloroethene (PCE). The primary challenges in DNAPL remediation are related to subsurface heterogeneity (EPA 2003; Chapman and Parker 2005; Guilbeault et al. 2005; Stroo et al. 2012). As a means to overcome heterogeneity, soil mixing with zero-valent iron (ZVI) and bentonite has become an established remediation approach for DNAPL source zones (Shackelford et al. 2005; Wadley et al. 2005; Bozzini et al. 2006; Shackelford and Sale 2011; Fjordboge et al. 2012b; Olson et al. 2012). Soil mixing with ZVI and bentonite utilizes two well-established concepts: ZVI-mediated degradation of chlorinated solvents (Gillham and O'Hannesin 1994; Johnson et al. 1996; Scherer et al. 1998; Arnold and Roberts 2000; Tratnyek et al. 2001; Ritter et al. 2002; Grant and Kueper 2004; Bi et al. 2010; Phillips et al. 2010; Jeon et al. 2011) and bentonite-induced reduction in hydraulic conductivity (Castelbaum and Shackelford 2009).

Figure 5-1 shows the conceptual model of a source zone before and after treatment with ZVI-Clay. Prior to mixing, groundwater flow through a heterogeneous source zone results in contaminant discharge from the source zone into a down-gradient contaminant plume. Properties of the post-treatment system are substantially different from those of the pre-mixing system: hydraulic conductivity is reduced, heterogeneity is eliminated, and ZVI particles are distributed throughout the treated soil zone (Wadley et al. 2005; Fjordboge et al. 2012a; Olson et al. 2012). Because of the reduction in  $K$ , groundwater flow tends to bypass the treated soils, thus reducing contaminant discharge and increasing contaminant residence time within the treated soils. The degree of reduction in  $K$  can be controlled, to an extent, via the amount of bentonite added (see Chapter 4). Within the vertical mixed columns, soils and contaminants, including DNAPL, are re-distributed and admixed with zero valent iron (Fjordboge et al. 2012b; Olson et al. 2012).

Research evaluating interaction between ZVI and DNAPL is fairly limited. Laboratory column experiments were conducted to evaluate injection of nano-scale ZVI in pooled (Fagerlund et al. 2012) or residual (Taghavy et al. 2010) PCE. In both experiments, results indicated that treatment effectiveness was contact-limited; extension of the treatment zone via down-gradient injection of nZVI was recommended to enhance contaminant-ZVI contact time. A field trial involving injection-based delivery of emulsified ZVI (EZVI) in a DNAPL source zone indicated excellent treatment performance where EZVI was present, but overall effectiveness was limited by a non-uniform distribution (Quinn et al. 2005). Use of soil mixing to deliver ZVI and bentonite can overcome contact limitations and enhance residence time. However, research into the interaction between reduction in  $K$  and ZVI-mediated degradation is limited. Furthermore, interaction between granular-scale ZVI and DNAPL has been limited to field-scale case studies. The research discussed herein is designed to address these knowledge gaps.

The overarching objective of this research is to advance our understanding of the interaction between the degradation rate and flow rate in homogenized mixed soils impacted with DNAPL. In

support of this objective, a mathematical model of NAPL dissolution, aqueous-phase transport, and degradation processes is developed. Column studies are conducted to test the model and determine parameter values for the model. Finally, the model is used to develop performance predictions for large-scale implementation of ZVI. A secondary objective of the research involves developing our insights regarding degradation pathways in a TCE-NAPL/ZVI system.



**Figure 5-1. Conceptual illustration of groundwater flow patterns before and after soil mixing remediation. The distance between arrows on the groundwater flow path-lines indicates (qualitatively) the distance a particle moves over time.**

## 5.2 Methods and Materials

Column experiments were conducted to test the mathematical model (described subsequently) and obtain parameter value estimates. Reactive transport studies were conducted in chromatography columns (Ace Glass, Vineland, NJ) measuring 610-mm in length and 41-mm I.D. with fritted-glass filters fixed on the bottom (effluent end) of the columns, as shown in Figure 5-2. The top of the column was sealed with a rubber stopper (chemical resistance was unnecessary at the column inlet as the feed solution contained no TCE). The experimental design consisted of a two-by-two matrix, including ZVI-treated and control columns at low and high flow rates. ZVI-treated columns contained 2% (by weight) ZVI; control columns were conducted in an identical manner but without ZVI. The columns were filled to a height of 500 mm with porous media that was spiked with TCE NAPL and homogenized. Layers of filter media, 20-mm in height, were emplaced above and below the TCE-spiked porous media. The upper portion of the column, about 70 mm in height, contained only inlet water. Inlet water contained no TCE; the only source of TCE in the columns was that initially spiked into the soils. The permeant fluid was pumped through the columns, using a peristaltic pump, in a top-down manner. A detailed description of materials and methods used in the column studies is presented in the following text.

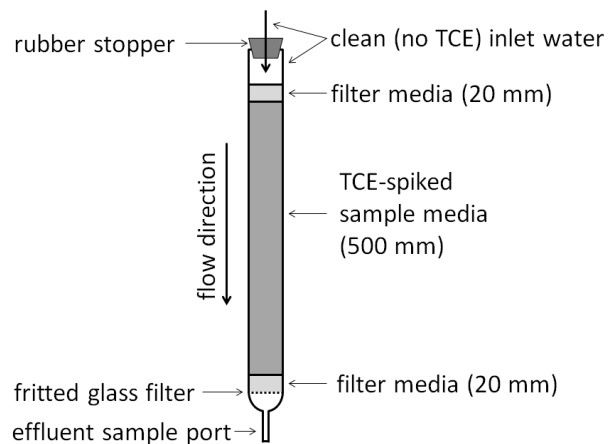


**Figure 5-2. Column reactor apparatus.**

### 5.2.1 Materials

Porous media used to fill the columns consisted of laboratory-grade, minus-100 mesh-size, silica sand (Carmeuse, Colorado Springs, CO). Filter media consisted of F-95 sand (US Silica, Frederick, MD). ZVI consisted of 50-70 mesh filings (Fisher, Pittsburgh, PA). The ZVI particles were washed in 1M HCl for two minutes; after washing, iron was rinsed in N<sub>2</sub>-sparged deionized water, rinsed in N<sub>2</sub>-sparged acetone, and then dried overnight in an anaerobic chamber with an atmosphere of about 1% hydrogen in nitrogen. The permeating fluid consisted of de-aired tap water (City of Fort Collins), which has been described previously (Castelbaum and Shackelford 2009). The model contaminant for the reactor studies was 97% TCE (Alfa Aesar, Ward Hill, MA). An organic-soluble ultraviolet (UV)-fluorescent tracer (product UVXPBB, purchased from LDP LLC, Carlstadt, NJ) was added to the TCE at 0.068% (by weight) so that the NAPL dissolution front could be observed during the experiments under UV light.

### 5.2.2 Column Experiments

Bentonite was excluded from the column reactors, due to the tendency for bentonite to wash out of the columns and clog filters (as discovered in unpublished initial trial experiments). Rather, water was pumped through the columns at low and high flow rates to simulate groundwater flow through treated soils with and without bentonite, respectively. The high-flow column experiments were conducted at a flow rate ( $Q$ ) of  $1.7 \text{ mL}\cdot\text{min}^{-1}$ , corresponding to a seepage velocity ( $v$ ) of  $4.5 \text{ m}\cdot\text{d}^{-1}$ , a Peclet number (Pe) of 300, and an average column residence time of 0.11 d. The low-flow column experiments were conducted at  $Q = 0.05 \text{ mL}\cdot\text{min}^{-1}$ , which corresponds to  $v = 0.13 \text{ m}\cdot\text{d}^{-1}$ ,  $\text{Pe} = 95$ , and a residence time of 3.7 d. These flow rates were selected as field-relevant values that are feasible to test under laboratory conditions. Experiments at both flow rates included ZVI-treated (2%-ZVI) and control (no-ZVI) columns.

*Column reactor preparation.* The conceptual model of the ZVI-Clay system (Figure 5-1) involves groundwater flowing through homogeneous porous media containing ZVI and NAPL. To simulate this system in laboratory-scale columns, porous media specimens for the column reactor studies were admixed and homogenized *ex situ* and then loaded into the column reactors. For columns containing ZVI, the dry ingredients –including 1200 g of sand and 24 g of ZVI – were mixed together first in 1-L glass jars. The solid materials were then filled to saturation with 380-mL of de-aired tap water. Finally, the specimens were spiked with neat TCE NAPL to target levels. The jars were placed on a vortex shaker for about 5 minutes to disperse the NAPL and then inspected under visual- and UV-light to ensure ZVI and NAPL distributions were homogeneous. For loading of the column reactors, de-aired tap water was initially injected into the bottom of each column. Specimens were added through standing water in the columns to minimize the amount of entrapped air. A 20-mm layer of clean (unspiked and untreated) filter media was then added. Next, the soil specimen was added to each column to a depth of 500-mm. The soil specimen was transferred directly from the glass jar into the column via a plastic funnel. The sample was loaded at a steady rate to prevent layer-formation within the column due to differential settlement of the materials.

After loading of the sample specimen, a 20-mm layer of filter media was emplaced near the top of the column. After loading of solid materials, the upper portion of the column was filled with clean tap water and the rubber stopper was emplaced, sealing the column.

*Column Operations.* Flow through the columns was begun within one hour of loading with porous media. As shown in the column configuration (Figure 5-2), flow was conducted in a top-down manner. Aside from minor deviations during sample collection, column effluent was collected in a 2-L graduated cylinder. Flow rates were monitored by tracking the cumulative effluent volume versus time. At the bottom of the column, the water-sampling port consisted of Viton® tubing and polyvinylidene fluoride (PVDF) Luer connectors; Teflon® tubing conducted effluent flow to the graduated cylinders.

*Sampling and Analysis.* Column effluent samples were collected regularly, approximately every 0.5 pore volumes of flow (with the exception of hours 2 to 9 in the high-flow column experiment, which occurred overnight). For sample collection, about 0.8 mL of effluent water were collected in a 1-mL glass syringe (gas-tight with a Luer tip). Immediate after sample collection, a 0.45- $\mu\text{m}$  syringe filter (PTFE membrane) and 1/2-inch 27-gauge hypodermic needle were attached to the syringe, and the sample was purged until 0.5 mL of water remained in the syringe. The remaining sample was then injected through the septa of a pre-sealed 20-mL headspace vial containing 9.5 mL of deionized water. The headspace vials were analyzed within 24 hours of sample collection.

Analysis was conducted using an Agilent 6890N gas chromatograph (GC) with flame ionization detector (FID) and a Tekmar 7000 headspace autosampler, equipped with a Restek (Bellefonte, PA) Rt-Q-Bond column (length = 30 m, I.D. = 0.32 mm, and film thickness = 10  $\mu\text{m}$ ). To analyze for TCE and related dechlorination products, the GC method included both temperature and flow ramping to optimize separation of highly-volatile degradation products (ethane, ethene, and acetylene) while minimizing the total run time needed for elution of heavier compounds such as TCE. The sample was injected at a 10:1

split ratio. The temperature was held at 45°C for 5 min and ramped at 20°C·min<sup>-1</sup> to 250°C. The flow was held at 1.0 mL·min<sup>-1</sup> for 5.5 min and then ramped at 12 mL·min<sup>-2</sup> to 4.0 mL·min<sup>-1</sup>.

Calibration for TCE, DCE isomers, and VC was conducted using standards prepared in methanol. Calibration for ethene, ethane, and acetylene was conducted using a Scotty® (Air Liquide, Plumsteadville, PA) calibration gas standard. Chloroacetylene (CA) was synthesized using a procedure similar to established methods (Denis et al. 1987) using 97%-purity cis-1,2-dichloroethene (cDCE) (ACROS Organics, Geel, Belgium) as a reductate and a 25-35% suspension of potassium borohydride (KH) in mineral oil (ACROS) as a reductant. A 1.7-g aliquot of the KH suspension was weighed out and the mineral oil was exchanged with tetrahydrofuran (THF) by mixing with pentane three times and with THF two times; liquid was decanted after each mixing step. Next, 9.25 mL of THF was added to the KH, followed by 758 µL of cDCE and 10 µL of methanol (as a catalyst). The reaction was allowed to proceed for one hour. CA was confirmed using GC/MS before analyzing using the previously-described headspace method to determine the retention time. Due to uncertainty in the CA concentration in the synthesized sample, the calibration factor for VC was used to quantify CA in samples (VC was selected due to a similar molecular weight to that of CA).

In the GC analysis, six peaks were routinely encountered in the chromatograms associated with ZVI-column samples (the peaks were not observed in any control-column samples) that did not correspond to compounds incorporated in the established TCE degradation network. To include these compounds in the TCE molar balance, the peak areas were added together and the average of the calibration factors for all of the known compounds (TCE, DCE isomers, VC, acetylene, ethene, and ethane) was calculated and applied to the total of the GC peak areas. The estimated concentration is reported as a single compound, *U*.

*Column Studies: Supplementary Analyses.* Additional analyses were conducted to obtain information on initial column concentrations and TCE solubility in the system being evaluated. To better

understand the initial concentrations in the experimental columns, a fifth column was prepared in the same manner as the other columns; however, the column was sacrificed for soil sampling immediately after preparation. For soil sample collection, soils were extruded from the column and six core samples were collected using 1.5-cm I.D. brass coring tubes. The cores were immediately placed in a 40-mL glass vial containing 30 mL of methanol. The extraction vials were placed on a vortex shaker for 5 min and then in an ultrasonication bath at 35°C for 30 min. The extract was analyzed on an HP 5890 Series II GC with an electron capture detector (ECD). Calibration standards of TCE in methanol were included in the analysis.

TCE solubility was measured by adding excess TCE to a water sample in a 40-mL vial. The TCE/water mixture was placed on a vortex mixer for about 15 minutes. Triplicate samples were collected from the aqueous phase and analyzed using headspace analytical methods as described previously for column study effluent samples.

### **5.3 Mathematical Modeling**

A mathematical model was developed to describe the reactive transport processes and scale-up observations made on a laboratory scale to field-scale applications. Following the previously-discussed conceptual model (Introduction), implementation of ZVI-Clay transforms a formerly-heterogeneous source zone into a (relatively) homogeneous body comprising soils, contaminants, and treatment reagents. The model assumes one-dimensional transport through a homogeneously-mixed NAPL source zone. Furthermore, factors that can be incorporated into the design of field-scale applications include the contaminant degradation rate, via the amount and/or type of ZVI used, and the hydraulic conductivity, via the amount of bentonite added. In terms of the mathematical modeling of a ZVI-Clay treated source zone, input values for the TCE degradation rate and groundwater seepage velocity can be varied to evaluate how the interaction of these parameters can affect treatment performance. In addition, to develop insights into the TCE degradation pathways in a ZVI-NAPL system, the TCE degradation

network has also been included in the model. ZVI-mediated TCE degradation follows a complex network that involves multiple pathways and intermediate products. Formation and/or degradation terms for intermediate and product species are coupled with transport equations for each species.

For the analysis described herein, two simplifications are noted. First, in the present system, retardation (sorption) of TCE and degradation products is treated as negligible. In field-scale systems sorption may affect reaction and transport rates, but the role of sorption is excluded from the present system. The second simplification involves the hydraulic gradient after mixing. Soil mixing typically involves addition of water, which may take time (months, typically) to drain from the low-K treated soil system. The flow pattern modeled in the present system is based on steady-state transport. This assumption would be valid under circumstances where (a) additional water added during mixing is drained quickly or (b) the water table in the treated zone is unaffected by mixing. In a real system, variations in the hydraulic gradient after mixing would affect the contaminant flux and/or discharge during the time when drainage occurs.

### 5.3.1 NAPL Dissolution

For the following analysis, we have assumed that TCE-NAPL dissolution is rapid relative to the other reaction and transport processes, such that NAPL and water are effectively in equilibrium. This assumption implies that the aqueous-phase TCE concentration is at solubility wherever NAPL is present. The equilibrium assumption is most applicable in homogeneous systems where NAPL is present in dispersed droplets – conditions that are unlikely to be encountered in the field (in the absence of mixing). In homogeneous column experiments, very short flow paths (1-3 cm) have been used to attain non-equilibrium conditions (Miller et al. 1990; Imhoff et al. 1994). By contrast, a rate-limited (i.e., non-equilibrium) NAPL dissolution model may be necessary to describe systems where distributions are heterogeneous (Powers et al. 1998; Sale and McWhorter 2001; Brusseau et al. 2002; Maji and Sudicky 2008), in multi-component NAPL systems (Borden and Pivoni 1992; Jawitz et al. 2003), or where

residence time is limited such that NAPL and water have inadequate time to equilibrate (Miller et al. 1990). Under typical field conditions, NAPL dissolution is limited by heterogeneity: NAPL is dispersed in sparse pools and ganglia, while groundwater flow is primarily limited to transmissive zones.

In a ZVI-Clay mixed-soil system, NAPL is re-distributed fairly uniformly throughout the mixed column (Fjordboge et al. 2012a) and mixing with bentonite facilitates emulsification of NAPLs (Roy-Perreault et al. 2005). Furthermore, hydraulically-transmissive zones, which may conduct most of the groundwater flow, are reduced or eliminated. Subsequently, following homogenization, contact between water and NAPL is much less restricted. This suggests that ZVI-Clay soil mixing would reduce contact-related NAPL dissolution limitations, thus encouraging use of the equilibrium assumption. Observations made in the column studies, including NAPL droplet size, distribution, and dissolution front behavior, further support use of the equilibrium assumption (additional details are provided in the Results section and in the Supporting Information, Appendix A).

The equations governing dissolution of TCE-NAPL are developed accordingly. The processes driving depletion of NAPL-phase TCE include dissolution into clean influent water and degradation. Assuming that (a) NAPL is immobile and (b) NAPL and water reach rapid equilibrium, influent water is saturated upon contact with NAPL. Thus, the velocity of the NAPL dissolution front is related to the groundwater velocity but is limited by the capacity of water to dissolve NAPL (i.e., the product of solubility and flow rate). Another implication of the NAPL-water equilibrium assumption is that the aqueous phase is replenished as rapidly as degradation occurs. Thus, the aqueous phase remains at solubility and NAPL is depleted at the rate of reaction. The TCE degradation reaction is modeled as a pseudo-first order process, but where NAPL is present, the aqueous-phase TCE concentration is fixed at solubility and TCE degradation is effectively zero-order. Furthermore, for the present model we have assumed the presence of sorbed and vapor phases to be negligible. On this basis, the spatial and temporal distribution of NAPL saturation is governed by the following equation (development of the NAPL dissolution governing equation is shown in the Supporting Information, Appendix A):

$$\frac{\partial}{\partial t} \left( \frac{\rho_N \phi S_N}{M_{TCE}} \right) = - \frac{v}{R^*} \frac{\partial}{\partial x} \left( \frac{\rho_N \phi S_N}{M_{TCE}} \right) - k_{TCE} S_w \phi C_{TCE}^* \quad (1)$$

where  $S_N$  and  $S_w$  (dimensionless) are the volumetric pore-saturations of NAPL and water, respectively,  $v$  ( $\text{m}\cdot\text{d}^{-1}$ ) is the groundwater seepage velocity,  $R^*$  is a modified retardation factor that relates the quantity of total TCE to the quantity of aqueous-phase TCE (see the Supporting Information),  $\phi$  (dimensionless) is the porosity,  $\rho_N$  is the NAPL density, which is  $1.46 \text{ g}\cdot\text{mL}^{-1}$  for TCE (Pankow and Cherry 1996),  $M_{TCE}$  ( $\text{g}\cdot\text{mol}^{-1}$ ) is the molecular weight of TCE,  $k_{TCE}$  ( $\text{d}^{-1}$ ) is the first-order TCE degradation rate coefficient, and  $C_{TCE}^*$  ( $\text{mol}\cdot\text{L}^{-1}$ ) is the concentration of TCE at solubility. In Equation 1, the lack of a diffusive-transport term is related to the equilibrium assumption; where NAPL is present, the aqueous phase concentration is at solubility and the concentration gradient is therefore zero. Assuming  $S_N \ll S_w$ , then  $S_w$  remains constant at approximately unity, even as  $S_N$  approaches 0. A substitution is applied, where  $\bar{\rho}_N$  ( $\text{mol}\cdot\text{L}^{-1}$ ) is the molar density of NAPL, calculated as  $\bar{\rho}_N = \rho_{NAPL}/M_{TCE}$ . Equation 1 can therefore be simplified as follows:

$$\frac{\partial}{\partial t} (\bar{\rho}_N S_N) = - \frac{v}{R^*} \frac{\partial}{\partial x} (\bar{\rho}_N S_N) - k_{TCE} C_{TCE}^* \quad (2)$$

The factor,  $R^*$ , can be written as follows (see the Supporting Information, Appendix A), with previously-noted simplifications applied:

$$R^* = 1 + \frac{\bar{\rho}_N S_N}{C_{TCE}^*} \quad (3)$$

The initial condition states that no NAPL is present up-gradient of the treated soil body and that NAPL saturation is uniform at all locations down-gradient of the treated soil interface. This is defined by the following function:

$$S_N(x, 0) = S_N^0 \cdot \begin{cases} 1 & \text{if } x \geq 0 \\ 0 & \text{if } x < 0 \end{cases}$$

where  $x = 0$  is the location of the interface between clean and treated soils and  $S_N^0$  is the initial saturation of NAPL. The following general solution to Equation 2, subject to the initial condition, is obtained:

$$\bar{\rho}_N S_N(x, t) = (\bar{\rho}_N S_N^0 - k_{TCE} C_{TCE}^* t) \cdot \begin{cases} 1 & \text{if } (\bar{\rho}_N S_N^0 - k_{TCE} C_{TCE}^* t) > 0 \\ 0 & \text{if } (\bar{\rho}_N S_N^0 - k_{TCE} C_{TCE}^* t) \leq 0 \end{cases} \cdot \begin{cases} 1 & \text{if } [x - L_f(t)] \geq 0 \\ 0 & \text{if } [x - L_f(t)] < 0 \end{cases} \quad (4)$$

where  $L_f(t)$  is the  $x$ -axis location of the NAPL dissolution front at time  $t$ . The step functions indicate that  $S_N \rightarrow 0$  under two conditions: at locations upstream of the NAPL dissolution front (i.e., when  $x < L_f(t)$ ) or at all locations when sufficient time has passed such that degradation has removed all NAPL in the system (i.e., when  $k_{TCE} C_{TCE}^* t > \bar{\rho}_N S_N^0$ ). Noting that  $R^*$  varies with time in this system (as described in more detail subsequently),  $L_f(t)$  is calculated as follows:

$$L_f(t) = \int_0^t \frac{v}{R^*(t)} dt \quad (5)$$

The factor,  $R^*$ , can be written as a function of time as follows:

$$R^*(t) = 1 + \frac{\bar{\rho}_N S_N^r(t)}{C_{TCE}^*} \quad (6)$$

where  $S_N^r$  is the saturation of NAPL remaining in locations where NAPL remains at time  $t$  (i.e., down-gradient of the dissolution front). The value of  $S_N^r$ , given pseudo-zero-order degradation of TCE and a uniform initial NAPL saturation of  $S_N^0$ , is related to  $t$  as follows:

$$\bar{\rho}_N S_N^r(t) = (\bar{\rho}_N S_N^0 - k_{TCE} C_{TCE}^* t) \cdot \begin{cases} 1 & \text{if } (\bar{\rho}_N S_N^0 - k_{TCE} C_{TCE}^* t) > 0 \\ 0 & \text{if } (\bar{\rho}_N S_N^0 - k_{TCE} C_{TCE}^* t) \leq 0 \end{cases} \quad (7)$$

By combining Equations 5, 6, and 7 and integrating, for a system with reaction (i.e., where  $k_{TCE} > 0$ ), the following equation is obtained for  $L_f(t)$ :

$$L_f(t) = \frac{v}{k_{TCE}} \left( \ln \frac{\left| 1 + \frac{\bar{\rho}_N S_N^0}{C_{TCE}^*} \right|}{\left| 1 + \frac{\bar{\rho}_N S_N^0}{C_{TCE}^*} - k_{TCE} t \right|} \right) \quad (8)$$

In the case of no reaction ( $k_{TCE} = 0$ ),  $R^*$  does not vary with time and integration yields the following:

$$L_f(t) = \frac{v}{1 + \frac{\bar{\rho}_N S_N^0}{C_{TCE}^*}} \cdot t \quad (9)$$

For use in subsequent calculations of aqueous-phase TCE reaction and transport, a step function is calculated, which returns a value of 1 where NAPL is present and a value of zero where NAPL has been depleted:

$$\Phi(x, t) = \begin{cases} 1 & \text{if } \bar{\rho}_N S_N(x, t) > 0 \\ 0 & \text{if } \bar{\rho}_N S_N(x, t) = 0 \end{cases} \quad (10)$$

As discussed subsequently, numerical methods are used to solve the system of PDEs governing reaction and transport for aqueous-phase TCE and related degradation products. Due to instability of the numerical solution when using the pure step function, the following step-function analytical approximation is used:

$$\Phi'(x, t) = \frac{1}{1 + \exp(-K_H \cdot \bar{\rho}_N S_N(x, t))} \quad (11)$$

where  $K_H$  is a coefficient of arbitrary units that controls the gradient of the analytical step function. For field and column modeling a value of  $K_H = 200 \cdot C_{TCE}^*{}^{-1}$  was used.

### 5.3.2 Aqueous Phase Reaction and Transport

*TCE.* The mass-balance equation for aqueous-phase TCE, assuming one-dimensional groundwater flow through homogeneous porous media, is as follows:

$$\frac{\partial C_{TCE}}{\partial t} = D_{TCE} \frac{\partial^2 C_{TCE}}{\partial x^2} - v \frac{\partial C_{TCE}}{\partial x} - k_{TCE} C_{TCE} + G \quad (12)$$

Where  $D_{TCE}$  ( $\text{cm}^2\text{s}^{-1}$ ) is the effective diffusion/dispersion coefficient for TCE and  $C_{TCE}$  ( $\text{mol}\cdot\text{L}^{-1}$ ) is the aqueous phase TCE concentration. The generation term,  $G$ , replenishes any loss, when NAPL is present locally. As such, where NAPL is present, the  $G$ -term cancels out any changes occurring in the aqueous phase due to reaction or transport ( $\partial C_{TCE}/\partial t = 0$ ). Where NAPL has been depleted, no generation occurs ( $G = 0$ ). As such, the following expression for  $G$  is used:

$$G = -\Phi(x, t) \left( D_{TCE} \frac{\partial^2 C_{TCE}}{\partial x^2} - v \frac{\partial C_{TCE}}{\partial x} - k_{TCE} C_{TCE} \right) \quad (13)$$

Combining Equations 12 and 13 yields the following equation for aqueous-phase TCE reaction and transport:

$$\frac{\partial C_{TCE}}{\partial t} = [1 - \Phi(x, t)] \left( D_{TCE} \frac{\partial^2 C_{TCE}}{\partial x^2} - v \frac{\partial C_{TCE}}{\partial x} - k_{TCE} C_{TCE} \right) \quad (14)$$

For initial conditions, the TCE-NAPL is homogeneously distributed throughout the model domain; assuming equilibrium between the NAPL and aqueous phases, the TCE concentration initially in the aqueous phase is equal to TCE solubility,  $C_{TCE}^*$ . A Dirichlet-type boundary condition is imposed at the left-hand boundary (i.e., the upgradient face of the source zone) and a Neumann-type boundary condition is imposed at the right-hand boundary. The right-hand boundary is selected at a distance,  $L'$  (m), which is far enough down-gradient of the model region of interest ( $x = 0$  to  $L$  m) such that a 0-gradient boundary condition applies (for a semi-infinite domain,  $L' \rightarrow \infty$ ;  $L'$  was used rather than  $\infty$  because the numerical model required a finite boundary location). Mathematically, the initial and boundary conditions are stated as follows:

$$\text{Initial condition: } C_{TCE}(x, 0) = C_{TCE}^*$$

$$\text{Left-hand boundary condition: } C_{TCE}(0, t) = 0$$

$$\text{Right-hand boundary condition: } \frac{\partial C_{TCE}}{\partial x}(L, t) = 0$$

*Degradation Products.* A widely-used reaction network model for ZVI-mediated degradation of TCE involves hydrogenation, hydrogenolysis, and  $\beta$ -elimination pathways (Arnold and Roberts 2000). For TCE and some of the intermediate species, multiple degradation pathways may be followed (Figure 5-3). The model system includes five intermediate species and leads to ethane as the primary degradation product. For the modeling conducted herein, the DCE isomers 11-DCE, *c*DCE, and *t*DCE have been lumped together as a single species, DCE. An additional species has been added to the model, under the notation *U*. This species has been added to account for unknown or unpredicted compounds that were observed in the column studies (as discussed below in more detail). The shorthand notation used for identification of species is as follows: DCE – dichloroethene (total of the three isomers, 11DCE, *t*DCE, and *c*DCE), VC – vinyl chloride, CA – chloroacetylene, A – acetylene, ET – ethene, ETA – ethane, U – unpredicted or unidentified species.

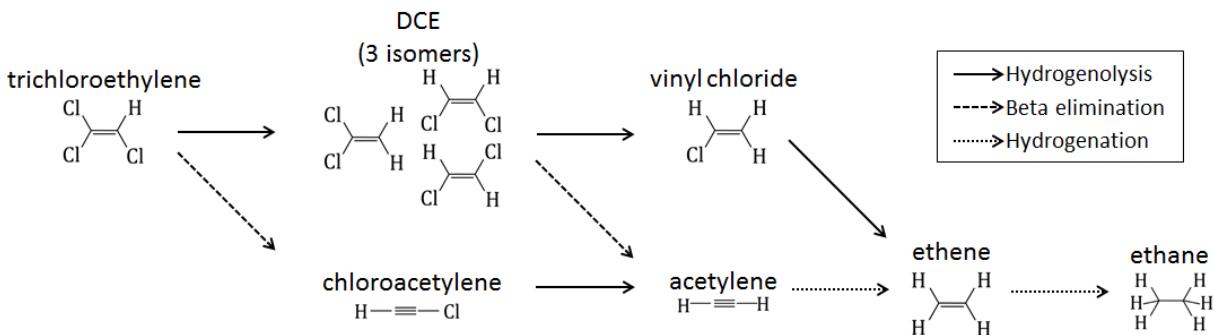


Figure 5-3. Degradation reaction network model for TCE.

In the degradation network model,  $\beta_1$  and  $\beta_2$  are the factors applied to the degradation rate coefficients for TCE and DCE, respectively, to indicate the relative amounts degraded via the  $\beta$ -elimination pathway. Another factor,  $\alpha$ , is applied to each reaction step to account for experimental products formed that are unidentified or not predicted by the model pathway. The governing equations for the degradation products are as follows:

$$\frac{\partial C_{DCE}}{\partial t} = D_{DCE} \frac{\partial^2 C_{DCE}}{\partial x^2} - v \frac{\partial C_{DCE}}{\partial x} + (1 - \beta_1)(1 - \alpha)k_{TCE}C_{TCE} - k_{DCE}C_{DCE} \quad (15)$$

$$\frac{\partial C_{VC}}{\partial t} = D_{VC} \frac{\partial^2 C_{VC}}{\partial x^2} - v \frac{\partial C_{VC}}{\partial x} + (1 - \beta_2)(1 - \alpha)k_{DCE}C_{DCE} - k_{VC}C_{VC} \quad (16)$$

$$\frac{\partial C_{CA}}{\partial t} = D_{CA} \frac{\partial^2 C_{CA}}{\partial x^2} - v \frac{\partial C_{CA}}{\partial x} + \beta_1(1 - \alpha)k_{TCE}C_{TCE} - k_{CA}C_{CA} \quad (17)$$

$$\frac{\partial C_A}{\partial t} = D_A \frac{\partial^2 C_A}{\partial x^2} - v \frac{\partial C_A}{\partial x} + \beta_2(1 - \alpha)k_{DCE}C_{DCE} + (1 - \alpha)k_{CA}C_{CA} - k_A C_A \quad (18)$$

$$\frac{\partial C_{ET}}{\partial t} = D_{ET} \frac{\partial^2 C_{ET}}{\partial x^2} - v \frac{\partial C_{ET}}{\partial x} + (1 - \alpha)k_{VC}C_{VC} + (1 - \alpha)k_A C_A - k_{ET}C_{ET} \quad (19)$$

$$\frac{\partial C_{ETA}}{\partial t} = D_{ETA} \frac{\partial^2 C_{ETA}}{\partial x^2} - v \frac{\partial C_{ETA}}{\partial x} + (1 - \alpha)k_{ET}C_{ET} \quad (20)$$

$$\frac{\partial C_U}{\partial t} = D_U \frac{\partial^2 C_U}{\partial x^2} - v \frac{\partial C_U}{\partial x} + \alpha[k_{TCE}C_{TCE} + k_{DCE}C_{DCE} + k_{VC}C_{VC} + k_{CA}C_{CA} + k_{ET}C_{ET}] \quad (21)$$

where  $D_i$  ( $\text{cm}^2\text{s}^{-1}$ ) is the effective diffusion/dispersion coefficient for species  $i$ . For the degradation network, initial and boundary conditions for species  $i$  are as follows:

Initial condition:  $C_i(x, 0) = 0$

Left-hand boundary condition:  $C_i(0, t) = 0$

Right-hand boundary condition:  $\frac{\partial C_i}{\partial x}(L', t) = 0$

The system of PDEs governing aqueous phase TCE and related degradation products were solved using numerical methods. These are described in the following section.

### 5.3.3 Numerical Solution to Aqueous Phase Reaction and Transport Equations

Model solutions were calculated using Mathcad® 15.0 software. The system of PDEs was solved in Mathcad using the Pdesolve function, which uses the numerical method-of-lines technique. A central differences numerical approximation scheme was selected. Convergence tolerance was set to 0.001 (default value) for all models. The Pdesolve function allows the user to select the time and distance step-sizes. Models were initially conducted with 200 steps in the  $x$ -domain and 50 steps in the  $t$ -domain. If instability or inaccuracy was noted in the solution, the domains were discretized into a larger number of steps in the  $x$ -domain.

*Input Parameters.* Input values included fixed-value parameters and parameters that could be adjusted to fit experimental data. Fixed values were used for both column-scale and field-scale modeling. Values for adjustable parameters were selected based on fitting of experimental data. For field scale modeling, values for the adjustable parameters were selected based on column-scale results.

Fixed values included system dimensions, porous media porosity, and transport parameters. Column reactor dimensions and porosity were discussed previously. Transport-related fixed-value parameters included  $v$  and  $D_i$ . The value of  $v$  was calculated for each column experiment based on the measured volume of water in the effluent reservoir over time. Values for  $D_i$  were calculated using

molecular diffusion coefficients for each species and properties of the porous media. The molecular diffusion coefficient for TCE in water was  $10.1 \times 10^{-5} \text{ cm}^2\text{s}^{-1}$  (Pankow and Cherry 1996). For the degradation products, molecular diffusion coefficients were calculated from their molecular weights relative to that of TCE using the following relationship (Schwarzenbach et al. 2003):

$$\frac{D_i^0}{D_{TCE}^0} = \left( \frac{M_i}{M_{TCE}} \right)^{-1/2} \quad (22)$$

Effective diffusion coefficients in porous media,  $D_i^*$  ( $\text{cm}^2\text{s}^{-1}$ ) for species  $i$ , were calculated as

$$D_i^* = \frac{D_i^0 \phi}{\tau_m} \quad (23)$$

where  $\tau_m$  is the tortuosity (dimensionless). Tortuosity was estimated as  $\tau_m = 1 - \ln(\phi^2)$  (Boudreau 1996). The bulk dispersion/diffusion coefficient,  $D_i$  ( $\text{cm}^2\text{s}^{-1}$ ) for species  $i$ , was calculated as follows:

$$D_i = \alpha v + D_i^* \quad (24)$$

with  $\alpha = 0.01 \cdot L$ .

Adjustable parameters included the initial TCE-NAPL concentration  $C_{NAPL}^0$ ; first-order degradation rate coefficients,  $k_i$ ; and pathway factors  $\beta_1$ ,  $\beta_2$ , and  $\alpha$ . Values for these parameters were estimated by trial-and-error fitting to experimental data. The model was first fit to TCE experimental data based on estimates for the parameters  $C_{NAPL}^0$  and  $k_{TCE}$ . The model fit was evaluated by comparison of experimentally measured column effluent values to those predicted by the model output. Model output was evaluated by calculating r-squared and mole balance values. Parameter values were refined until no further improvements were observed. Next, degradation rate coefficients were estimated for the degradation network (Figure 5-3). As a first approximation for the rate coefficients, values were calculated for each reaction step based on literature data (Arnold and Roberts 2000). The experimental system was solved using these parameter values and the model output compared to experimental values.

Next, parameter values were modified until further improvements in model fitting of experimental data were obtained. Values were selected such that total amount of each product model discharged from the model system was within 10% of the total moles measured in the effluent of the corresponding column experiment.

As discussed previously, compounds were present in the effluent of the ZVI-treated columns that were not accounted for in the TCE degradation model (these compounds were also not present in the no-ZVI control column effluent). These unidentified/unpredicted products, herein grouped together under the species identifier  $U$ , were incorporated into the model by applying an alternative pathway for each reaction step wherein a fraction, determined by a factor,  $\alpha$ , was transformed into the  $U$  compounds. The value of  $\alpha$  was fit as an experimental parameter such that  $U$  in the model was within 10% of the  $U$  discharged from the columns in the experiments. Although this method provides only a rough estimate for unknown (or unpredicted) species, this method provided a means to include unidentified species in the model for comparison to experimental data. Further investigation into these unknown species is recommended for future research, as they may provide important information about reaction pathways in a ZVI-bentonite-NAPL system.

*Model Stability and Accuracy.* With each model simulation, model output was evaluated for stability and accuracy. The evaluation consisted of visual inspection of data plots and calculation of a molar-balance. Data plots consisted of TCE and degradation product concentrations plotted versus position or time. Stable solutions resulted in smooth concentration profiles, whereas unstable solutions resulted in fluctuations. The second method of model evaluation involved mole-balance calculation. The molar balance was calculated as:

$$\frac{\sum_i n_i^{effluent} + \sum_i n_i^{remaining}}{n_{TCE}^0} \quad (25)$$

where  $i$  refers to each species in the system including TCE and degradation products,  $n_i^{effluent}$  is the cumulative number of moles of species  $i$  that has been discharged in the system effluent,  $n_i^{remaining}$  is the total moles of species  $i$  remaining in the system, and  $n_{TCE}^0$  is the total initial moles of TCE in the system (i.e., NAPL and aqueous-phase TCE present at time 0). Model output was considered valid when the molar balance was  $1.0 \pm 0.01$ . If the molar balance was outside of this range, the step sizes were refined and the model re-run.

## 5.4 Results

### 5.4.1 Column Studies

The column studies were conducted at two flow rates ( $0.13$  and  $4.5 \text{ m}\cdot\text{d}^{-1}$ ) and under two experimental conditions (no-ZVI control and soil admixed with 2% ZVI) to test the mathematical model and development of insights into degradation rates and pathways in a homogenized ZVI-NAPL system at different flow rates. Column study results are presented in this section. Modeling of column study data is discussed in the following section.

*TCE Concentrations.* TCE concentrations measured in the column-study effluent water samples are shown in Figure 5-4. The reported column effluent concentrations represent contaminant molar flux across a cross-section of porous media; thus, these values represent flux-averaged concentrations, as opposed to resident concentrations (i.e., the contaminant concentrations that would be measured directly within the soil-pore water) (Shackelford 1994). In general, effluent TCE concentrations remained at levels near solubility until NAPL within the column was depleted. After NAPL was depleted, TCE concentrations declined rapidly. In the no-ZVI control columns, complete depletion of NAPL (as indicated by a decline in the effluent TCE concentration) required about 0.8 days in the high-flow columns and about 24 days in the low-flow columns. In terms of pore volumes of flow (PVF), complete dissolution of TCE occurred at 7.6 PVF in the high-flow control column and 6.3 PVF in the low-flow reactor. The difference in these values may be attributed to variability in initial concentrations.

The impact of ZVI on treatment performance at both flow rates is also evaluated. In the high-flow reactor, TCE elution curves for the control and ZVI-containing columns essentially overlap, indicating that the presence of ZVI had little impact on the NAPL longevity. In the low-flow columns, complete dissolution of TCE occurred at about 20 days (5.3 PVF) in the ZVI-containing column, clearly earlier than in the control column. Thus, the presence of ZVI appears to have had a greater impact on source-zone NAPL longevity in the low-flow reactors than in the high-flow reactors. Taken together, these results indicate that NAPL longevity was primarily controlled by the capacity for water to remove TCE from the system (i.e., as governed by the water flow rate with concentrations limited to solubility) and the initial amount of TCE in the column reactors. Under the conditions imposed in the column reactor experiments, the impact of ZVI on source-zone longevity was marginal and highly dependent upon the flow rate. The extended residence time in the low-flow reactor provided an improvement in the fraction of TCE degraded.

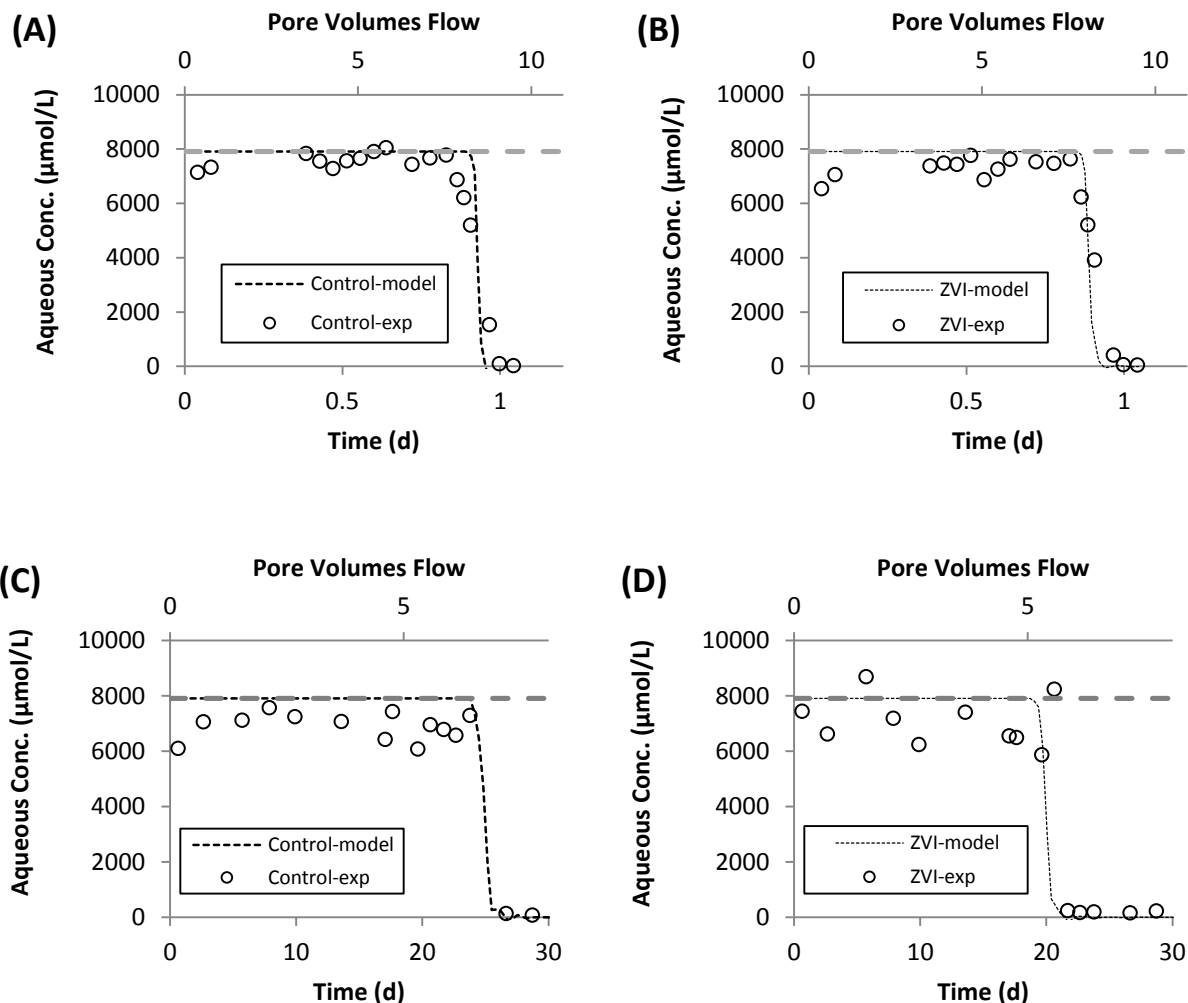


Figure 5-4. TCE effluent concentrations versus time: experimental data (o) and model output (----). Data is shown for the following columns: (A) high-flow control column, (B) high-flow ZVI column, (C) low-flow control column and (D) low-flow ZVI column.

*TCE degradation products.* Additional evidence of TCE degradation comes from analysis of degradation products in the column effluent. Concentration versus time data for products detected in the effluent from the high-flow and low-flow reactors are shown in Figure 5-5 and Figure 5-6, respectively. In the high-flow columns, observed degradation products (and peak concentrations) included acetylene (24  $\mu\text{M}$ ), ethene (8.2  $\mu\text{M}$ ), ethane (3.9  $\mu\text{M}$ ), and cDCE (1.2  $\mu\text{M}$ ). In the low-flow reactor, observed degradation products included ethene (325  $\mu\text{M}$ ), ethane (45  $\mu\text{M}$ ), DCE (73  $\mu\text{M}$ ), VC (0.73  $\mu\text{M}$ ), and CA

(0.65  $\mu\text{M}$ ). Acetylene was observed in the low-flow column only at early times ( $<1$  PVF) but was not detected thereafter. The higher concentrations of degradation products indicate that more TCE was degraded in low-flow column (residence time = 3.7 days) than in the high-flow column (residence time = 0.11 days). A notable amount of unidentified/unpredicted species ( $U$ ) were also observed in both columns.

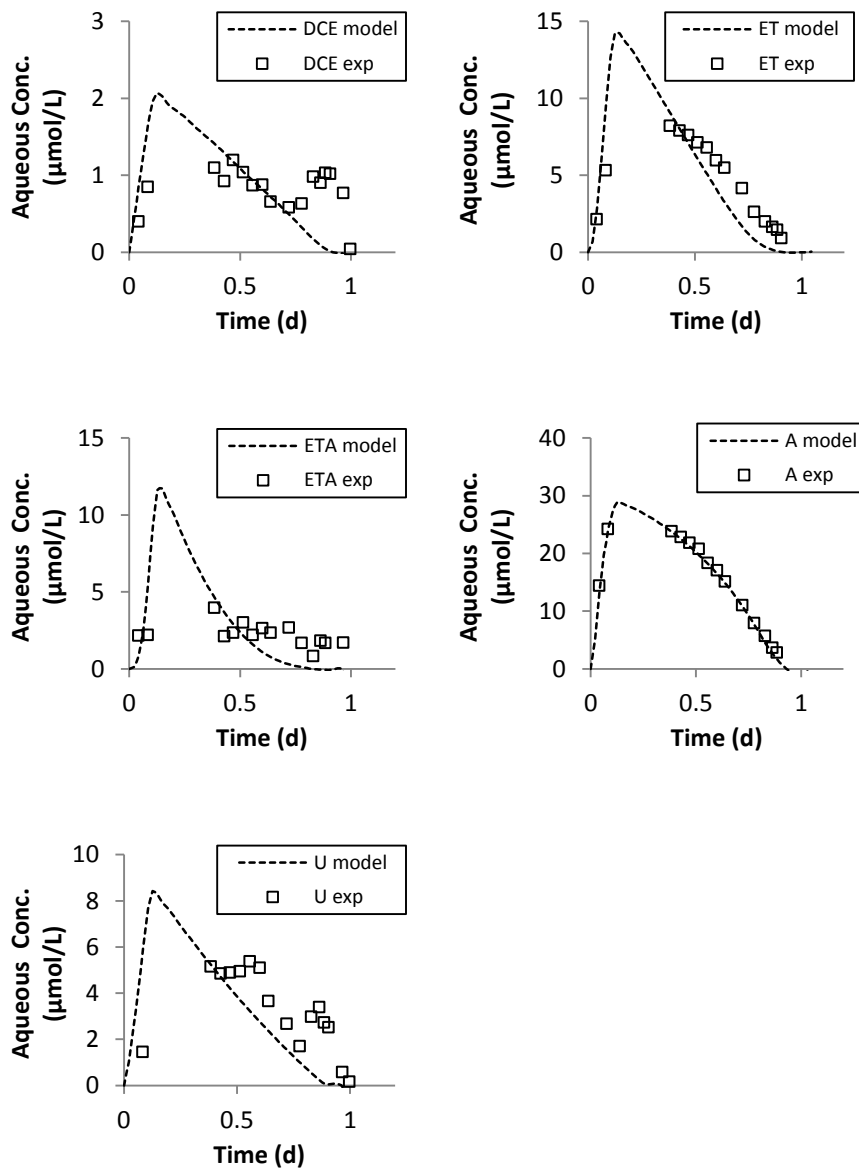


Figure 5-5. Model fitting of column effluent data in the high-flow system ( $\nu = 4.5 \text{ m}\cdot\text{d}^{-1}$ ) with ZVI. Chloroacetylene (CA) and vinyl chloride (VC) were not detected in the high-flow column effluent.

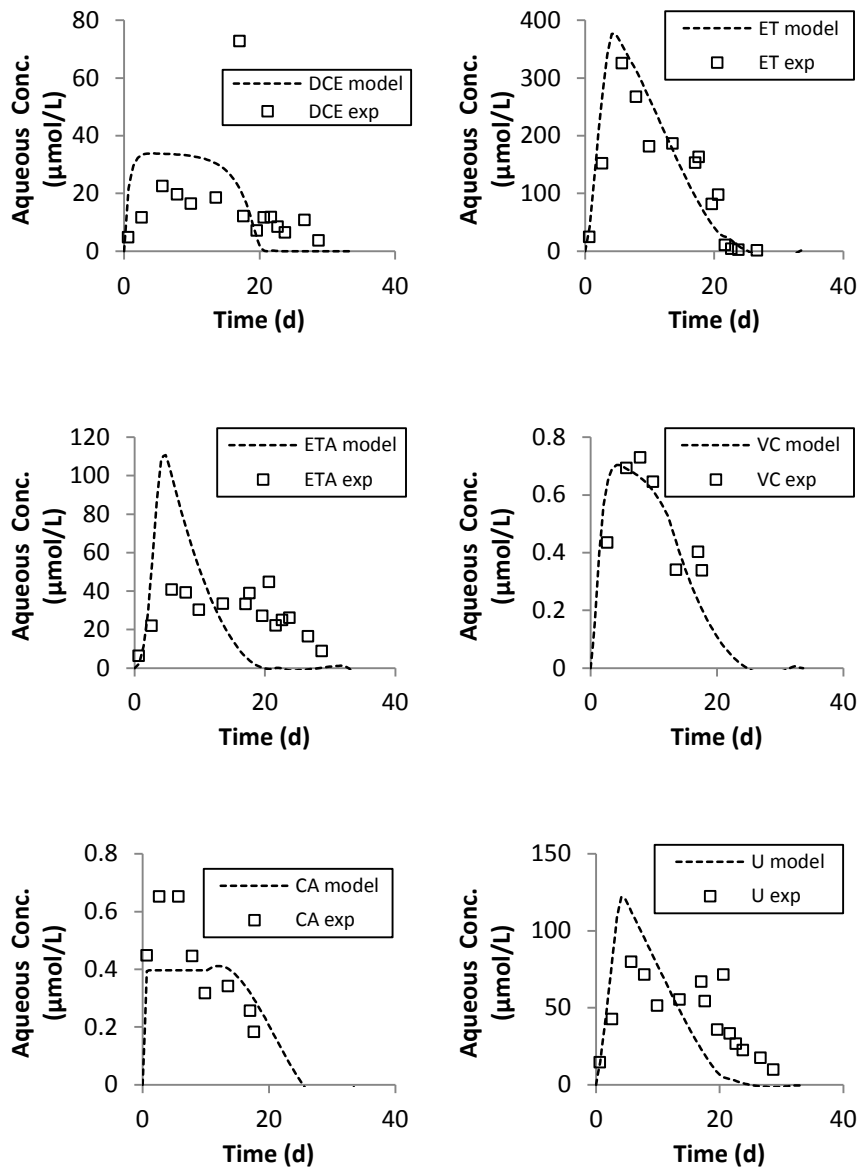


Figure 5-6. Model fitting of column effluent data in low-flow system ( $v = 0.13 \text{ m}\cdot\text{d}^{-1}$ ) with ZVI. Aside from irregular detection at early times ( $<1$  PVF), acetylene (A) was not detected in the low-flow column effluent.

*NAPL dissolution.* The dissolution behavior of the TCE-NAPL, which was spiked with a UV-fluorescent tracer, was observed throughout the column experiments. Photographs taken during the column studies, indicating the NAPL droplet size and NAPL dissolution front in the high- and low-flow

columns are shown in the Supporting Information. NAPL was initially present in dispersed droplets with a typical size on the order of 0.1 mm (Figure A-1 in the Supporting Information, located in Appendix A). The NAPL dissolution front varied slightly between the low- and high-flow columns. In the low-flow columns, the dissolution front occurred over a very short distance (<10 mm; Figure A-2 in the Supporting Information). In the high-flow columns, the dissolution front occurred over a wider interval than in the high flow column (10-50 mm; Figure A-3 in the Supporting Information), but was still very short compared to the length of the column reactors. The variable length of the dissolution front in the high-flow reactors appears to have resulted more from flow fingering, possibly resulting imperfect uniformity of flow within the column, than non-equilibrium dissolution.

The short length of the NAPL-dissolution front is consistent with previous work. Flow lengths of 1-3 cm have often been required to capture non-equilibrium NAPL dissolution behavior (Miller et al. 1990; Imhoff et al. 1994). When compared to the conditions under which non-equilibrium modeling is required, observations of column study NAPL support use of the equilibrium assumption.

*Column Studies: Supplementary Analyses.* Supplemental column study data included analysis for initial concentrations and TCE solubility. A sacrificial column, which was prepared and sampled immediately to determine initial concentration, was found to contain  $2040 \pm 340 \text{ mg} \cdot \text{kg}^{-1}$  of total TCE (dry soil basis), which corresponds to a volumetric pore-space NAPL saturation of 0.0053 (at  $\phi = 0.41$ ). The solubility of TCE was measured to be  $1040 \pm 140 \text{ mg} \cdot \text{L}^{-1}$ ; literature TCE solubility has been reported as  $1100 \text{ mg} \cdot \text{L}^{-1}$  (Pankow and Cherry 1996).

#### 5.4.2 Modeling of Experimental Data

To test the mathematical model and develop insights into processes governing treatment in the column experiments, the model was applied to experimental data.

*TCE: NAPL Dissolution and Degradation.* TCE degradation was modeled as a first-order process at concentrations below solubility and zero-order in the presence of NAPL. As mentioned previously, TCE depletion in column effluent occurred nearly simultaneously in the ZVI and no-ZVI control columns (the short residence time in the 0.5-m columns was insufficient to achieve greater treatment differential in the ZVI-treated columns). As such, the TCE degradation rate coefficients were calculated based on the effluent degradation products to be 0.079 and 0.024 d<sup>-1</sup>, respectively, in the high-flow and low-flow systems. The faster apparent degradation rate in the high-flow system may indicate mass transfer limitations; nevertheless, the rate coefficients at both flow rates are of similar magnitude. In the presence of uniformly distributed NAPL, the aqueous-phase TCE concentration is maintained near solubility. Thus, TCE degradation is effectively a zero-order process, with zero-order TCE degradation rates of 630 and 160 μmol·L<sup>-1</sup>·d<sup>-1</sup>, respectively, in the high-flow and low-flow systems.

*TCE: Degradation Network.* Although analyzing degradation pathways was not a primary objective of this research, rigorous analysis of degradation pathways has not been conducted in a ZVI-NAPL system (to our knowledge). Thus, we included all of the potential products in the degradation scheme shown in Figure 5-3 in our analysis. The TCE degradation network model includes several parameters, including rate coefficients and pathway factors. As discussed previously, initial estimates for parameter values were calculated based on literature data (Arnold and Roberts 2000). Parameter values were then adjusted to improve fitting of the column effluent data. For all contaminants, model-estimated discharge is within 10% of experimentally-measured discharge. Parameter values and literature values are shown in Table 5-1. The literature values are applicable to this experiment as they are based on ZVI-mediated degradation of TCE and related products. However, the literature values are based on a system in which neither NAPL nor soil were present, initial concentrations were well below solubility (<200 μmol·L<sup>-1</sup>, reactions occurred in mixed-batch reactors, and the ZVI concentrations were about 3 g·L<sup>-1</sup> (as compared to 80 g·L<sup>-1</sup> in the present experiment). Thus, discrepancies in degradation rates and pathways may be attributed to noted differences in the study conditions.

**Table 5-1. Parameter values used to model the TCE degradation reaction network**

	Fast-flow column (v = 4.5 m/d)			Slow-flow column (v = 0.13 m/d)			Literature <sup>(D)</sup>	
	k <sup>1st</sup> (A)	β-fraction <sup>(B)</sup>	U-fraction <sup>(C)</sup>	k <sup>1st</sup>	β-fraction	U-fraction	k <sup>1st</sup>	β-fraction
<b>TCE</b>	0.079	0.97	0.05	0.023	0.70	0.065	0.53	0.94
<b>DCE</b>	1.5	0.94	0.05	1.5	0.98	0.065	1.6	0.97
<b>VC</b>	-- <sup>(E)</sup>		0.05	1.3		0.065	1.7	
<b>CA</b>	-- <sup>(E)</sup>		0.05	300		0.065	38	
<b>A</b>	15		0.05	500		0.065	31	
<b>ET</b>	19		0.05	0.17		0.065	0.48	

(A) 1<sup>st</sup>-order degradation coefficient

(B) Fraction degraded via β-elimination pathway

(C) Fraction degraded to “U” compounds

(D) Literature coefficients were calculated from values presented by Arnold and Roberts (2000). TCE, DCE, CA, A were calculated from  $K^3S_t$  (μM/h)·K (1/μM); VC and E were presented as  $K^3S_t$  (1/h) (see Arnold and Roberts 2000, Table 1).

(E) These compounds were non-detect, so no parameter estimates are provided.

Comparisons of model-calculated effluent concentrations for the degradation products to experimental data are shown for the high- and low-flow columns in Figure 5-5 and Figure 5-6, respectively. In general, our analysis indicates that both TCE and DCE (excepting the 1,1-DCE isomers) are primarily degraded via the β-elimination pathway. We estimate that 97% and 70% of TCE is degraded via the β-elimination pathway in the high-flow and low-flow columns, respectively. The literature value (Table 5-1) indicates that 94% of TCE was degraded via the β-elimination pathway. The relatively lower ratio in the low-flow column may indicate that the combination of high concentrations (i.e., the presence of NAPL) and extended residence time in the low-flow column results in saturation of ZVI surface sites favoring β-elimination. For DCE degradation, we estimated 94% (high flow) and 98% (low flow) followed β-elimination, which compares reasonably well to 97% in the literature value. The degradation rate of chloroacetylene is rapid compared to the rate of formation, thus little accumulation is observed (none was observed in the fast-flow column). Acetylene is formed in high levels in the fast flow system but has generally been depleted, presumably through subsequent reduction to ethene, in the low flow system. A small amount of vinyl chloride is observed in the low-flow system and none is observed in the high-flow system; thus, insufficient data is generated to change the VC degradation coefficient

from that calculated from literature. Ethane may be formed from ethene, but also may result from degradation of chlorinated ethanes that were identified among the degradation products (see following paragraph). In the low-flow system, a lag is apparent for degradation product formation. The lag may be the result of products partitioning into gas-phase cavities in the system which may form from hydrogen production, which associated with anaerobic corrosion of ZVI (Zhang and Gillham 2005).

Some unknown/unidentified products were observed in the GC chromatograms associated with samples collected from the ZVI columns. Six such peaks were regularly present in ZVI-column effluent samples. The compounds behind four of these peaks have not been identified (although GC-mass spectroscopic (GC/MS) analysis was conducted, concentrations appear to have been too low for GC/MS identification). Two of these peaks were identified as chloroethane and 1,2-dichloroethane (1,2-DCA), which are not included in the standard ZVI-TCE degradation network. In the low-flow column the effluent chloroethane concentration peaked at  $12 \mu\text{mol}\cdot\text{L}^{-1}$ , approximately 4% of the peak level for ethene (the highest concentration constituent in the low-flow column effluent). In the high-flow column the effluent chloroethane concentration peaked at  $1.6 \mu\text{mol}\cdot\text{L}^{-1}$ , approximately 6% of the peak levels for acetylene (the highest concentration constituent in the low-flow column effluent). Concentrations of 1,2-DCA were generally less than those measured for chloroethane. Formation of chlorinated ethanes suggests that hydrogenation steps may be reducing the  $\pi$ -bond associated with chlorinated ethenes. Previous studies that have investigated degradation pathways of TCE in the presence of ZVI have not been identified these products. These studies have been conducted in the context of ZVI permeable reactive barriers (PRBs), in which the aqueous phase TCE concentration has generally been much lower. Thus, the pathways may result from limited dechlorination rates due to saturation of ZVI surface sites. Mechanisms of such degradation steps are outside of the research focus area of the present experiment, but investigation is recommended for future research. Other unidentified compounds may consist of C4 (or higher) hydrocarbons such as butadienes.

The analysis of the degradation network presented herein has noted limitations: due to the large number of parameters and related challenges with fitting parameters in the system of PDEs, the coefficients are not necessarily unique; also, due to the use of trial-and-error for parameter fitting, confidence intervals for fitting parameters are not available (these could be better understood by conducting kinetic studies in no-flow systems, which were not conducted as part of this research).

#### 5.4.3 Model Prediction of Field Performance

A primary objective of the research involved development of a mathematical model to predict treatment performance under large-size and low-flow conditions that may be present after field-scale soil mixing of ZVI and bentonite in a NAPL source zone. In support of this objective, the following analysis presents model-predicted treatment performance under ranges of values for  $L$ ,  $v$ , and  $k_{TCE}$ . Model output consists of concentration data for TCE, TCE degradation products, and NAPL saturation as a function of 1-D space and time. Primary performance metrics, calculated from the model output, include contaminant molar discharge and flux. Finally, analysis of the NAPL longevity and saturation profile at various times is presented.

*TCE Discharge.* A common metric for source-zone treatment involves Contaminant Mass Discharge (CMD), or total contaminant mass that is released into a downgradient plume. For the analysis conducted herein, the total (time-integrated) CMD is calculated and normalized to the TCE mass initially present in the system. The resulting parameter is the fractional contaminant discharge,  $f_D$ . The parameter  $f_D$  indicates the ultimate fate of TCE initially present in the treated zone:  $f_D = 1.0$  indicates that all TCE is eventually discharged, whereas  $f_D = 0.01$  indicates that 99% of the TCE initially present is degraded.

Figure 5-7 shows calculated values of  $f_D$ , as a function of source-zone length, over seepage velocities ranging from 0.0001 to 10 m·d<sup>-1</sup>. In all cases shown in Figure 5-7, the degradation rate coefficient,  $k_{TCE}$ , is fixed at 0.05 d<sup>-1</sup>. In a model source zone of 10-m in length, the calculated  $f_D$  value at  $v$

$= 1 \text{ m}\cdot\text{d}^{-1}$  is 0.68. The normalized TCE discharge values at  $v = 0.1, 0.01, 0.001,$  and  $0.0001 \text{ m}\cdot\text{d}^{-1}$  are 0.20, 0.020, 0.0020, and 0.00020, respectively. Thus, in intermediate- to low-flow systems ( $v < 0.1 \text{ m}\cdot\text{d}^{-1}$ )  $v$  and  $f_D$  are approximately proportional (at a treated zone length of  $>10 \text{ m}$ ). In high-flow systems ( $v = 1$  or  $10 \text{ m}\cdot\text{d}^{-1}$ ), the reaction efficiency is limited by the short residence time in the system, and the relationship of proportionality does not hold.

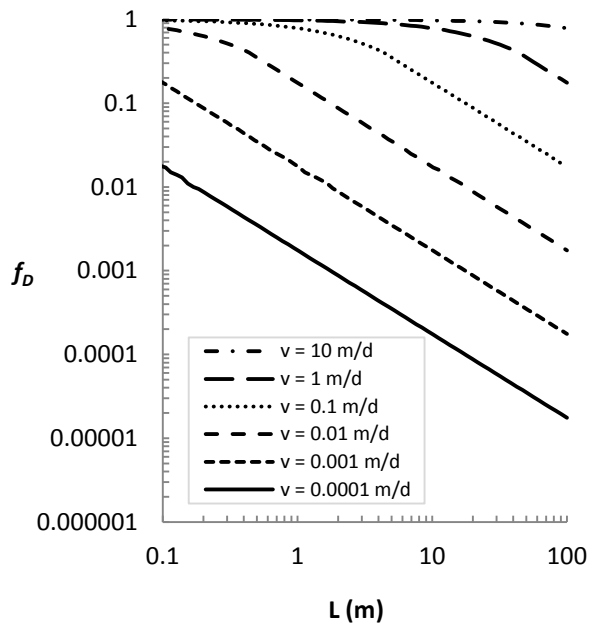


**Figure 5-7. TCE time-integrated discharge, normalized to the total TCE initially present in the system, in the case where  $k_{TCE}$  is fixed at  $0.05 \text{ m}\cdot\text{d}^{-1}$ .**

These results are applicable to systems where  $k_{TCE}$  is fixed at  $0.05 \text{ d}^{-1}$ . In field-scale treatment, a number of factors can impact degradation rates, many of which can be incorporated in treatment design. Use of nano-scale ZVI, which has been reported to have a specific surface area of 30-times that of coarser ZVI particles (Lowry and Johnson 2004), can increase the reaction rate in a system. Alternatively, implementation costs may be reduced by using a lesser amount of granular-scale ZVI, which will result in

a diminished degradation reaction rate. To address the implications of varying the degradation rates, the sensitivity of  $f_D$  to changes in  $k_{TCE}$  was analyzed.

Figure 5-8 shows the model-calculated  $f_D$  in a 10-m source zone for  $k_{TCE}$  values of 0, 0.005, 0.05, 0.5  $\text{d}^{-1}$  at groundwater seepage velocities of 1, 0.01, and 0.0001  $\text{m}\cdot\text{d}^{-1}$ . In the case of no degradation ( $k_{TCE} = 0$ ),  $f_D$  is equal to 1.0, regardless of the flow rate. In the high-flow system, sensitivity of  $f_D$  to  $k_{TCE}$  is greater, in absolute terms, than at lower flow rates; this is most apparent on a linear scale. In the intermediate- and low-flow systems,  $k_{TCE}$  and  $f_D$  are approximately inversely proportional; however, the absolute reduction is less as  $f_D$  values are low (typically less than 0.01) even at the lowest modeled reaction rate. These results suggest that the benefits of reactivity can be maximized by a simultaneous reduction in groundwater flow velocity. Furthermore, in the medium- and low-flow systems, similar treatment benefits are observed via either an order-of-magnitude reduction in  $K$  or an order-of-magnitude increase in  $k_{TCE}$ .

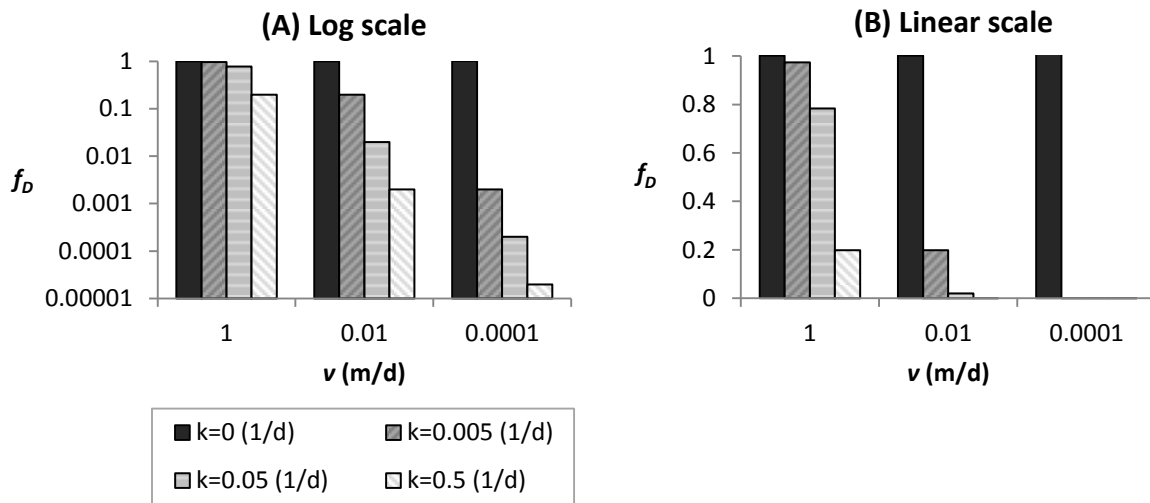


Figure 5-8. TCE discharge from a 10-m source: sensitivity to change in reaction rate,  $k_{TCE}$ , across a range of seepage velocities. Data are shown on a logarithmic scale (A) and linear scale (B).

*Contaminant Flux.* The molar flux of species  $i$ ,  $J_i$  ( $\text{mol m}^{-2}\text{d}^{-1}$ ), that crosses the down-gradient face of the treated soil body ( $x = L$ ) at time  $t$  is calculated as follows:

$$J_i(L, t) = v C_i(L, t) \quad (26)$$

Equation 26 suggests that  $J_i$  is directly proportional to  $v$  and  $C_i$ . Under the model scenario,  $v$  is fixed at a constant value after mixing. Thus, changes in  $J_i$  after mixing must result from changes in  $C_i$  at the downgradient face of the treated soil body.

Figure 5-9 shows model-calculated TCE molar flux,  $J_{TCE}$ , versus time for six treatment scenarios, including three flow rates ( $v = 1, 0.01, \text{ or } 0.0001 \text{ m}\cdot\text{d}^{-1}$ ) in systems with reaction ( $k_{TCE} = 0.05 \text{ d}^{-1}$ ) or without reaction. When TCE-NAPL remains present in the system, the concentration at  $L$  remains constant at  $C_{TCE}^*$ . Thus, under the conditions of the model system, the initial  $J_{TCE}$  values are directly proportional to  $v$  and are independent of  $k_{TCE}$ . In the high-, medium, and low-flow systems, the initial  $J_{TCE}$  values are  $7.9 \times 10^6$ ,  $7.9 \times 10^4$ , and  $7.9 \times 10^2 \text{ }\mu\text{mol}\cdot\text{m}^{-2}\text{d}^{-1}$ , respectively. The flux reduction in the low-flow system occurs at the expense of longevity: NAPL persists for 80 days in the high flow system but persists for 790,000 days (2000 years) in the low-flow system, in the absence of any degradation. However, the impact of degradation is greatest in the low-flow system. The duration of high contaminant flux is only slightly reduced in the high-flow system with reaction. In the low-flow system, inclusion of degradation reduces the duration of flux substantially.

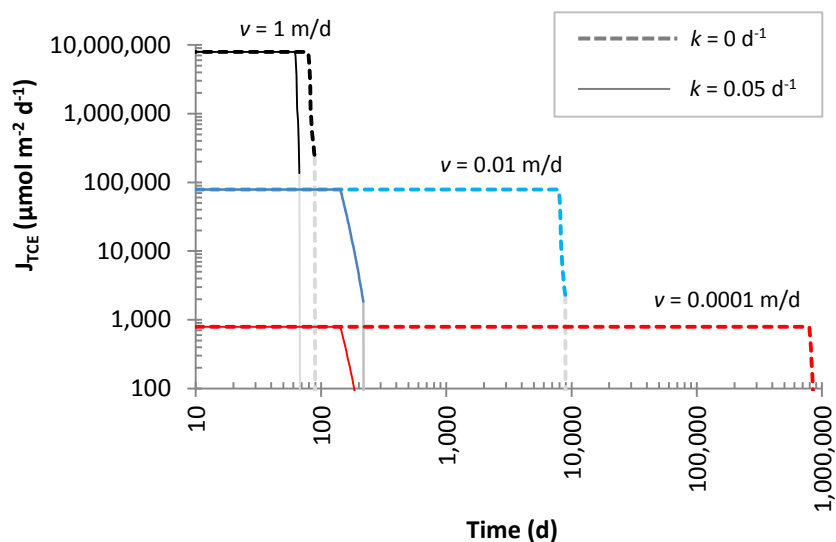


Figure 5-9. TCE molar flux across the down-gradient face of a 10-m-long source zone for the model scenarios of high-, mid-, and low-flow, each with and without ZVI-mediated degradation. Extrapolated data is shown in light gray.

Figure 5-10 shows the molar flux of all components in the TCE degradation network, based on modeled discharge from a 10-m long source zone. The molar flux values for degradation products shown in Figure 5-10 are theoretical in that neither solubility limitations nor partitioning of degradation products into non-aqueous phases (gas, NAPL, or solid) are accounted for. Although molar-flux values in a real system may differ from those presented, the results provide useful insights. First, at each of the modeled flow rates, chlorinated intermediates including DCE and VC account for a very small fraction of the molar discharge. DCE flux is approximately two orders of magnitude lower than that of TCE and VC flux is approximately two orders of magnitude lower than that of DCE. Thus, the degraded fraction of TCE is primarily discharged in the form of the non-chlorinated products ethene and ethane. Another observation is that in the mid- and low-flow systems, ethane flux surpasses that of TCE and persists after TCE flux has declined (i.e., after TCE-NAPL has been depleted). The reasons for this are two-fold: first, the rate of reaction is rapid, relative to that of discharge, such that degradation products accumulate in the system; second, the total amount of TCE in the aqueous phase is small compared to the total TCE in the

system (i.e., aqueous- plus NAPL-phase TCE). As TCE-NAPL is dissolved and then converted into degradation products, which are only slowly discharged from the system, the quantity of degradation products present may surpass the solubility-limited aqueous-phase concentrations of TCE.

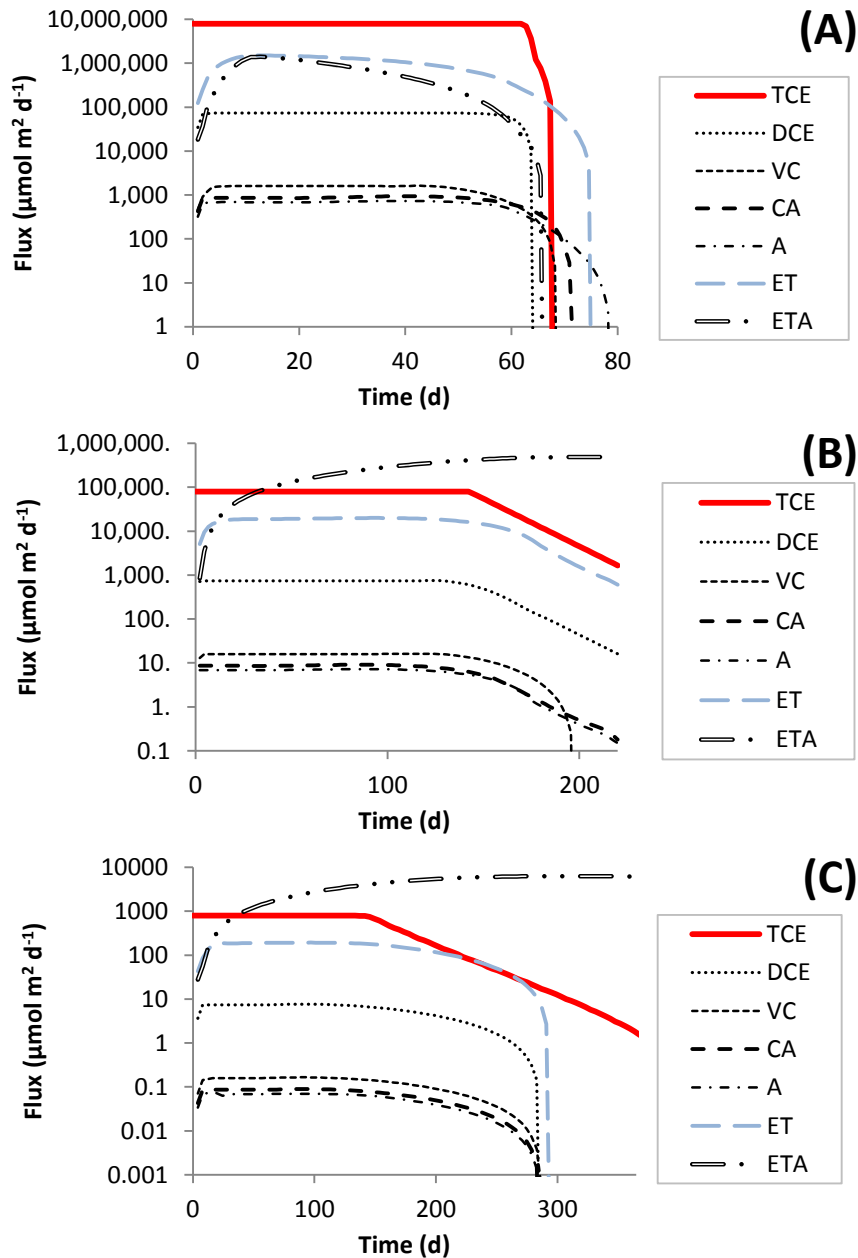


Figure 5-10. Model-predicted flux of TCE and degradation products: (A)  $v = 1 \text{ m}\cdot\text{d}^{-1}$ , (B)  $v = 0.01 \text{ m}\cdot\text{d}^{-1}$ , and (C)  $v = 0.0001 \text{ m}\cdot\text{d}^{-1}$ . In all cases,  $k_{\text{TCE}} = 0.05 \text{ d}^{-1}$ .

*NAPL Behavior.* The preceding discussion has focused on contaminant flux and discharge, which are common metrics for source-zone remediation. The analysis has been based on model-predicted aqueous-phase concentrations at the down-gradient face of the treated soil body. The NAPL phase is immobile and therefore does not contribute directly to contaminant mass discharged from the system. However, NAPL behavior governs discharge behavior. We now shift our focus to the NAPL phase within the system.

The NAPL saturation is initially uniform across the treated soil body. Two processes contribute to the removal of NAPL: (a) dissolution into clean influent water and (b) replenishment of TCE removed from the aqueous phase due to ZVI-mediated degradation. Dissolution into influent water occurs at the up-gradient face of the NAPL body and is marked by a dissolution front, which advances along the  $x$ -axis with the passage of time. NAPL depletion due to degradation occurs uniformly across the treated soil body, and results in a uniform decline in the NAPL saturation across the zone where NAPL remains. These processes are illustrated in Figure 5-11, which shows the progression of NAPL saturation profiles versus  $x$ -axis position at various times.

Figure 5-11 shows modeled NAPL saturation profiles for systems with reaction ( $k_{TCE} = 0.05 \text{ d}^{-1}$ ) and without reaction at groundwater seepage velocities of 1, 0.01, and 0.0001  $\text{m d}^{-1}$ . In the absence of degradation, a similar set of curves are generated in the high-, medium, and low-flow systems. However, the time scale is highly dependent on the flow rate, as the NAPL dissolution front crosses the 10-m source zone after approximately 82, 8200, and 820,000 days, respectively, in the high-, medium-, and low-flow systems. Conversely, in systems that include degradation, different patterns in the propagation of the NAPL dissolution front are noted. In the high-flow system, the NAPL concentration is diminished concurrently with progress in the  $x$ -axis direction of the dissolution front. In systems with reduced flow rates, the NAPL concentration is diminished with little-to-no clear movement of the dissolution front in the  $x$ -axis direction. These patterns suggest that NAPL longevity is controlled by degradation in medium- and low-flow rate systems. In high-flow systems, the impact of degradation is limited and NAPL

longevity is controlled primarily by the groundwater seepage velocity. With no degradation, all TCE is eventually discharged from the system and the NAPL longevity is controlled entirely by the groundwater seepage velocity.

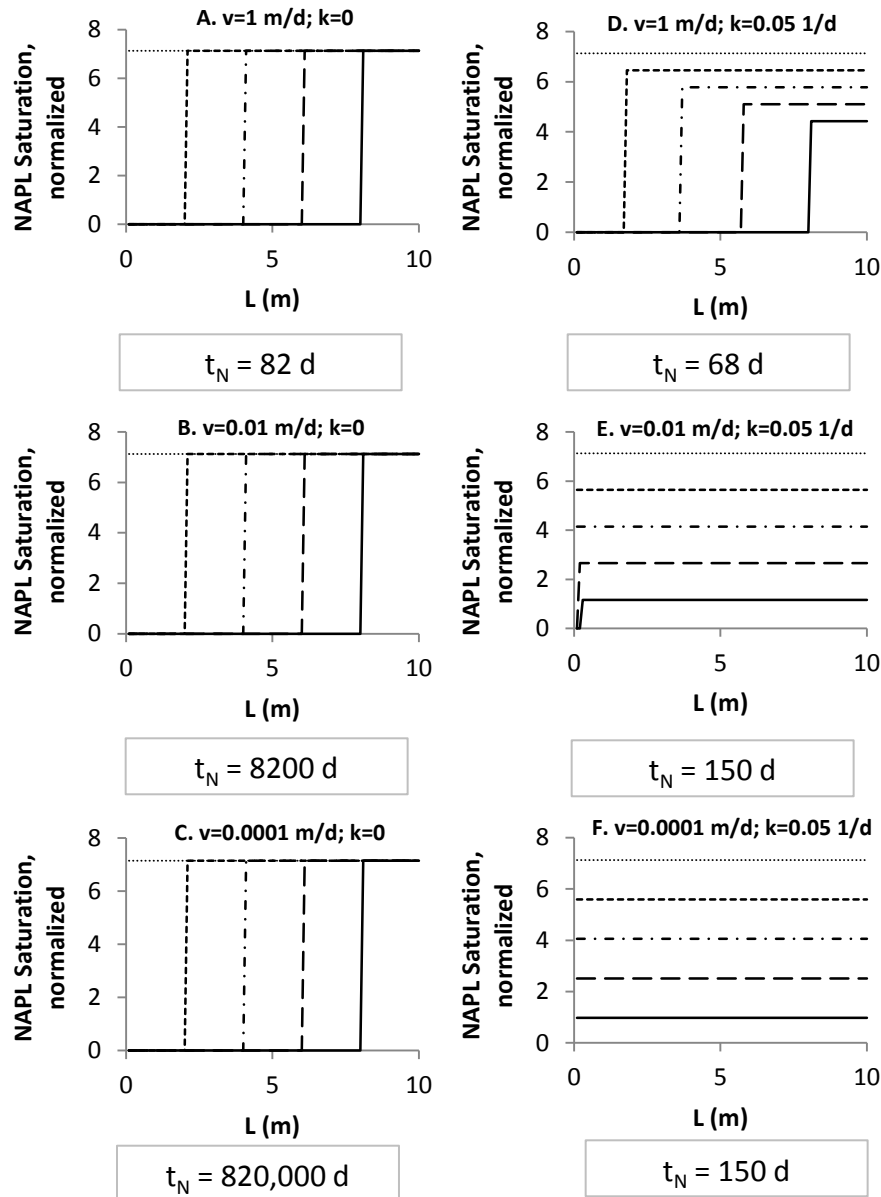


Figure 5-11. Profile of NAPL saturation, normalized to the TCE concentration at solubility ( $S_N \bar{p}_N / C_{TCE}^*$ ), in a 10-m long source. A, B, and C show model simulation results at a range of seepage velocities in systems with no reaction ( $k_{TCE} = 0$ ). D, E, and F show results in systems with reaction ( $k_{TCE} = 0.05 \text{ d}^{-1}$ ). Lines indicate NAPL saturation at times corresponding to the following multiples of the time of NAPL longevity,  $t_N$ :  $0 \cdot t_N$  (.....),  $0.2 \cdot t_N$  (-----),  $0.4 \cdot t_N$  (- · - · -),  $0.6 \cdot t_N$  (- - - -), and  $0.8 \cdot t_N$  (——). The model-calculated value for  $t_N$  is shown in the legend for each chart.

Figure 5-12 shows model-predicted NAPL longevity under conditions of variable flow rate and degradation rate. Flow rate was varied over six orders-of-magnitude, ranging from 0.0001 to 10 m·d<sup>-1</sup>. At each of these flow rates,  $k_{TCE}$  was evaluated at values of 0, 0.005, 0.05, and 0.5 m·d<sup>-1</sup>. With no degradation, a linear response between longevity and seepage velocity is observed. At high degradation rates and/or low flow rates, NAPL longevity is independent of the flow rate and is approximately inversely proportional to  $k_{TCE}$ . In terms of the Damköhler number,  $Da$  (dimensionless), where  $Da = k_{TCE} \cdot L \cdot v^{-1}$ , longevity is independent of the flow rate when  $Da > 5$ .

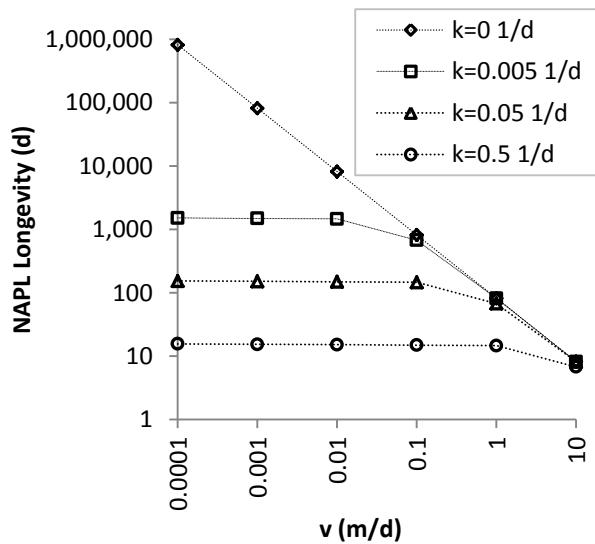


Figure 5-12. Model-predicted NAPL longevity, or time required before all NAPL is depleted from the treated soil zone, versus groundwater seepage velocity. Data series are grouped by the first-order TCE degradation rate coefficient,  $k$ . Data points represent results of individual model simulations; lines are shown to guide the eye.

#### 5.4.4 Comparison of Model to Field Applications

The model output predicts near-complete degradation of TCE over the course of about 150 days, given a degradation rate commensurate with addition of 2% ZVI. By comparison, a field application at Marine Corps Base Camp Lejeune, North Carolina, USA, a TCE-NAPL source zone was treated with 2% ZVI and 3% bentonite. TCE was depleted to detection limits at most locations across the site within 45

days. However, average initial concentrations were lower than those used for modeling. Degradation products observed across most of the site were consistent with the trends noted in the column studies. At one location, elevated levels of cDCE and VC were observed but these concentrations were reduced to levels approaching detection limits over the course of about three years.

At a field application in Skuldelev, Denmark, a PCE-NAPL source zone was treated with 3% ZVI and 1% bentonite. The average initial PCE concentration was reported to be 180 mg/kg. PCE degradation was observed with an average rate of  $0.015 \text{ d}^{-1}$  and overall concentration reductions of >99% were observed. Discharge in the 19 months after treatment was observed in a multi-level transect located 3m downgradient of the treated soils. Four phases of treatment were observed: baseline (pre-treatment), initial rapid decline, temporary increase, and a long-term tailing phase. The baseline and initial rapid decline phases are consistent with the observations presented within this research. Unless concentrations are measured very near the face of the treated soil body, the long-term treatment characteristics in a down-gradient monitoring well are likely to be controlled by contaminant release from storage, including low-permeability zones and sorbed onto the solid phase. Such processes are likely to control down-gradient effects of treatment but are highly site-specific and are not included in the present experiment.

Two of the reported field applications were tested for hydraulic conductivity in the mixed soil zone before and after mixing. In one application, addition of 3% bentonite to media of moderately high conductivity resulted in a reduction Site-wide average pre- and post-mixing hydraulic conductivity values were  $2 \times 10^{-5}$  and  $5 \times 10^{-8} \text{ m}\cdot\text{s}^{-1}$ , respectively, indicating a reduction of about 2.5 orders of magnitude. In another application, addition of 1% bentonite resulted in an average reduction by about an order of magnitude (Bozzini et al. 2006). This reduction in  $K$  is roughly consistent with the observation that in source materials of moderately high permeability,  $K$  is reduced by approximately one order of magnitude for each 1% bentonite added.

## 5.5 Conclusions

The overarching objective of the research conducted herein was to evaluate the interaction between the degradation rate and groundwater seepage velocity in homogenized mixed soils. In support of this objective, a mathematical model was developed to capture processes including NAPL dissolution, aqueous phase transport, and homogeneous first-order degradation. Column studies were conducted to test the model and determine values for model parameters. Finally, the model was used to predict performance following field-scale remediation.

Processes captured by the mathematical model include NAPL dissolution, advective and diffusive transport of dissolved-phase constituents, and degradation. NAPL dissolution was modeled as an equilibrium process. Observations of NAPL dissolution in the column experiments support this assumption. The standard ZVI-mediated degradation network for TCE was implemented.

In the column study experiments, a relatively small fraction of the TCE initially present was degraded via reaction with ZVI. The limited amount of TCE degradation observed in the column studies is attributed to the limited residence time within the columns. Formation of degradation products indicated that TCE degradation did indeed occur. Kinetic modeling was conducted based on the measured degradation products. Variable degradation rates were noted in high-flow versus low flow columns, but results were of similar magnitude. The difference is possibly attributed to gas formation, which was more pronounced in the low-flow column. The model was found to adequately predict column study effluent concentrations; although data fitting was not perfect for all constituents, the general trends and concentrations predicted by the model were similar to those observed in the column study effluent. Most of the TCE was degraded via the  $\beta$ -elimination pathway - chlorinated intermediate compounds were only detected at low levels.

The model was used to predict field- scale treatment performance. When scaled up, a much more significant fraction of TCE is degraded than was observed in the column studies. This is due to a longer residence time in field-scale systems. Modeling of field-scale treatment suggests that the benefits of reactivity can be maximized by a simultaneous reduction in groundwater flow velocity, which can be achieved via soil mixing with bentonite. Furthermore, in the medium- and low-flow systems, similar treatment benefits are observed via either an order-of-magnitude reduction in  $K$  or an order-of-magnitude increase in  $k_{TCE}$ . NAPL saturation profiles and longevity were also analyzed. These patterns suggest that NAPL longevity is controlled by degradation in medium- and low-flow rate systems. In high-flow systems, the impact of degradation is limited and NAPL longevity is controlled primarily by the groundwater seepage velocity. With no degradation, all TCE is eventually discharged from the system and the NAPL longevity is controlled entirely by the groundwater seepage velocity.

## REFERENCES

- Arnold, W. A., and A. L. Roberts. 2000. Pathways and kinetics of chlorinated ethylene and chlorinated acetylene reaction with Fe(0) particles. *Environmental Science & Technology* 34 (9):1794-1805.
- Bi, E. P., J. F. Devlin, B. Huang, and R. Firdous. 2010. Transport and Kinetic Studies To Characterize Reactive and Nonreactive Sites on Granular Iron. *Environmental Science & Technology* 44 (14):5564-5569.
- Borden, R. C., and M. D. Pivoni. 1992. Hydrocarbon Dissolution and Transport - A Comparison of Equilibrium and Kinetic Models. *Journal of Contaminant Hydrology* 10 (4):309-323.
- Boudreau, B. P. 1996. The diffusive tortuosity of fine-grained unlithified sediments. *Geochimica Et Cosmochimica Acta* 60 (16):3139-3142.
- Bozzini, C., T. Simpkin, T. Sale, D. Hood, and B. Lowder. 2006. DNAPL Remediation at Camp Lejeune using ZVI-Clay Soil Mixing. In *Fifth Battelle Conference on Remediation of Chlorinated and Recalcitrant Compounds*. Monterrey, CA.
- Brusseau, M. L., Z. H. Zhang, N. T. Nelson, R. B. Cain, G. R. Tick, and M. Oostrom. 2002. Dissolution of nonuniformly distributed immiscible liquid: Intermediate-scale experiments and mathematical modeling. *Environmental Science & Technology* 36 (5):1033-1041.
- Castelbaum, D., and C. D. Shackelford. 2009. Hydraulic conductivity of bentonite slurry mixed sands. *Journal of Geotechnical and Geoenvironmental Engineering* 135 (12):1941-1956.
- Chapman, S. W., and B. L. Parker. 2005. Plume persistence due to aquitard back diffusion following dense nonaqueous phase liquid source removal or isolation. *Water Resources Research* 41 (12):W12411.
- Day, S. R., and C. Ryan. 1995. Containment, stabilization and treatment of contaminated soils using in-situ soil mixing. In *Geoenvironment 2000: Characterization, Containment, Remediation, and Performance in Environmental Geotechnics, Vols 1 and 2*, edited by Y. B. Acar and D. E. Daniel. New York: ASCE.
- Denis, J. N., A. Moyano, and A. E. Greene. 1987. Practical Synthesis of Dichloroacetylene. *Journal of Organic Chemistry* 52 (15):3461-3462.
- EPA. 2003. *The DNAPL remediation challenge: Is there a case for source depletion?* Edited by M. C. Kavanaugh and P. S. C. Rao. Cincinnati, OH: U.S. Environmental Protection Agency, National Risk Management Research Laboratory.
- Fagerlund, F., T. H. Illangasekare, T. Phenrat, H. J. Kim, and G. V. Lowry. 2012. PCE dissolution and simultaneous dechlorination by nanoscale zero-valent iron particles in a DNAPL source zone. *Journal of Contaminant Hydrology* 131 (1-4):9-28.

Fjordboge, A. S., I. V. Lange, P. L. Bjerg, P. J. Binning, C. Riis, and P. Kjeldsen. 2012a. ZVI-Clay remediation of a chlorinated solvent source zone, Skuldelev, Denmark: 2. Groundwater contaminant mass discharge reduction. *Journal of Contaminant Hydrology* 140:67-79.

Fjordboge, A. S., C. Riis, A. G. Christensen, and P. Kjeldsen. 2012b. ZVI-Clay remediation of a chlorinated solvent source zone, Skuldelev, Denmark: 1. Site description and contaminant source mass reduction. *Journal of Contaminant Hydrology* 140:56-66.

Gillham, R. W., and S. F. O'Hannesin. 1994. Enhanced degradation of halogenated aliphatics by zero-valent iron. *Ground Water* 32 (6):958-967.

Grant, G. P., and B. H. Kueper. 2004. The influence of high initial concentration aqueous-phase TCE on the performance of iron wall systems. *Journal of Contaminant Hydrology* 74 (1-4):299-312.

Guilbeault, M. A., B. L. Parker, and J. A. Cherry. 2005. Mass and flux distributions from DNAPL zones in sandy aquifers. *Ground Water* 43 (1):70-86.

Imhoff, Paul T., Peter R. Jaffé, and George F. Pinder. 1994. An experimental study of complete dissolution of a nonaqueous phase liquid in saturated porous media. *Water Resources Research* 30 (2):307-320.

Jasperse, B. H., and C. R. Ryan. 1987. Geotech import - Deep soil mixing. *Civil Engineering* 57 (12):66-68.

Jawitz, James W., Dongping Dai, P. Suresh C. Rao, Michael D. Annable, and R. Dean Rhue. 2003. Rate-Limited Solubilization of Multicomponent Nonaqueous-Phase Liquids by Flushing with Cosolvents and Surfactants: Modeling Data from Laboratory and Field Experiments. *Environmental Science & Technology* 37 (9):1983-1991.

Jeen, S. W., R. W. Gillham, and A. Przepiora. 2011. Predictions of long-term performance of granular iron permeable reactive barriers: Field-scale evaluation. *Journal of Contaminant Hydrology* 123 (1-2):50-64.

Johnson, T. L., M. M. Scherer, and P. G. Tratnyek. 1996. Kinetics of halogenated organic compound degradation by iron metal. *Environmental Science & Technology* 30 (8):2634-2640.

Lowry, G. V., and K. M. Johnson. 2004. Congener-specific dechlorination of dissolved PCBs by microscale and nanoscale zerovalent iron in a water/methanol solution. *Environmental Science & Technology* 38 (19):5208-5216.

Maji, R., and E. A. Sudicky. 2008. Influence of mass transfer characteristics for DNAPL source depletion and contaminant flux in a highly characterized glaciofluvial aquifer. *Journal of Contaminant Hydrology* 102 (1-2):105-119.

Miller, C. T., M. M. Poiriermneill, and A. S. Mayer. 1990. Dissolution of Trapped Nonaqueous Phase Liquids - Mass-Transfer Characteristics. *Water Resources Research* 26 (11):2783-2796.

- Olson, Mitchell R., Thomas C. Sale, Charles D. Shackelford, Christopher Bozzini, and Jessica Skeeane. 2012. Chlorinated Solvent Source-Zone Remediation via ZVI-Clay Soil Mixing: 1-Year Results. *Ground Water Monitoring & Remediation* 32 (3):63-74.
- Pankow, J.F., and J.A. Cherry. 1996. *Dense chlorinated solvents and other DNAPLs in groundwater: History, behavior, and remediation*. Portland, OR: Waterloo Press.
- Paria, S., and P. K. Yuet. 2006. Solidification-stabilization of organic and inorganic contaminants using portland cement: a literature review. *Environmental Reviews* 14 (4):217-255.
- Phillips, D. H., T. Van Nooten, L. Bastiaens, M. I. Russell, K. Dickson, S. Plant, J. M. E. Ahad, T. Newton, T. Elliot, and R. M. Kalin. 2010. Ten year performance evaluation of a field-scale zero-valent iron permeable reactive barrier installed to remediate trichloroethene contaminated groundwater. *Environmental Science & Technology* 44 (10):3861-3869.
- Powers, S. E., I. M. Nambi, and G. W. Curry. 1998. Non-aqueous phase liquid dissolution in heterogeneous systems: Mechanisms and a local equilibrium modeling approach. *Water Resources Research* 34 (12):3293-3302.
- Quinn, J., C. Geiger, C. Clausen, K. Brooks, C. Coon, S. O'Hara, T. Krug, D. Major, W. S. Yoon, A. Gavaskar, and T. Holdsworth. 2005. Field demonstration of DNAPL dehalogenation using emulsified zero-valent iron. *Environmental Science & Technology* 39 (5):1309-1318.
- Ritter, K., M. S. Odziemkowski, and R. W. Gillham. 2002. An in situ study of the role of surface films on granular iron in the permeable iron wall technology. *Journal of Contaminant Hydrology* 55 (1-2):87-111.
- Roy-Perreault, A., B. H. Kueper, and J. Rawson. 2005. Formation and stability of polychlorinated biphenyl Pickering emulsions. *Journal of Contaminant Hydrology* 77 (1-2):17-39.
- Sale, T. C., and D. B. McWhorter. 2001. Steady state mass transfer from single-component dense nonaqueous phase liquids in uniform flow fields. *Water Resources Research* 37 (2):393-404.
- Scherer, M. M., B. A. Balko, D. A. Gallagher, and P. G. Tratnyek. 1998. Correlation analysis of rate constants for dechlorination by zero-valent iron. *Environmental Science & Technology* 32 (19):3026-3033.
- Schwarzenbach, R. P., P. M. Gschwend, and D. M. Imboden. 2003. *Environmental Organic Chemistry*. 2nd ed. New York: Wiley.
- Shackelford, C. D. 1994. Critical Concepts for Column Testing. *Journal of Geotechnical Engineering-ASCE* 120 (10):1804-1828.
- Shackelford, C. D., and T. C. Sale. 2011. Using the ZVI-clay technology for source zone remediation. *Geo-Strata* 15 (2):36-42.
- Shackelford, C. D., T. C. Sale, and M.R. Liberati. 2005. In-situ remediation of chlorinated solvents using zero valent iron and clay mixtures: A case history. In *Waste Containment and Remediation*, edited by A. Alshawabkeh, C. H. Benson, P. J. Culligan, J. C. Evans, B. A. Gross, D. Narejo, R. Reddy, C. D. Shackelford and J. G. Zornberg. Geotechnical Special Publication 142 (CD ROM), Reston, VA: ASCE.

Siegrist, R. L., O. R. West, M. I. Morris, D. A. Pickering, D. W. Greene, C. A. Muhr, D. D. Davenport, and J. S. Gierke. 1995. In-situ mixed region vapor stripping in low-permeability media. 2. Full-scale field experiments. *Environmental Science & Technology* 29 (9):2198-2207.

Siegrist, Robert L., Michelle Crimi, and Richard A. Brown. 2011. Chemical Oxidation: Technology Description and Status

In Situ Chemical Oxidation for Groundwater Remediation, edited by R. L. Siegrist, M. Crimi and T. J. Simpkin: Springer New York.

Stroo, H. F., A. Leeson, J. A. Marqusee, P. C. Johnson, C. H. Ward, M. C. Kavanaugh, T. C. Sale, C. J. Newell, K. D. Pennell, C. A. Lebron, and M. Unger. 2012. Chlorinated Ethene Source Remediation: Lessons Learned. *Environmental Science & Technology* 46 (12):6438-6447.

Taghavy, A., J. Costanza, K. D. Pennell, and L. M. Abriola. 2010. Effectiveness of nanoscale zero-valent iron for treatment of a PCE-DNAPL source zone. *Journal of Contaminant Hydrology* 118 (3-4):128-142.

Tratnyek, P. G., M. M. Scherer, B. L. Deng, and S. D. Hu. 2001. Effects of natural organic matter, anthropogenic surfactants, and model quinones on the reduction of contaminants by zero-valent iron. *Water Research* 35 (18):4435-4443.

Wadley, S. L. S., R. W. Gillham, and L. Gui. 2005. Remediation of DNAPL source zones with granular iron: Laboratory and field tests. *Ground Water* 43 (1):9-18.

Zhang, Y. S., and R. K. Gillham. 2005. Effects of gas generation and precipitates on performance of Fe degrees PRBs. *Ground Water* 43 (1):113-121.

Zimmerman, J. R., U. Ghosh, R. N. Millward, T. S. Bridges, and R. G. Luthy. 2004. Addition of carbon sorbents to reduce PCB and PAH bioavailability in marine sediments: Physicochemical tests. *Environmental Science & Technology* 38 (20):5458-5464.

## CHAPTER 6

### LONG-TERM POTENTIAL OF IN SITU CHEMICAL REDUCTION FOR TREATMENT OF POLYCHLORINATED BIPHENYLS IN SOILS

#### *Synopsis of Chapter*

Polychlorinated biphenyls (PCBs) are well-known for being hydrophobic and persistent in the environment. Although many treatment approaches have been demonstrated to result in degradation of PCBs in water or water/cosolvent systems, few examples exist where such approaches have been applied successfully for PCB degradation in soil-water systems. A possible explanation for the limited treatment of PCBs in soil-water systems is that reactants that are capable of degrading PCBs in the aqueous phase are unlikely to persist long enough to achieve meaningful treatment of slowly-desorbing PCBs associated with the soil phase. To investigate this explanation, laboratory studies were conducted to evaluate chemical reductants, including zero valent metals, palladium (Pd) catalyst, and emulsified zero valent iron (EZVI), for dechlorination of PCBs in the presence and absence of soil. In the absence of soil, Pd-catalyzed treatments (Pd with electrolytic ZVI or iron/aluminum alloy) achieved rapid destruction of a model PCB congener, 2-chlorobiphenyl, with half-lives ranging from 43 to 110 min. For treatment of soils containing Aroclor 1248 at an initial concentration of approximately  $1500 \text{ mg}\cdot\text{kg}^{-1}$ , Pd-catalyzed treatments achieved no measurable enhancement over the background PCB depletion rate (i.e., that measured in the untreated control) of  $5.3 \text{ mg}\cdot\text{kg}^{-1}\cdot\text{week}^{-1}$ . In the presence of soils, EZVI was the only approach evaluated that resulted in a clear enhancement in PCB dechlorination rates. EZVI achieved PCB concentration reductions of greater than 50 % at an average rate of  $19 \text{ mg}\cdot\text{kg}^{-1}\cdot\text{week}^{-1}$ . The results suggest that slow PCB desorption limits treatment effectiveness in soils.

## 6.1 Introduction

In 1976, the Toxic Substances and Control Act (TSCA) ended commercial production of polychlorinated biphenyls (PCBs) in the United States; world-wide production of PCBs was greatly reduced in 2001 with the Stockholm Convention on Persistent Organic Pollutants. After the cessation of commercial-scale PCB production, global concentrations of PCBs in air, water, and soil have declined (Mackay and Cherry 1989). Nevertheless, PCBs continue to present environmental and social challenges. Methods that have typically been employed for treatment of PCB-impacted soils and sediments include thermal oxidation (incineration), chemical oxidation, biodegradation, stabilization/sequestration, and thermal desorption. Although capable of reducing environmental risks of PCBs under certain circumstances, each of these is subject to limitations. For example, thermal and chemical oxidation technologies risk formation of polychlorinated dibenzo-*p*-dioxins and dibenzofurans (Manzano et al. 2003). Biodegradation of PCBs has been widely studied (e.g., Korte et al. 2002; Kouznetsova et al. 2007; Krembs et al. 2010) but is often slow and may result in incomplete dechlorination. Stabilization/sequestration can effectively reduce mobility and bioavailability of PCBs (Burriss et al. 1995) but does not ultimately result in removal of PCBs from the environment. Thermal desorption can be effective at reducing total PCB concentrations but requires high temperatures (>200°C) (Mackenzie et al. 2006; Manzano et al. 2003) which may be cost prohibitive for certain situations and may be challenging to implement in high groundwater flow conditions.

An approach that could overcome these limitations involves *in situ* use of chemical reductants. A recent review addresses the advantages and limitations of several chemical reductants for degradation of PCBs (Jeen et al. 2011). Of the extensive list of treatments identified in the review, only eight addressed treatment of PCBs in soil or sediment (Agarwal et al. 2009; Klausen et al. 2003; Johnson et al. 1996; Siegrist et al. 2011; Koelmans et al. 2009; Kjellerup et al. 2008; Karn et al. 2009; Varanasi et al. 2007). Generally, these studies reflect conditions that are unlikely to be applied for *in situ* treatment. Extreme

temperature (greater than 300°C) or pressure (20 MPa at 100°C) conditions were often required for substantial degradation of PCBs (Klausen et al. 2003; Kjellerup et al. 2008; Varanasi et al. 2007). Although the authors did not always state their envisioned method of implementation, we assume that such conditions are intended primarily for *ex situ* applications. Treatment of PCBs in soils under ambient temperature and pressure conditions utilized reactive media loading rates of 25 to 250% of the mass of soil treated (Siegrist et al. 2011), which may present challenges in terms of cost and deliverability. In addition, several studies addressed the use of surfactants or cosolvents to enhance liquid-phase availability of PCBs (Agarwal et al. 2009; Koelmans et al. 2009; Karn et al. 2009). Under laboratory study conditions, surfactants and cosolvents have been effective in enhancing PCB desorption rates from soil and sediment, but have often resulted in limited reaction rates (e.g., Agarwal et al. 2009; Koelmans et al. 2009; Devor et al. 2008). Information presented by Wu et al. (2011) suggests that few, if any, instances of degradation of PCB in soil-water systems under *in situ* conditions have been achieved.

PCBs are difficult to degrade in soils and sediments for two primary reasons: (1) high chemical stability and (2) high hydrophobicity, which leads to low availability in the aqueous phase. In the presence of soils, equilibrium phase partitioning calculations indicate that the fraction of PCBs in the aqueous phase may range from 0.79% for mono-chlorobiphenyl (CBP) to 0.00023% for deca-CBP (see the Supporting Information). Therefore, any treatment applied to the aqueous phase may affect only a very small fraction of the total PCB mass.

The hypothesis addressed by this research is that PCBs present a treatment conundrum, wherein reactive media exist that are capable of degrading persistent compounds such as PCBs, but such reactive media are unlikely to persist long enough under *in situ* conditions to achieve meaningful treatment of PCBs in soils. The objectives of the study include (a) comparing treatment performance of chemical reductants, including zero-valent metals and Pd-catalyst, in water and soil-water systems and (b) evaluating the long-term potential of these chemical reductants to enhance the degradation rates of PCBs in soil-water systems. For treatment of PCBs in the presence of soils, the envisioned implementation

approach utilizes soil mixing for delivery of reactive media and stabilizing agents, an approach that has been advanced for remediation of soils impacted with chlorinated aliphatic compounds (Dercova et al. 1999; Wadley et al. 2005). Moreover, the studies focus on conditions that conceivably can be implemented *in situ* at contaminated sites.

## 6.2 Materials and Methods

### 6.2.1 Materials

The studies were conducted using soils, groundwater, and field-weathered PCB dense non-aqueous phase liquid (DNAPL) collected from the Outboard Marine Corporation (OMC) Superfund Site, Waukegan, IL. Soil samples consisted of medium-grained, poorly-sorted sand. Groundwater and PCB DNAPL, which consisted of nearly-pure Aroclor 1248, were collected from on-site monitoring wells.

Treatment reagents included 50-200 mesh zero-valent iron (Fe) filings and 40-80 mesh zero-valent magnesium (Mg) obtained from Peerless Metal Powders and Abrasive (Detroit, MI) and Fisher Scientific (Pittsburgh, PA), respectively. OnMaterials (Akron, OH) provided electrolytic Fe (Fe\*), metallic iron/aluminum alloy (Fe/Al), and 1% zero-valent palladium (Pd) on alumina (Pd-Al<sub>2</sub>O<sub>3</sub>). The Fe\*, Fe/Al, and Pd-Al<sub>2</sub>O<sub>3</sub> were shipped and stored in propylene glycol (PG). Emulsified zero-valent iron (EZVI) was produced following procedures similar to those outlined by Quinn et al. (2005). Materials used to make EZVI included BASF (Evans City, PA) Microspheres 200-plus zero-valent Fe, food-grade corn oil and SPAN-85 surfactant (Sigma-Aldrich, St. Louis, MO). The EZVI was prepared in a kitchen-grade blender by mixing 100 mL of water, 80 mL of corn oil, 3 mL of surfactant, and 20 g of micro-scale Fe. A 10% bentonite slurry mixture was prepared with Black Hills Bond unaltered sodium bentonite (Black Hills Bentonite, Mills, WY) and tap water (City of Fort Collins). All other chemicals used were ACS grade.

### 6.2.2 Aqueous Study Methods

The aqueous-phase study was conducted to validate reactivity of select treatments toward 2-chlorobiphenyl, which was selected as the model PCB congener due to a relatively high solubility (2.9 mg/L). Five treatment sets were included: Fe\*, Fe\*+Pd, Fe/Al, Fe/Al+Pd, and an untreated control (additional details are provided in the Supporting Information); each treatment set was prepared in triplicate. The study was conducted in 60-mL borosilicate glass vials equipped with Mininert® caps. In preparation for the study, the Fe\*, Fe/Al, and Pd-Al<sub>2</sub>O<sub>3</sub> (all in PG) were transferred into the dry vials under atmospheric conditions. The vials were then placed into an anaerobic chamber, where 50 mL of site groundwater were added. Next, 50 µL of a spiking solution, comprising 2-chlorobiphenyl (Ultra Scientific, North Kingstown, RI) in methanol, were added to obtain an initial concentration of 10 µM. Vials were then rotated in a tumbler at 20 rpm until sampling.

For sample collection, 500 µL of the liquid phase were removed through the Mininert® cap using a 500- µL glass gas-tight syringe. The liquid sample was added to a 2-mL glass vial containing 500 µL of *n*-hexane. The extraction vial was placed on a vortex shaker (Scientific Manufacturing Industries, Bohemia, NY) for 60 seconds. A portion of the organic phase was then removed for analysis.

### 6.2.3 Soils Study Methods

Soil-phase studies were conducted to evaluate the potential of select reductants to achieve reductive degradation of PCBs under conditions that conceivably can be applied for *in situ* treatment. The treatments applied in the soil-phase study included Fe, Mg, Fe\*, Fe\*+Pd, Fe/Al, Fe/Al+Pd, EZVI without clay, and EZVI with clay (see the Supporting Information for additional details). Two controls were included that consisted of soils mixed with or without bentonite clay. Most treatments consisted of 5% reductant (i.e., mass of reductant per mass of dry soil), the maximum amount that can be applied under field soil-mixing conditions before delivery and distribution become problematic (Wadley et al.

2005) and 2% bentonite. The rationale for including bentonite is that the envisioned method of emplacement would involve soil mixing; bentonite serves as a drilling fluid, which facilitates uniform reagent delivery (Dercova et al. 1999), and can facilitate formation of a Pickering emulsion with PCB DNAPL (Hildebrand et al. 2009a).

The study was conducted in 125-mL glass vials containing 100 g of site soils. Soils were spiked to an initial PCB concentration of about  $1500 \text{ mg}\cdot\text{kg}^{-1}$  by continuously mixing site soils, groundwater, and site-collected PCB DNAPL on a tumbler at 20 rpm for several days. The PCB-spiked soils were admixed with treatment reagents in an anaerobic chamber. For treatment application, reagents were blended with a 10% clay-in-water slurry, which was then admixed with PCB-spiked soils within each vial using a stainless steel spatula. Vials were stored in an anaerobic chamber until sampling. To simulate environmental conditions, no attempt was made to enhance or inhibit biological activity.

For the studies including soils, non-sacrificial sampling was conducted 11 and 66 weeks after treatments were applied. Approximately 20 g of wet soil was removed from each vial. PCB extraction from the samples was then conducted following EPA method 3550 using a 50/50 blend of hexane and acetone. Ultrasonication was performed using a Misonix (Farmingdale, NY) S-4000 with a 1.9-cm (3/4-inch) horn. After extraction, the acetone/hexane mixture was exchanged with hexane and concentrated to a volume of about 10 mL.

#### 6.2.4 Analysis

PCB analysis was completed by direct injection of the hexane extract into an Agilent 6890 GC with an Agilent 5973N mass spectrometer (MS). For the soil-phase and aqueous-phase PCB studies, the GC was equipped with an Agilent DB-5 column (30 m length  $\times$  0.32 mm ID,  $\times$  0.25  $\mu\text{m}$  film thickness) and a Restek Rxi®-624Sil MS column (30 m  $\times$  0.25 mm  $\times$  1.4  $\mu\text{m}$ ), respectively.

## 6.2.5 Statistical Analysis

Statistical analysis of the aqueous-phase study results was based on the standard errors calculated from triplicate sampling. The soil phase study did not include replicate analyses. In the absence of replicate samples, statistical analysis was conducted by grouping treatments based on select properties (e.g., EZVI treatments, which included a desorbing agent, versus other treatments that excluded desorbing agents) and comparing population means. Populations were compared using the Student's t-test: two-sample assuming equal variances (Microsoft Excel).

## 6.3 Results and Discussion

### 6.3.1 Treatment of PCBs in Aqueous-Phase Systems

The aqueous-phase study was conducted to evaluate reactivity of Fe\* and Fe/Al, with and without Pd catalyst, to reductively dechlorinate PCBs in the absence of soils. Figure 6-1 shows that neither degradation of 2-chlorobiphenyl nor biphenyl production were observed over a 24-hour period in treatment sets that excluded Pd. The lack of PCB degradation in vials containing zero-valent metals without Pd catalyst is consistent with results reported in previous studies (e.g., Lowry and Johnson 2004). In treatment sets that included Pd, degradation of 2-chlorobiphenyl and corresponding production of biphenyl was observed. Degradation of 2-chlorobiphenyl appears to have been more rapid in vials containing Fe\*+Pd ( $t_{1/2} = 43 \pm 3$  min) than in those containing Fe/Al+Pd ( $t_{1/2} = 110 \pm 70$  min), although the half-lives were statistically similar ( $p$ -value = 0.02). The PCB mass balances, including both 2-chlorobiphenyl and biphenyl, for Fe\*+Pd and Fe/Al+Pd were  $75 \pm 9\%$  and  $71 \pm 4\%$ , respectively. The incomplete mass balances may indicate sorption losses or formation of other degradation products. Mass balances for 2-chlorobiphenyl in the untreated control, Fe, and Fe/Al batches were all approximately 100%, thus indicating that sorption alone is unlikely to account for the incomplete recovery. Other

potential reductive degradation products, such as bicyclohexyl or cyclohexylbenzene (Jeen et al. 2011), were not detected during GC/MS analysis of sample extracts.

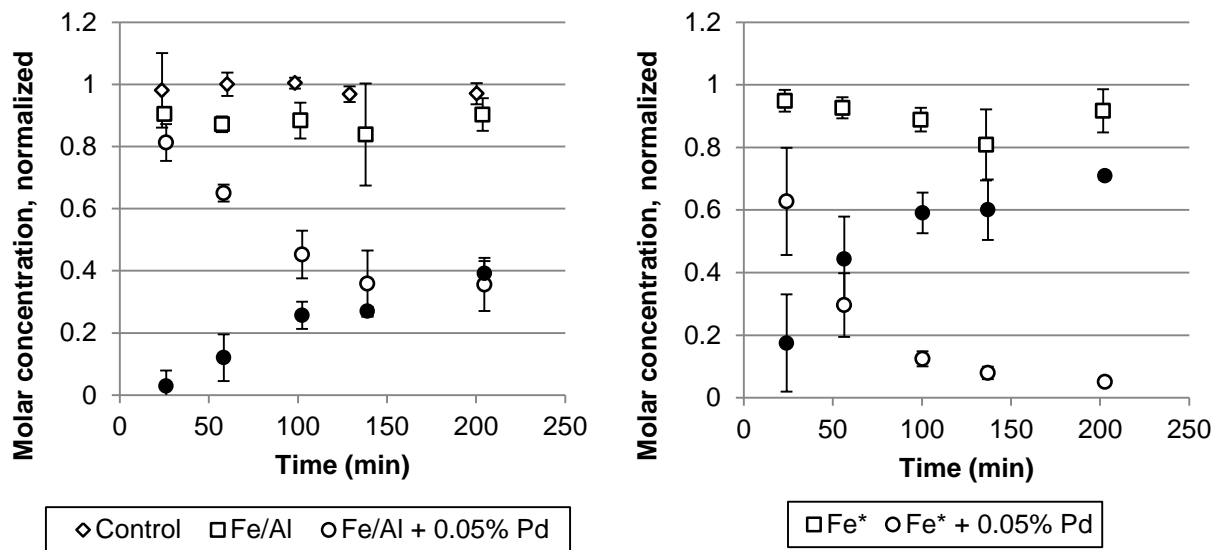


**Figure 6-1. Reductive dechlorination of 2-chlorobiphenyl (hollow data points) and formation of biphenyl (solid data points) by Fe/Al (left) and electrolytic Fe (right) in aqueous phase-based studies. Biphenyl production was only observed in treatments that included Pd catalyst. Results are shown for treatments with 0.05% Pd and without Pd. The untreated (no reductant added) control is shown in the figure to the left. Data points represent the mean values of triplicate samples and error bars represent the standard deviations of the calculated mean values.**

The potential for Pd-catalyzed reductive hydrodechlorination of liquid-phase PCBs has been well-documented (Jeen et al. 2011; Batchelor et al. 2002; Devor et al. 2008; Schuth and Reinhard 1998; Bozzini et al. 2006). In general, removal of liquid-phase PCBs has been observed with half-lives on the order of minutes to hours, which is comparable to the half-lives measured in this study. Thus, results are consistent with previous research and confirm the potential reactivity of the Pd-catalyzed treatments toward aqueous-phase PCBs.

### 6.3.2 Treatment of PCBs in the Presence of Soils

In contrast to the relatively short liquid-phase studies, the soil-phase studies were conducted to evaluate the long-term treatment potential of reductants including zero valent metals, Pd catalyst, and EZVI. To effectively demonstrate long-term treatment potential, the soil-phase study was conducted for over one year.

In the experiments conducted in soil-water systems, reductions in PCB concentrations between 11- and 66-weeks were observed in all samples, except the control with bentonite clay (Figure 6-2). Mean PCB concentrations at 11- and 66-weeks were  $1530 \pm 160$  and  $1110 \pm 100$   $\text{mg}\cdot\text{kg}^{-1}$ , respectively. In the no-clay control, PCB concentrations were reduced by 19% between 11 and 66 weeks, corresponding to an average degradation rate of  $5.3$   $\text{mg}\cdot\text{kg}^{-1}\text{week}^{-1}$ . The control with clay was the only treatment in which no degradation is apparent between 11- and 66-weeks. The apparent lack of degradation in the clay-containing control may be attributed to an anomalously low PCB concentration observed in this sample at 11 weeks; the concentration at 66-weeks is similar to that observed in other treatments. In soils treated with zero valent metals, including Fe, Mg, Fe\*, and Fe/Al, the average PCB concentration reduction was 23% (corresponding to an average degradation rate of  $6.3$   $\text{mg}\cdot\text{kg}^{-1}\text{week}^{-1}$ ). In soils treated with Pd catalyst the average PCB concentration reduction was 21% ( $5.9$   $\text{mg}\cdot\text{kg}^{-1}\text{week}^{-1}$ ). In EZVI-treated soils, the average PCB concentration reduction was 56% ( $19$   $\text{mg}\cdot\text{kg}^{-1}\text{week}^{-1}$ ).

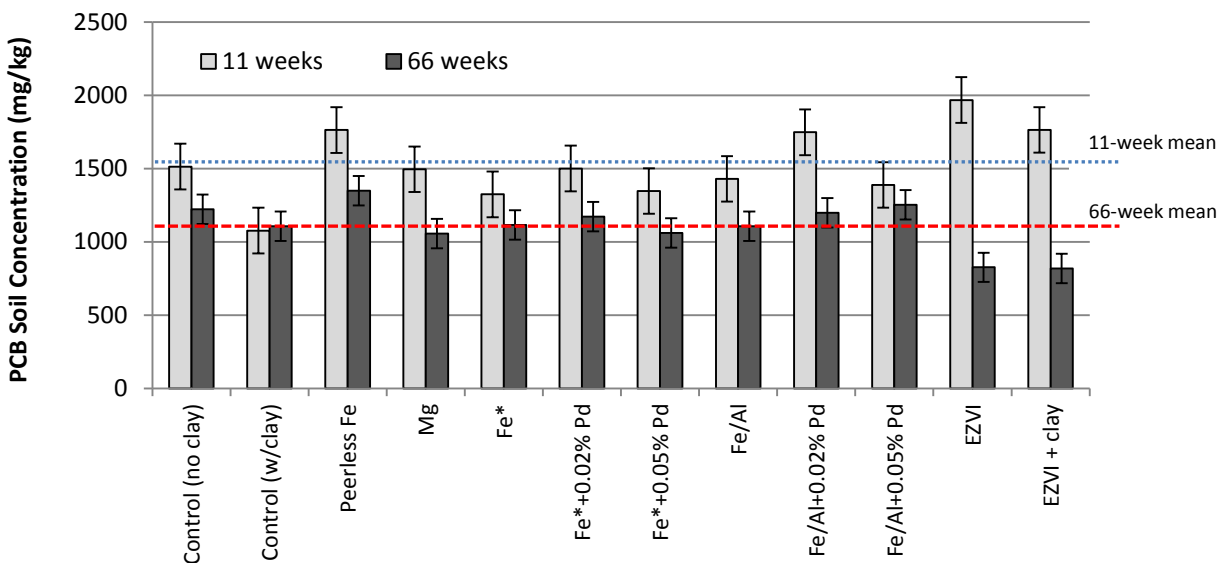


**Figure 6-2. Total PCB concentration at 11 and 66 weeks after treatment. Error bars represent 95% confidence intervals calculated for all 11-week or all 66-week data. Mean values at 11 weeks (1530 mg/kg) and 66 weeks (1110 mg/kg) are indicated by dashed lines. Fe\* indicates electrolytic zero-valent iron.**

PCB homolog distributions (see Figure 6-3; additional discussion is provided in the Supporting Information) were calculated from the sum of GC/MS chromatogram peak areas for each homolog. Homolog distributions are presented for di-, tri-, tetra-, and penta-CBP homologs. Lesser amounts of mono- and hexa- CBP were also detected, but at levels that are too small to be apparent in Figure 6-3. Biphenyl was not produced in measureable quantities in any of the treated vials.

PCB concentration reductions were observed across the spectrum of treatments applied, no-clay control included. Thus, it is likely that natural attenuation processes including aging, such as diffusion-limited intra-particle transport and strong sorption within the soil matrix (Cornelissen et al. 2005), or biologically-mediated reductive dechlorination are responsible for much of the observed concentration decline. A modest increase in mono- and di-CBP observed in all of the non-EZVI treatments, no-clay control included, provides evidence that some degradation has occurred. Nevertheless, when compared to the field sample of PCB oil, changes in the homolog distributions in all non-EZVI treatments at 11 and 66

weeks are relatively minor. The only treatments that stand out in terms of the degree of PCB concentration reduction and changes in homolog distribution are those that involved EZVI.

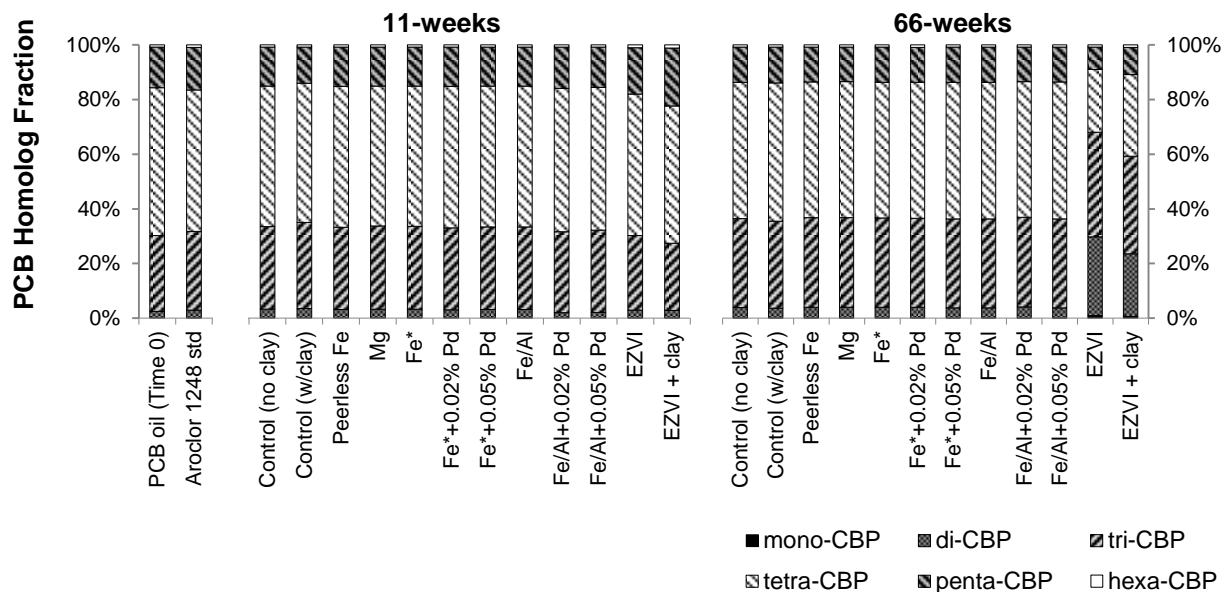


**Figure 6-3. Homolog distribution (showing mono- through hexa-CBP) after 11 weeks (center) and 66 weeks (right). For comparison, the homolog distribution of the field-collected sample of PCB oil and an Aroclor 1248 standard (Ultra Scientific) are also shown (left). Fe\* indicates electrolytic zero-valent iron.**

### 6.3.3 Zero Valent Metals and Pd Catalysis

In the present experiment, treatment reagents that were able to rapidly degrade PCBs in the liquid phase (Fe/Al+Pd and Fe\*+Pd) did not provide any clear enhancement in the rates of PCB degradation in soils after 66 weeks. In the four treatments that included a Pd-catalyst, the average degradation rate between 11- and 66-weeks was  $5.9 \text{ mg}\cdot\text{kg}^{-1}\text{week}^{-1}$ , which is not statistically different from the average achieved by all non-EZVI treatments,  $5.4 \text{ mg}\cdot\text{kg}^{-1}\text{week}^{-1}$  (p-value = 0.76). The average degradation rate in soils treated with zero valent metals (Mg, Fe, Fe\*, and Fe/Al) in the absence of Pd catalyst was  $6.3 \text{ mg}\cdot\text{kg}^{-1}\text{week}^{-1}$ , which is also similar to the non-EZVI average decline rate (p-value = 0.57). Furthermore,

66- week homolog data (Figure 6-3) indicate no clear difference in PCB congener distributions between the untreated controls and any of the treatments involving zero valent metals and/or Pd catalyst. Successful reductive dechlorination of PCBs is expected to result in enrichment of lesser chlorinated homologs and corresponding depletion of higher-chlorinated homologs.

The absence of any clear long-term enhancement in the rate of PCB degradation when zero valent metals and/or Pd catalysts were applied in the presence of soils can likely be explained by slow desorption of PCBs and a lack of persistent reactive media. Reductive processes mediated by zero-valent metals (Lowry and Reinhard 2000) or heterogeneous catalysis (Schwarzenbach et al. 2003) require reactants to adsorb onto the reductant or catalyst surface. From this, we can infer that these reagents are not likely to directly degrade contaminants that are sorbed in the soil phase. Thus, overall PCB degradation rates may be controlled by the rate of PCB desorption from soils. Furthermore, a decline in catalytic activity of Pd over time (Lowry and Johnson 2004) and even complete and rapid Pd deactivation in the presence of soils (Agarwal et al. 2009) have been reported. Cited mechanisms for catalyst deactivation include oxidation/passivation and surface poisoning, especially by sulfide species, which are common in subsurface environments under reducing conditions (Hildebrand et al. 2009b; Coq et al. 1986).

As discussed in section 1.0, the number of studies that have involved direct application of zero-valent metals and/or Pd catalysis to soil-phase PCBs is fairly limited. He et al. (2011) evaluated treatment of soils spiked with tri- and penta-CBP using reagent loadings that were substantially higher (25 to 250% of the treated soil mass, versus 5% as used in the present study); up to 78% removal of PCBs was observed, but PCB degradation rates declined substantially after 48 hours. Varanasi et al. (2007) utilized nano-scale ZVI for treatment of field-PCB contaminated soils; PCB depletion with corresponding increase in lesser-chlorinated congeners or biphenyl was reported only at temperatures of greater than 300°C. Agarwal et al. (2009) reported that no dechlorination was observed after treatment of PCB-impacted Waukegan harbor sediments using a Pd-Mg system that showed much promise for treatment of

liquid-phase PCBs. Results of the soil-phase study presented herein are consistent with these reported results, when the study conditions (e.g., use of smaller reagent amounts at ambient temperature conditions) are taken into consideration.

#### 6.3.4 EZVI

In terms of the PCB degradation achieved between 11 and 66 weeks, EZVI stands out from all of the other treatments. The mean PCB concentrations for EZVI and other treatments at 66 weeks were 822 and 1160 mg·kg<sup>-1</sup>, respectively. When the soils treated with EZVI are compared to all other soil treatments, t-test results indicate that the population means are significantly different (p-value = 0.0006). Between 11 and 66 weeks, PCB concentrations in EZVI soils with and without clay were reduced by 54 and 58%, respectively, compared to the average reduction of 19% for all non-EZVI treatments.

The average 11-to-66 week PCB degradation rate in EZVI vials was 19 mg·kg<sup>-1</sup>week<sup>-1</sup>, which is significantly faster than the non EZVI average degradation rate (p-value = 0.0001). By comparison, Abramowicz (2002) reported PCB biodegradation rate of 46 mg·kg<sup>-1</sup>week<sup>-1</sup> (see the Supporting Information) in sediments initially containing PCBs at 1500 mg·kg<sup>-1</sup> under conditions optimized for biodegradation (i.e., in Hudson river sediments containing indigenous PCB-degrading microorganisms and with nutrients supplied). In the absence of nutrients or other amendments, a lag time of about eight weeks was required before meaningful degradation occurred, and then only with diminished PCB biodegradation rates.

Homolog distributions (Figure 6-3) provide additional evidence of PCB degradation in EZVI-treated soils. At 66-weeks, enrichment in the lesser-chlorinated di-CBP congener is observed with corresponding depletion in the higher-chlorinated tetra- and penta-CBP congeners. The di-CBP fraction increased from 4% (average in non-EZVI soils) to 23 and 29% in EZVI soils with and without bentonite, respectively. Conversely, the tetra-CBP fraction decreased from 50% (average without EZVI) to 27%

(average with EZVI) and penta-CBP decreased from 13% to 9.1%. Enrichment in mono-CBP was also observed in EZVI-treated soils, although at levels too small to be apparent in Figure 6-3 (see the Supporting Information).

Whether the primary degradation mechanism was biological or abiotic is not clear, given available data, but inferences can be made from work conducted by others. Following an EZVI field demonstration applied to a trichloroethylene (TCE) source zone, both biological and abiotic processes were reported to have contributed to overall TCE degradation (Quinn et al. 2005). However, in liquid-phase studies conducted with PCBs at ambient temperatures, zero valent metals have been generally unsuccessful in degrading PCBs in the absence of a catalyst (e.g., Lowry and Johnson 2004). Furthermore, the degradation rates and treatment patterns (i.e., an initial lag-period of several weeks followed by a period of degradation) observed in EZVI-treated soils are generally consistent with previously reported PCB biodegradation trends (Korte et al. 2002). This suggests that biodegradation was the primary mechanism behind PCB degradation in soils treated with EZVI. Future work should include evaluation of individual components of EZVI (e.g., zero valent metal, corn oil, and surfactant) to improve our understanding of their relative impacts in degradation of PCB in the presence of soils.

The fact that significant reductive dechlorination of PCBs occurs only in the EZVI-treated soils, which included corn oil and surfactant, suggests a key role of the two organic additives. Increased PCB biodegradation rates have been reported in soils amended with carbon sources (Krembs et al. 2010; Kouznetsova et al. 2007). Enhanced PCB availability over 24 months was reported in the presence of non-aqueous phase comprising industrial waste oil and grease (Luo et al. 2008). Thus, results of previous work suggest that the presence of liquid-phase organic carbon may enhance both PCB desorption and biological activity, which ultimately led to observable PCB degradation in the study.

## 6.4 Conclusions

Our research hypothesis stated that PCBs present a treatment conundrum, wherein reactive media that are capable of creating the thermodynamic conditions necessary for PCB degradation are unlikely to persist long enough under *in situ* conditions to achieve meaningful treatment of PCBs. In general, the experimental results support this hypothesis. Treatments that involved Pd-catalyst were capable of rapidly depleting aqueous phase PCBs, but showed no meaningful enhancement in the rate of PCB depletion in soils over extended periods of contact time (>1 year). In the absence of a Pd catalyst, zero valent metals were unable to degrade PCBs in short-term aqueous-phase studies or achieve any significant enhancements in the PCB degradation rates observed in long-term studies including soils. EZVI was the only treatment approach that seemed to improve long-term treatment results for PCBs in the presence of soils. The desorption agents – corn oil and surfactant – may offer a means to overcome the hypothesized treatment conundrum by increasing the liquid-phase availability of PCBs as well as stimulating beneficial microbiological activity. Although the presence of surfactants/cosolvents has been previously shown to decrease reactivity (as discussed in section 1.0), results of this study suggest that the use of a degradable and immobile non-aqueous phase as a component of the treatment system may help facilitate long-term PCB degradation. Even so, the incomplete treatment observed over a period of greater than one year indicates that the potential for near-complete removal of PCBs from soil-water systems may be limited.

## 6.5 Attribution of Credit

This research was conducted as part of a treatability study evaluating treatment options for the OMC Superfund Site and was funded, in part, by the United States Environmental Protection Agency. Field samples from the OMC Superfund Site were provided by CH2M HILL. We also thank Clint Bickmore of OnMaterials for providing reactive materials and Suzanne O'Hara of GeoSyntec for support in formulating EZVI.

## REFERENCES

- Agarwal, S., S. R. Al-Abed, and D. D. Dionysiou. 2009. A feasibility study on Pd/Mg application in historically contaminated sediments and PCB spiked substrates. *Journal of Hazardous Materials* 172 (2-3):1156-1162.
- Batchelor, B., A. M. Hapka, G. J. Igwe, R. H. Jensen, M.F. McDevitt, D.S. Schultz, and J.M. Whang. 2002. *Method for Remediating Contaminated Soils* edited by U. S. P. a. T. Office. United States: E. I. du Pont de Nemours and Company.
- Bozzini, C., T. Simpkin, T. Sale, D. Hood, and B. Lowder. 2006. DNAPL Remediation at Camp Lejeune using ZVI-Clay Soil Mixing. In *Fifth Battelle Conference on Remediation of Chlorinated and Recalcitrant Compounds*. Monterrey, CA.
- Burris, D. R., T. J. Campbell, and V. S. Manoranjan. 1995. Sorption of trichloroethylene and tetrachloroethylene in a batch reactive metallic iron-water system. *Environmental Science & Technology* 29 (11):2850-2855.
- Coq, B., G. Ferrat, and F. Figueras. 1986. Conversion of Chlorobenzene over Palladium and Rhodium Catalysts of Widely Varying Dispersion. *Journal of Catalysis* 101 (2):434-445.
- Cornelissen, G., O. Gustafsson, T. D. Bucheli, M. T. O. Jonker, A. A. Koelmans, and P. C. M. Van Noort. 2005. Extensive sorption of organic compounds to black carbon, coal, and kerogen in sediments and soils: Mechanisms and consequences for distribution, bioaccumulation, and biodegradation. *Environmental Science & Technology* 39 (18):6881-6895.
- Dercova, K., B. Vrana, R. Tandlich, and L. Subova. 1999. Fenton's type reaction and chemical pretreatment of PCBs. *Chemosphere* 39 (15):2621-2628.
- Devor, R., K. Carvalho-Knighton, B. Aitken, P. Maloney, E. Holland, L. Talalaj, R. Fidler, S. Elsheimer, C. A. Clausen, and C. L. Geiger. 2008. Dechlorination comparison of mono-substituted PCBs with Mg/Pd in different solvent systems. *Chemosphere* 73 (6):896-900.
- Hildebrand, H., K. Mackenzie, and F. D. Kopinke. 2009a. Highly Active Pd-on-Magnetite Nanocatalysts for Aqueous Phase Hydrodechlorination Reactions. *Environmental Science & Technology* 43 (9):3254-3259.
- Hildebrand, H., K. Mackenzie, and F. D. Kopinke. 2009b. Pd/Fe<sub>3</sub>O<sub>4</sub> nano-catalysts for selective dehalogenation in wastewater treatment processes-Influence of water constituents. *Applied Catalysis B-Environmental* 91 (1-2):389-396.
- Jeen, S. W., R. W. Gillham, and A. Przepiora. 2011. Predictions of long-term performance of granular iron permeable reactive barriers: Field-scale evaluation. *Journal of Contaminant Hydrology* 123 (1-2):50-64.
- Johnson, T. L., M. M. Scherer, and P. G. Tratnyek. 1996. Kinetics of halogenated organic compound degradation by iron metal. *Environmental Science & Technology* 30 (8):2634-2640.

- Karn, B., T. Kuiken, and M. Otto. 2009. Nanotechnology and in Situ Remediation: A Review of the Benefits and Potential Risks. *Environmental Health Perspectives* 117 (12):1823-1831.
- Kjellerup, B. V., X. L. Sun, U. Ghosh, H. D. May, and K. R. Sowers. 2008. Site-specific microbial communities in three PCB-impacted sediments are associated with different in situ dechlorinating activities. *Environmental Microbiology* 10 (5):1296-1309.
- Klausen, J., P. J. Vikesland, T. Kohn, D. R. Burris, W. P. Ball, and A. L. Roberts. 2003. Longevity of granular iron in groundwater treatment processes: Solution composition effects on reduction of organohalides and nitroaromatic compounds. *Environmental Science & Technology* 37 (6):1208-1218.
- Koelmans, A. A., K. Kaag, A. Sneekes, and Ethm Peeters. 2009. Triple Domain in Situ Sorption Modeling of Organochlorine Pesticides, Polychlorobiphenyls, Polyaromatic Hydrocarbons, Polychlorinated Dibenzo-p-Dioxins, and Polychlorinated Dibenzofurans in Aquatic Sediments. *Environmental Science & Technology* 43 (23):8847-8853.
- Korte, N. E., O. R. West, L. Liang, B. Gu, J. L. Zutman, and Q. Fernando. 2002. The effect of solvent concentration on the use of palladized-iron for the step-wise dechlorination of polychlorinated biphenyls in soil extracts. *Waste Management* 22 (3):343-349.
- Kouznetsova, I., P. Bayer, M. Ebert, and M. Finkel. 2007. Modelling the long-term performance of zero-valent iron using a spatio-temporal approach for iron aging. *Journal of Contaminant Hydrology* 90 (1-2):58-80.
- Krembs, F. J., R. L. Siegrist, M. L. Crimi, R. F. Furrer, and B. G. Petri. 2010. ISCO for Groundwater Remediation: Analysis of Field Applications and Performance. *Ground Water Monitoring and Remediation* 30 (4):42-53.
- Lowry, G. V., and K. M. Johnson. 2004. Congener-specific dechlorination of dissolved PCBs by microscale and nanoscale zerovalent iron in a water/methanol solution. *Environmental Science & Technology* 38 (19):5208-5216.
- Lowry, G. V., and M. Reinhard. 2000. Pd-catalyzed TCE dechlorination in groundwater: Solute effects, biological control, and oxidative catalyst regeneration. *Environmental Science & Technology* 34 (15):3217-3223.
- Luo, W., E. M. D'Angelo, and M. S. Coyne. 2008. Organic carbon effects on aerobic polychlorinated biphenyl removal and bacterial community composition in soils and sediments. *Chemosphere* 70 (3):364-373.
- Mackay, D. M., and J. A. Cherry. 1989. Groundwater contamination: Pump-and-treat remediation. *Environmental Science & Technology* 23 (6):630-636.
- Mackenzie, Katrin, Heike Frenzel, and Frank-Dieter Kopinke. 2006. Hydrodehalogenation of halogenated hydrocarbons in water with Pd catalysts: Reaction rates and surface competition. *Applied Catalysis B: Environmental* 63 (3-4):161-167.
- Manzano, M. A., J. A. Perales, D. Sales, and J. M. Quiroga. 2003. Microbial degradation and chemical oxidation of sandy sediment contaminated with polychlorinated biphenyl. *Environmental Engineering Science* 20 (2):91-101.

Quinn, J., C. Geiger, C. Clausen, K. Brooks, C. Coon, S. O'Hara, T. Krug, D. Major, W. S. Yoon, A. Gavaskar, and T. Holdsworth. 2005. Field demonstration of DNAPL dehalogenation using emulsified zero-valent iron. *Environmental Science & Technology* 39 (5):1309-1318.

Schuth, C., and M. Reinhard. 1998. Hydrodechlorination and hydrogenation of aromatic compounds over palladium on alumina in hydrogen-saturated water. *Applied Catalysis B-Environmental* 18 (3-4):215-221.

Schwarzenbach, R. P., P. M. Gschwend, and D. M. Imboden. 2003. *Environmental Organic Chemistry*. 2nd ed. New York: Wiley.

Siegrist, R.L., M. Crimi, T.J. Simpkin, and R.C. Borden. 2011. *In situ chemical oxidation for groundwater remediation*. Edited by R. L. Siegrist, M. Crimi, T. J. Simpkin and R. C. Borden, *Springer eBook collection*. New York: Springer.

Varanasi, P., A. Fullana, and S. Sidhu. 2007. Remediation of PCB contaminated soils using iron nanoparticles. *Chemosphere* 66 (6):1031-1038.

Wadley, S. L. S., R. W. Gillham, and L. Gui. 2005. Remediation of DNAPL source zones with granular iron: Laboratory and field tests. *Ground Water* 43 (1):9-18.

## CHAPTER 7

### CONCLUSIONS AND RECOMMENDATIONS

Despite extensive research, few technologies exist that are capable of reducing concentrations in chlorinated solvent source zones to drinking water standards (EPA 2003). Remediation success is often limited by the heterogeneous nature of the subsurface. Most remediation technologies require a precise knowledge of where contaminants are located in the subsurface and, furthermore, the ability to deliver reagents to those locations (Stroo et al. 2012). For source zones containing NAPLs, locating all contaminant mass can be difficult. At aged sites, a significant portion of the contaminant mass can diffuse into low-permeability (low-k) zones, thus limiting our ability to achieve reagent-contaminant contact. Soil mixing is a delivery method that can be used to overcome the limitations associated with subsurface heterogeneity (Wadley et al. 2005; Olson et al. 2012). Soil mixing transforms an initially-heterogeneous distribution, in both permeability and contaminant mass, into a (relatively) uniform body with treatment reagents distributed throughout. Use of soil-mixing for delivery of ZVI and bentonite (Clay) into chlorinated solvent source zones is an emerging treatment approach. After treatment, ZVI mediates reductive dechlorination of chlorinated solvents and bentonite provides stabilization by reducing hydraulic conductivity of treated soils. The ZVI-Clay technology has been applied in 13 field projects (as of December 2013), all of which have been considered successful in achieving site-specific remediation objectives. Through these projects, research questions have been raised. For example, variations in contaminant degradation rates have been observed across field applications, despite mixing with a uniform and consistent amount of ZVI. Also, our understanding of the interaction between ZVI-mediated degradation and flow reduction has been limited, prior to this research.

The research presented herein was conducted with the overarching objective of advancing our understanding of the processes occurring in soils after treatment via soil mixing with chemical reductants,

such as ZVI, and bentonite. Novel aspects of the research presented herein include (a) a detailed analysis of reaction kinetics and hydraulics in a field-scale mixed-soil system, (b) evaluation of reaction kinetics in a ZVI/TCE system across a range of TCE concentrations, both above and below the solubility threshold, (c) evaluation of the interaction between flow reduction and kinetics in a homogenized system, (d) advancement of an equilibrium model for NAPL dissolution in a ZVI-Clay mixed-soil system, and (e) comparison of treatment potential for chemical reductants to degrade polychlorinated biphenyls (PCBs) in systems with and without soils. Key findings of the work conducted herein are discussed in subsequent paragraphs.

An analysis of performance data following full-scale field application at Site 89, Camp Lejeune, North Carolina (Olson et al. 2012) indicated that ZVI-Clay can simultaneously reduce contaminant concentrations and hydraulic conductivity by multiple orders of magnitude. Within one year of treatment, soil and groundwater concentrations were reduced median values of >99%. Further reductions were observed over the subsequent two years after mixing. In addition, hydraulic conductivity following field treatment was reduced by 2.5 orders of magnitude.

Building on the field-data analysis, reaction kinetics and groundwater flow hydraulics were further addressed in subsequent chapters. Reaction rates were evaluated across a range of initial TCE concentrations, both above and below the NAPL-solubility threshold (i.e., the concentration of TCE above which NAPL will be present). Michaelis-Menton kinetics adequately described degradation rates below the NAPL threshold, while the degradation rate above the NAPL threshold was independent of the amount of NAPL in the system. Hydraulics analysis consisted of measuring hydraulic conductivity,  $K$ , in the treated soils as a function of bentonite content, BC, at levels typical of ZVI-Clay soil mixing application (i.e., BC < 4%, soil weight basis). In soils of moderately high initial permeability,  $K$  was reduced by about an order of magnitude for each 1% bentonite added; in soils of low initial permeability,  $K$  reductions were minor with addition of up to 4% bentonite.

The concepts of ZVI-mediated treatment of TCE-NAPL and bentonite-induced reduction in  $K$  were then combined to develop a mathematical model of the ZVI-Clay mixed-soil system. The objective in developing the model was to evaluate the interaction between degradation and flow reduction following field-scale ZVI-Clay treatment. The model consists of a system of PDEs governing TCE-NAPL dissolution and reactive transport of dissolved-phase constituents. An equilibrium modeling approach was adopted to describe dissolution of NAPL; a PDE was developed accordingly and an analytical solution for NAPL dissolution was obtained. Numerical methods were used to solve the reactive-transport PDEs for TCE and related degradation products. To validate the model, laboratory-scale column experiments were conducted. The model provided a good fit for measured column-effluent concentrations and observations made in the column study support use of the equilibrium assumption for NAPL dissolution. The model was then used to predict field-scale performance metrics including contaminant mass flux (i.e., contaminant mass crossing the down-gradient face of the treated soil body) and time-integrated contaminant discharge. Modeling of field-scale applications indicates that reduction in the flow rate has an enormous impact on the TCE discharge; the fraction of TCE initially present in the system that is ultimately degraded, rather than lost down-gradient, can reach 99.9% or greater in systems where  $K$  is reduced by multiple orders of magnitude. This illustrates the importance of residence time in conjunction with ZVI-mediated degradation. These results are consistent with the observations made following field application at Site 89.

Finally, an evaluation of the ZVI-Clay soil mixing approach for treatment of polychlorinated biphenyls (PCBs) was evaluated (Olson et al. 2013). PCBs are strongly hydrophobic and persistent in the environment (Erickson 1997), and reductive dechlorination of PCBs has been widely demonstrated to require more extreme conditions than degradation of the chlorinated solvents (e.g., Lowry and Johnson 2004; Varanasi et al. 2007). The experiments described herein were based on the observation that, in recent literature, several treatments have been advanced based on degradation of liquid-phase PCBs, but few examples exist where such treatments have been successfully applied for degradation of PCBs in the

presence of soils. The experiments consisted of batch-reactor studies evaluating reductive dechlorination of PCBs in the presence and absence of soils. Results indicated that Pd-catalyzed treatments achieved rapid destruction of a model PCB congener (2-chlorobiphenyl) in the aqueous-phase studies, but in the presence of soils did not enhance degradation of a commercial PCB mixture (Aroclor 1248) over background rates. In the presence of soils, emulsified zero valent iron, EZVI (Quinn et al. 2005), was the only approach evaluated that resulted in a clear enhancement in PCB dechlorination rates. The combination of a desorption agent (corn oil and/or surfactant) and degradation appears to have enhanced the PCB degradation rate in the EZVI system; whether the observed degradation-rate enhancement was due to biological or abiotic processes is not clear, given available data. Nevertheless, results highlight the importance of considering desorption limitations when evaluating treatment approaches for PCBs.

The research presented in this dissertation was conducted with the objective of improving treatment performance of future ZVI-Clay field projects. The primary impact of this research, as seen by the author, involves the interaction between flow rates and contaminant degradation. The conclusion that flow reduction by a given factor has similar results as increasing degradation rates by the same factor may have important implications. In high-K media, addition of bentonite can be as important as addition of ZVI.

The research presented herein has provided a significant contribution to our understanding of ZVI-Clay mixed soil systems, but has also raised additional questions. Additional research questions are as follows:

- A primary assumption in the work conducted herein is that mixed soils are homogeneous. Following field implementation, rigorous documentation of the degree to which homogeneity is obtained would be helpful. This may include: (a) depth-discrete sampling for soil and contaminant distribution, before and after mixing, (b) mixing with a dye such that NAPL distribution and droplet size could be observed after mixing is complete, (c) using magnetic

susceptibility techniques to scan soil cores, thus generating continuous iron-content data, and (d) using advanced techniques such as nuclear magnetic resonance (NMR) to characterize post-mixing distributions.

- Uncertainty remains around the treatment pattern observed in one monitoring well – MW-2A – following field-scale implementation of ZVI-Clay at Site 89, Camp Lejeune, NC. Research conducted herein indicates that initial TCE concentration may have contributed to the apparent anomalous treatment, but results were not conclusive. The degradation products that were observed (temporarily) in this monitoring well, VC and *c*DCE, are often cited as indicating biological degradation. A previous thermal-remediation application in this vicinity may have affected microbial populations in the vicinity, either positively or negatively. Additional field analyses such as stable isotope analysis may help to better understand the interaction between biological and abiotic processes following field-scale treatment.
- Degradation pathways in TCE-NAPL / ZVI systems were discussed (Chapters 3 and 5). However, the experiments described in Chapter 3 were initial rate studies, which were conducted over a short time period that is not ideal for pathway analysis. Studies conducted in Chapter 5 included transport, which complicates interpretation of pathways; furthermore, residence time within the columns was limited to a few days. Rigorous pathway analysis will require long-term batch experiments, which were not conducted as part of this research, but are recommended for future research.
- The model developed in Chapter 5 may have broader applications in the discipline of groundwater and soil remediation. The concept of controlling residence time to enhance treatment performance may provide benefits to other remediation practices, such as injection-based delivery systems. Further investigation is warranted.
- Results presented in Chapter 6 suggest that enhanced desorption is a necessary component in treatment of polychlorinated biphenyls (PCBs) in the presence of soils. However, given results of

the experiment, we were unable to state with certainty whether observed degradation of PCBs was due primarily to biological or abiotic processes. This could be addressed by conducting additional control experiments with care taken to isolate the inherent processes, i.e., desorption agents, bio-stimulation, and abiotic degradation.

## REFERENCES

- EPA. 2003. *The DNAPL remediation challenge: Is there a case for source depletion?* Edited by M. C. Kavanaugh and P. S. C. Rao. Cincinnati, OH: U.S. Environmental Protection Agency, National Risk Management Research Laboratory.
- Erickson, Mitchell D. 1997. *Analytical chemistry of PCBs*. Boca Raton, Fla.: CRC/Lewis Publ.
- Lowry, G. V., and K. M. Johnson. 2004. Congener-specific dechlorination of dissolved PCBs by microscale and nanoscale zerovalent iron in a water/methanol solution. *Environmental Science & Technology* 38 (19):5208-5216.
- Olson, M. R., J. Blotvogel, T. Borch, T.C. Sale, M.A. Petersen, and R.A. Royer. 2013. Long-Term Potential of In Situ Chemical Reduction for Treatment of Polychlorinated Biphenyls in Soils *Chemosphere* in review.
- Olson, Mitchell R., Thomas C. Sale, Charles D. Shackelford, Christopher Bozzini, and Jessica Skeean. 2012. Chlorinated Solvent Source-Zone Remediation via ZVI-Clay Soil Mixing: 1-Year Results. *Ground Water Monitoring & Remediation* 32 (3):63-74.
- Quinn, J., C. Geiger, C. Clausen, K. Brooks, C. Coon, S. O'Hara, T. Krug, D. Major, W. S. Yoon, A. Gavaskar, and T. Holdsworth. 2005. Field demonstration of DNAPL dehalogenation using emulsified zero-valent iron. *Environmental Science & Technology* 39 (5):1309-1318.
- Stroo, H. F., A. Leeson, J. A. Marqusee, P. C. Johnson, C. H. Ward, M. C. Kavanaugh, T. C. Sale, C. J. Newell, K. D. Pennell, C. A. Lebron, and M. Unger. 2012. Chlorinated Ethene Source Remediation: Lessons Learned. *Environmental Science & Technology* 46 (12):6438-6447.
- Varanasi, P., A. Fullana, and S. Sidhu. 2007. Remediation of PCB contaminated soils using iron nanoparticles. *Chemosphere* 66 (6):1031-1038.
- Wadley, S. L. S., R. W. Gillham, and L. Gui. 2005. Remediation of DNAPL source zones with granular iron: Laboratory and field tests. *Ground Water* 43 (1):9-18.

APPENDIX A

SUPPORTING INFORMATION FOR  
DISSOLUTION, TRANSPORT, AND DEGRADATION OF TCE NAPL IN SOILS MIXED  
WITH ZVI AND BENTONITE: COLUMN STUDIES AND MODELING

## A.1 Development of the NAPL Equation

The governing equation for non-aqueous phase liquid (NAPL)-phase trichloroethene (TCE) is developed by conducting a mass balance on total TCE (i.e., the sum of dissolved-phase and NAPL-phase TCE, neglecting sorption) in an element of the system. Primary assumptions include: (a) TCE-NAPL is immobile; (b) TCE-NAPL and aqueous-phase TCE are in equilibrium, thus, where NAPL is present, the aqueous phase TCE concentration is fixed at solubility; (c) the groundwater flow velocity field is uniform; and (d) degradation of TCE is pseudo-first-order in the aqueous phase TCE concentration. From assumption (b), the concentration gradient is 0 in the presence of NAPL, thus the diffusive transport flux is assumed to be negligible. The possible presence of sorbed and vapor-phases are ignored.

Processes governing the mass balance are (a) advective flux of aqueous-phase TCE across the system boundaries and (b) degradation of TCE, which occurs uniformly within the system. The advective flux term,  $J$  ( $\text{mol}\cdot\text{m}^{-2}\text{d}^{-1}$ ), is calculated as follows:

$$J = v \cdot C_w \quad (1)$$

where  $v$  is the groundwater seepage velocity and  $C_w$  ( $\text{mol}\cdot\text{L}^{-1}$ ) is the water-phase concentration of TCE. Degradation is assumed to be first-order in the aqueous phase TCE concentration. Assuming the NAPL and water reach rapid equilibrium, the aqueous-phase concentration is fixed at solubility and degradation is effectively 0-order. Thus, the degradation rate,  $R$  ( $\text{mol}\cdot\text{L}^{-1}\text{d}^{-1}$ ), is calculated as:

$$R = -k_{TCE}C_w^* \quad (2)$$

where  $k_{TCE}$  ( $\text{d}^{-1}$ ) is the 1<sup>st</sup>-order degradation rate coefficient and  $C_w^*$  ( $\text{mol}\cdot\text{L}^{-1}$ ) refers to the moles of TCE in the aqueous-phase, at solubility, per bulk volume. From Equations 1 and 2, the mass balance on total TCE within a representative element volume (REV) of thickness  $\Delta x$  can be written as:

$$\frac{\partial C_t}{\partial t} = \frac{J^{in} - J^{out}}{\Delta x} - R = \frac{v \cdot C_w^{in} - v \cdot C_w^{out}}{\Delta x} - k_{TCE} C_w^* = -v \frac{(C_w^{out} - C_w^{in})}{\Delta x} - k_{TCE} C_w^* \quad (3)$$

where  $C_t$  ( $\text{mol} \cdot \text{L}^{-1}$ ) is the total TCE (water- and NAPL-phase) moles per pore volume. Taking the limit as  $\Delta x \rightarrow 0$ ,

$$\frac{\partial C_t}{\partial t} = -v \frac{\partial C_w}{\partial x} - k_{TCE} C_w^* \quad (4)$$

Next, we would like to express all concentrations in terms of  $C_t$ . We can relate  $C_w$  and  $C_t$  through use of a modified retardation factor,  $R^*$  (dimensionless), which is defined as the ratio of  $C_t$  to  $C_w$ . To calculate  $R^*$ , we start with a mass balance on TCE within the REV:

$$C_t = C_w + C_N \quad (5)$$

where  $C_t$ ,  $C_w$ , and  $C_N$  ( $\text{mol} \cdot \text{L}^{-1}$ ) are the moles of total TCE, water-phase TCE, and NAPL-phase TCE, respectively, per bulk volume. Rearranging, we can write the following expression for  $R^*$ :

$$R^* = \frac{C_t}{C_w} = 1 + \frac{C_N}{C_w} \quad (6)$$

By combining with Equation 8, Equation 3 can be written as:

$$\frac{\partial C_t}{\partial t} = -\frac{v}{R^*} \frac{\partial C_t}{\partial x} - k_{TCE} C_w^* \quad (7)$$

Finally, to treat aqueous-phase and NAPL-phase TCE independently, we will convert Equation 7 to apply to TCE in the NAPL phase. To accomplish this, Equation 5 is differentiated with respect to  $x$  and with respect to  $t$ .

$$\frac{dC_t}{dx} = \frac{dC_w}{dx} + \frac{dC_N}{dx} \quad (8)$$

$$\frac{dC_t}{dt} = \frac{dC_w}{dt} + \frac{dC_N}{dt} \quad (9)$$

The water-phase TCE concentration is constant and uniform where NAPL is present, thus both  $dC_w/dx$  and  $dC_w/dt \rightarrow 0$ . Therefore, Equations 8 and 9 can be simplified as follows:

$$\frac{dC_t}{dx} = \frac{dC_N}{dx} \quad (10)$$

$$\frac{dC_t}{dt} = \frac{dC_N}{dt} \quad (11)$$

Substituting these into Equation 7 yields the following:

$$\frac{\partial C_N}{\partial t} = -\frac{v}{R^*} \frac{\partial C_N}{\partial x} - k_{TCE} C_w^* \quad (12)$$

Noting that  $C_N$  and  $C_w^*$  refer to the total moles in the respective phases per bulk volume, the following substitutions can be applied:

$$C_N = \frac{\rho_N \phi S_N}{M_{TCE}} \quad (13)$$

$$C_w^* = S_w \phi C_{TCE}^* \quad (14)$$

where  $\rho_N$  ( $\text{g}\cdot\text{L}^{-1}$ ) is the NAPL density,  $\phi$  is the porosity,  $S_N$  and  $S_w$  are the fractions of the pore volume saturated with the NAPL-phase and water-phases, respectively, and  $C_{TCE}^*$  ( $\text{mol}\cdot\text{L}^{-1}$ ) is the solubility concentration of TCE in the water phase. Thus, the PDE governing TCE-NAPL dissolution is as follows:

$$\frac{\partial}{\partial t} \left( \frac{\rho_N \phi S_N}{M_{TCE}} \right) = -\frac{v}{R^*} \frac{\partial}{\partial x} \left( \frac{\rho_N \phi S_N}{M_{TCE}} \right) - k_{TCE} S_w \phi C_{TCE}^* \quad (15)$$

Through substitution of Equations 13 and 14 into Equation 6, we can write the following expression for  $R^*$ :

$$R^* = 1 + \frac{\rho_N \phi S_N}{S_w \phi C_{TCE}^*} = 1 + \frac{\rho_N S_N}{M_{TCE} S_w C_{TCE}^*} \quad (16)$$

## A.2 Column Study Photographs

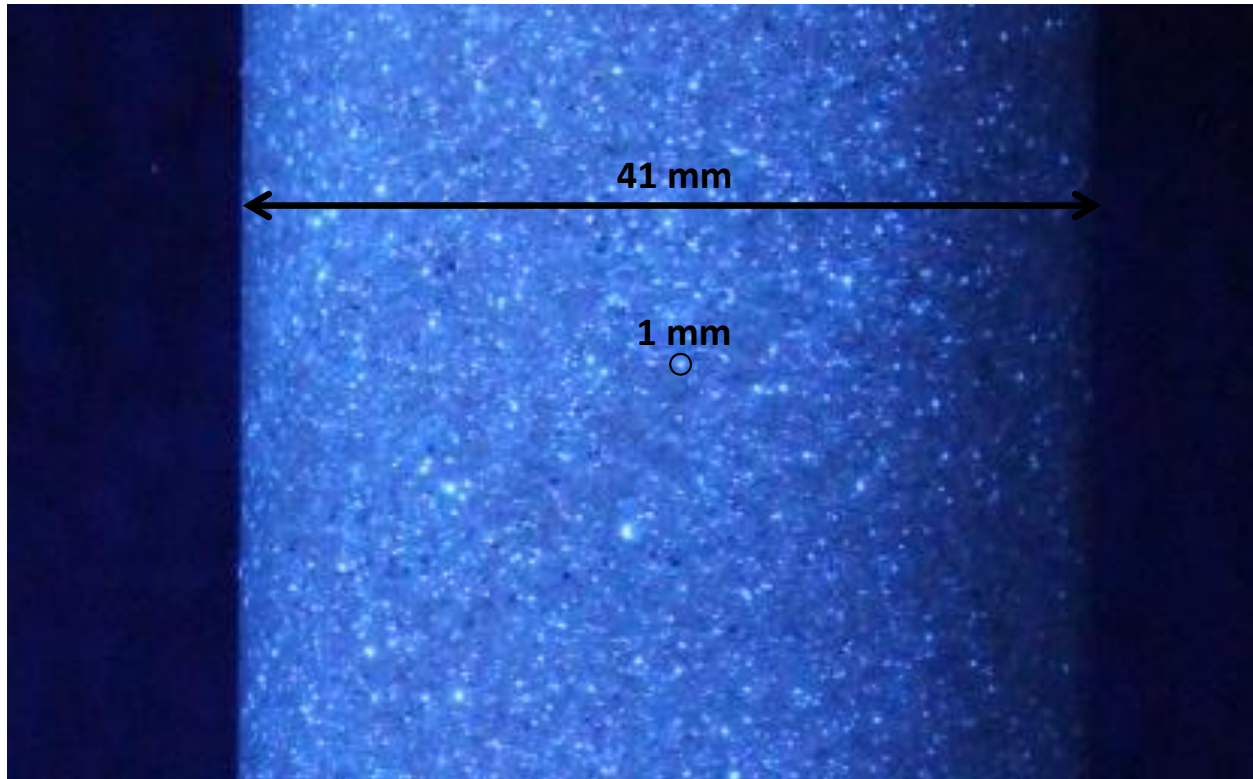


Figure A-1. Close-up of photograph, taken under UV light, of a NAPL-containing column at time 0. The non-aqueous phase liquid (NAPL) trichloroethylene (TCE) was dyed with 0.068% (by weight) of a UV-fluorescent tracer, such that the TCE-NAPL distribution could be observed under UV light. The scale indicates the column inside diameter (41 mm) and the black circle indicates the approximate image-size of a 1-mm droplet.

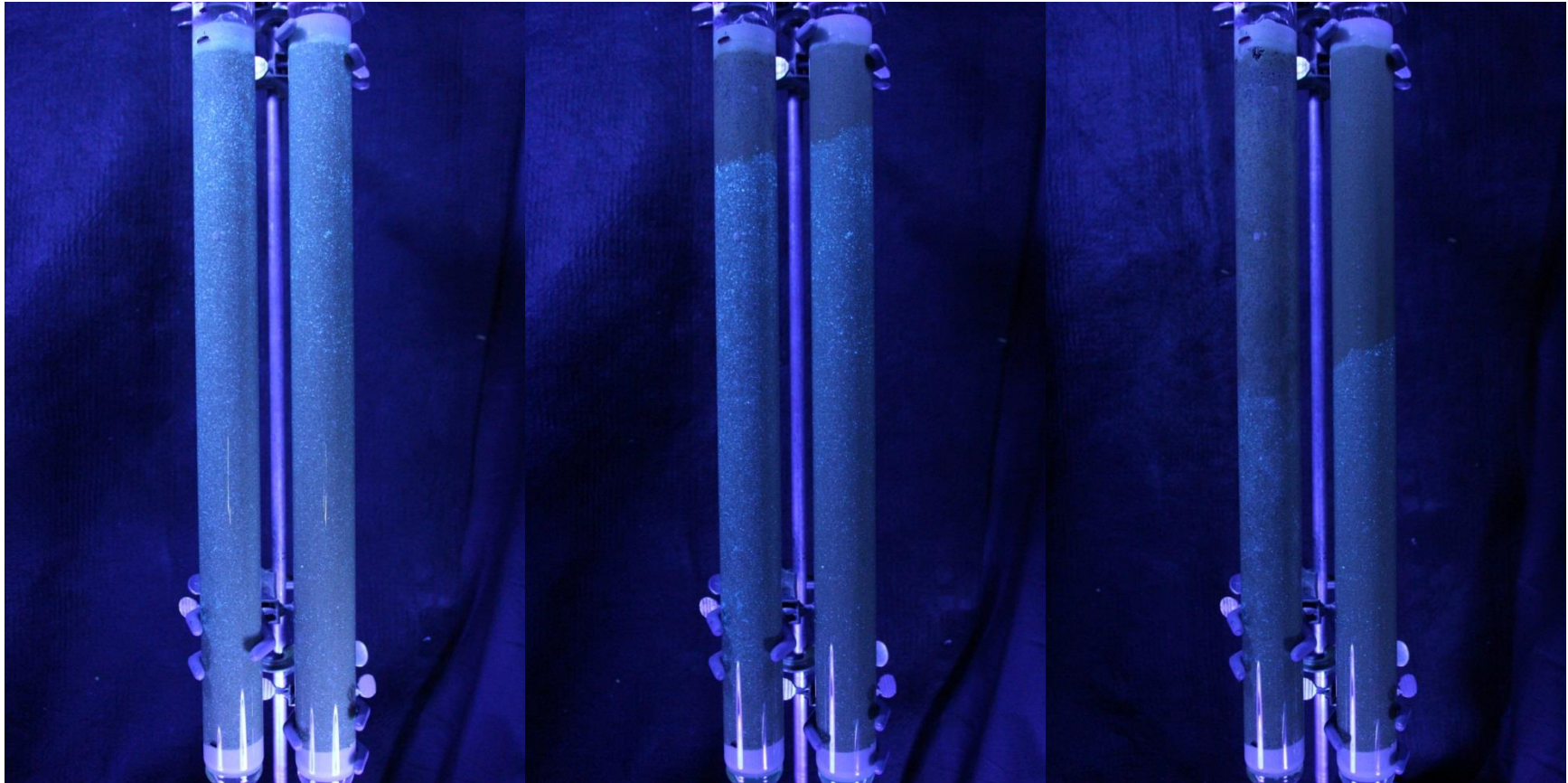


Figure A-2. Low-flow column study photos taken under UV light. The TCE-NAPL was dyed with 0.068% of a UV-fluorescent tracer, such that the NAPL distribution could be observed under UV light. Photos are shown for time 0 (left), 4 days (center) and 12 days (right). The right-hand figure shows the column when approximately 50% of the initial TCE mass has been discharged from the column. In all of the photos, the left column contains 2% ZVI and the right column is the no-ZVI control.

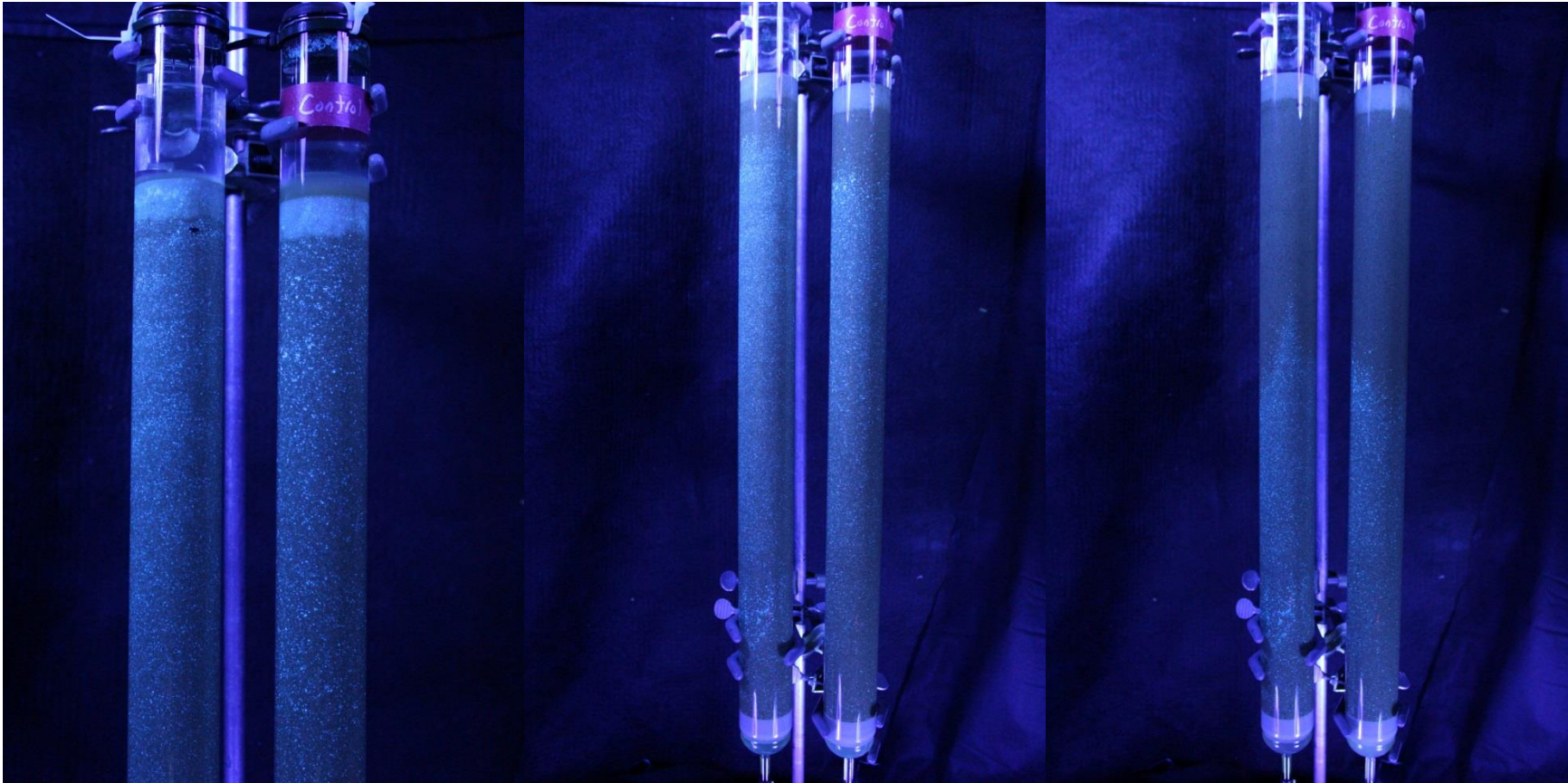


Figure A-3. High-flow column study photos taken under UV light. The TCE-NAPL was dyed with 0.068% of a UV-fluorescent tracer, such that the NAPL distribution could be observed under UV light. Photos are shown for time 0 (left), 0.08 days (2 hr; center) and 0.4 days (10 hr; right). The right-hand figure shows the column when approximately 50% of the initial TCE mass has been discharged from the column. In all of the photos, the left column contains 2% ZVI and the right column is the no-ZVI control.

## APPENDIX B

### SUPPORTING INFORMATION FOR LONG-TERM POTENTIAL OF IN SITU CHEMICAL REDUCTION FOR TREATMENT OF POLYCHLORINATED BIPHENYLS IN SOILS

## B.1 Chlorobiphenyl (CBP) Homolog Solubility and Calculation of Partitioning Coefficient

PCB homolog	Solubility <sup>1</sup> (µg/L)	log K <sub>oc</sub> <sup>1</sup>	fraction of CBP in aqueous phase <sup>2</sup>
mono-CBP	2900	4.1	0.0079
di-CBP	721	4.51	0.0031
tri-CBP	175	4.92	0.0012
tetra-CBP	41.8	5.32	0.00048
penta-CBP	9.83	5.73	0.00019
hexa-CBP	2.29	6.14	0.000072
hepta-CBP	0.527	6.54	0.000029
octa-CBP	0.121	6.95	0.000011
nona-CBP	0.0274	7.35	0.0000045
deca-CBP	0.00619	7.64	0.0000023

<sup>1</sup> EPA, U.S. 1983. Environmental Transport and Transformation of Polychlorinated Biphenyls. Washington, DC U.S. Environmental Protection Agency. P. 80.

<sup>2</sup> Calculated as  $C_s/C_w = K_{oc}f_{oc}$  for a system comprising 1 kg of soil with an  $f_{oc}$  of 0.01 and 1 L of water.

$C_s$ : soil concentration (µg/kg)

$C_w$ : concentration of PCBs in water (µg/L)

$K_{oc}$ : partition coefficient between water phase and soil organic carbon (L/kg)

$f_{oc}$ : fraction of organic carbon in soils (mass/mass)

## B.2 Aqueous-Phase and Soil-Phase Study Experimental Design Details

### *Aqueous-Phase Study*

Description	Treatment details	Reactant Source	Bentonite added	Mass dry soil (g)	Volume water (mL)	Mass zero valent metal (g)
Control (no clay)	--	--	--	--	50	--
ZVI	5% Fe* <sup>1</sup>	OnMaterials	--	--	50	2.5
ZVI + Pd	5% Fe*+0.05% Pd	OnMaterials	--	--	50	2.5
Fe/Al	5% Fe/Al	OnMaterials	--	--	50	2.5
Fe/Al + Pd	5% Fe/Al+0.05% Pd	OnMaterials	--	--	50	2.5

### *Soil-Phase Study*

Description	Treatment details	Reactant Source	Bentonite added	Mass dry soil (g)	Volume water (mL)	Mass zero valent metal (g)
Control (no clay)	--	--	--	84	31	4.2
Control (w/clay)	--	--	2%	84	31	4.2
Peerless Fe	5% Fe (Peerless)	Peerless	2%	84	31	4.2
Mg	5% Mg (Fisher)	Fisher Scientific	2%	84	31	4.2
ZVI	5% Fe*	OnMaterials	2%	84	31	4.2
ZVI + Pd	5% Fe*+0.02% Pd	OnMaterials	2%	84	31	4.2
ZVI + Pd	5% Fe*+0.05% Pd	OnMaterials	2%	84	31	4.2
Fe/Al	5% Fe/Al	OnMaterials	2%	84	31	4.2
Fe/Al + Pd	5% Fe/Al+0.02% Pd	OnMaterials	2%	84	31	4.2
Fe/Al + Pd	5% Fe/Al+0.05% Pd	OnMaterials	2%	84	31	4.2
EZVI	5% EZVI	--	--	84	31	4.2
EZVI	5% EZVI	--	2%	84	31	4.2

<sup>1</sup> Fe\* indicates electrolytic iron (i.e., zero valent iron produced by electrolytic reduction of dissolved iron ions).

### **B.3 Soil Phase Study Methods: Calculating Homolog Distribution and Total PCBs**

The procedure for quantifying homolog distributions and total PCB concentrations is as follows:

- Based on GC/MS analysis, approximately 50 peaks in the GC chromatogram were identified as PCBs.
- For a select sample, GC/MS identification was used to assign a homolog to each peak in the GC chromatogram.
- For all remaining samples, homologs were assigned to GC chromatogram peaks based on similarity of retention times.
- Homolog distribution - peak areas were added for all peaks assigned to each homolog. The reported percent distributions represent the fraction of total PCB peak area that corresponds to peaks assigned to each homolog.
- Total PCBs – peak areas were added for all peaks identified as PCB. The sum of peak-area values was converted to liquid-phase concentration in the extract using a single calibration factor (based on a five-point calibration curve prepared from a 1000 ppm standard solution of Aroclor 1248 in hexane, purchased from Ultra Scientific, North Kingstown, RI). Values were converted to a wet-soil basis using the volume of concentrated hexane (i.e., after the solvent exchange and concentration step) and sample mass of wet soil.

#### **B.4 Soil Phase Study: Discussion and Statistical Evaluation of Homolog Distribution**

PCB homolog distributions (manuscript Figure 3) were calculated from the sum of GC chromatogram peak areas for each homolog. Visual observation of the data indicates that any shifts in PCB homolog distributions at 11 weeks are small compared to those observed at 66 weeks. At 11 weeks, a slight enrichment in the more-highly chlorinated homologs was apparent in EZVI-treated soils. This may be attributed to induced desorption of PCBs from the soil matrix, mediated by the presence of a hydrophobic phase – corn oil – and surfactant in the system. Although too small to be apparent in Figure 3 (main body of paper), slightly elevated fractions of mono-CBP congeners were also observed in the EZVI vials. The mono-CBP in EZVI soils comprised approximately 0.1% of total PCBs. In 11-week samples, t-test comparison of EZVI samples to all other samples indicates that the fractions of di- and tetra-CBP homologs were similar for the two populations ( $P$ -value  $> 0.05$ ), while the fractions of mono-, tri-, and hexa-CBP congeners were significantly different ( $P$ - values  $< 0.001$ ).

After 66-weeks, a more prevalent shift in homolog distribution was observed. In EZVI-treated soils, with or without bentonite, enrichment in the lesser-chlorinated congeners was observed. Mono-CBP was observed in all of the 66-week samples, presumably due to biodegradation of PCBs. In non-EZVI soils, mono-PCB comprised 0.1 to 0.2% of total PCBs. In the EZVI vials with and without bentonite, mono-CBP comprised 0.5 and 0.9% of total PCBs, respectively. In 66-week samples, t-test comparison of EZVI samples to all other samples indicates that the fractions of all PCB homologs were statistically different ( $P$ -values  $< 0.001$ ).

GC/MS chromatograms of the untreated control and EZVI soil samples at 66 weeks are shown in Figure B-1. The sample GC chromatograms further illustrate the observed shift to lesser-chlorinated congeners. Approximate GC retention time ranges for the PCB homologs based on 66-week data are also indicated on Figure B-1.

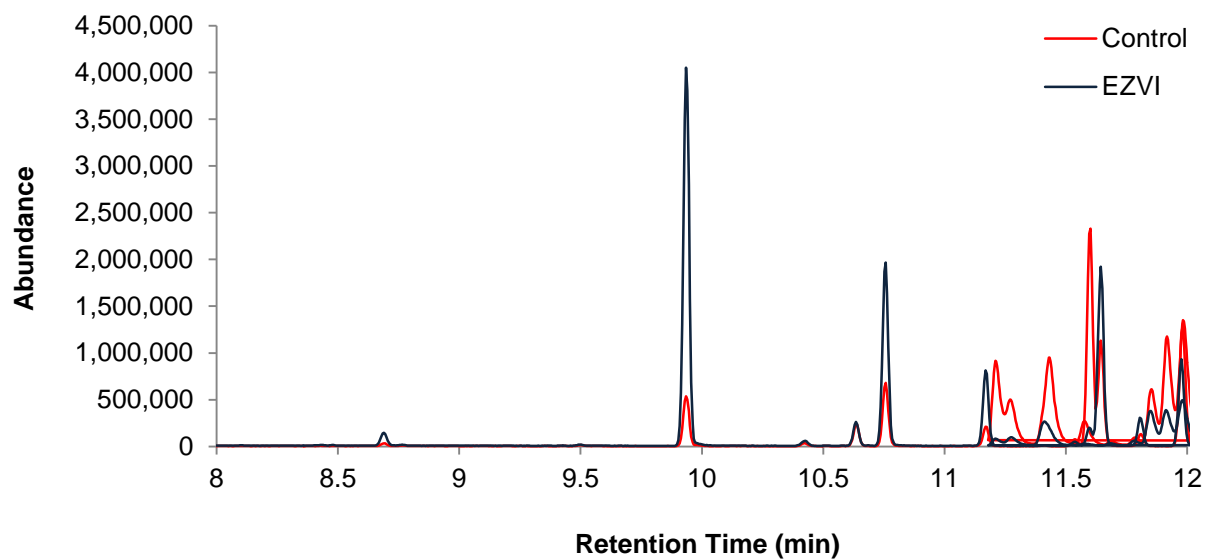
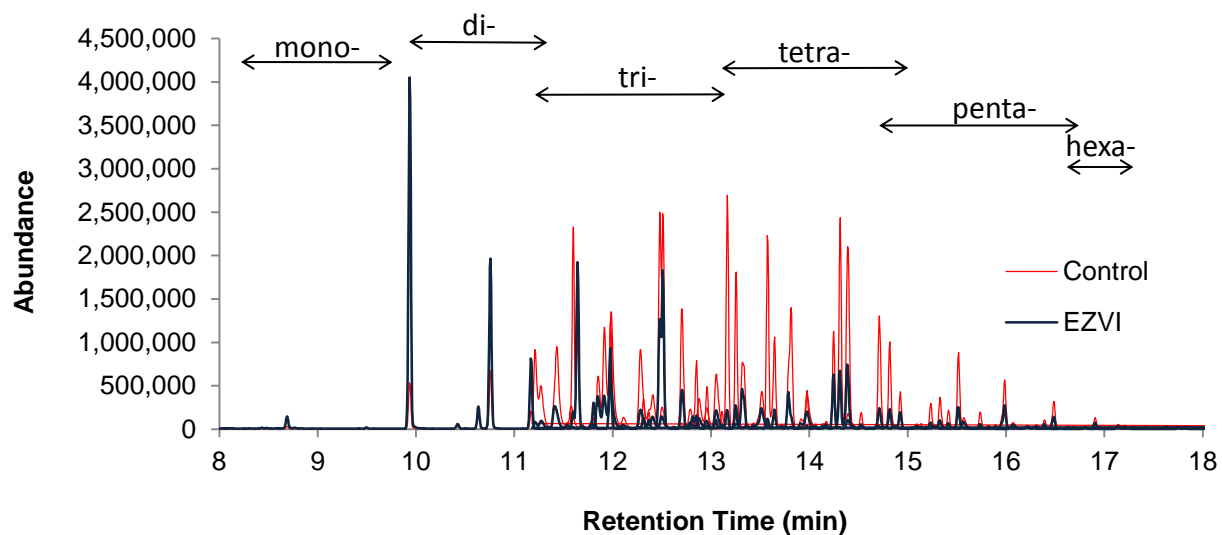


Figure B-1. Top: GC chromatogram data comparison of untreated control and EZVI-treated soils after 66 weeks of reaction. Approximate ranges for retention times by homolog are indicated. Bottom: Close-up of the early retention times, where enrichment of lesser-chlorinated congeners is observed in EZVI-treated vials.

## B.5 Soil Phase Study: Rate Unit Conversion

Abramowicz et al. (1993)<sup>1</sup> presented PCB degradation rate in terms of 1.3  $\mu\text{mol}$ -chlorine per gram of sediment per week. This is converted to units used in the present manuscript ( $\text{mg kg}^{-1} \text{ week}^{-1}$ ), using a molecular weight of chloride (Cl) of 35.5 g/mol, as follows:

$$1.3 \frac{\mu\text{mol Cl}}{\text{g} \cdot \text{week}} \cdot 35.5 \frac{\text{g Cl}}{\text{mol Cl}} = 46 \frac{\text{mg}}{\text{kg} \cdot \text{week}}$$

<sup>1</sup>Abramowicz, D. A., M. J. Brennan, H. M. Vandort, and E. L. Gallagher. 1993. Factors Influencing the Rate of Polychlorinated Biphenyl Dechlorination in Hudson River Sediments. *Environmental Science & Technology* 27 (6):1125-1131.